Studies on enzymatic synthesis of functional sugars

A Dissertation Submitted to the Graduate School of Bioagricultural Sciences,

Nagoya University in Partial Fulfillment of the Requirements

for the Degree of Doctor of Agricultural Sciences

March, 2013

Teruyo Ojima

Laboratory of Molecular Biotechnology,

Division of Biotechnology,

Department of Bioengineering Sciences,

Graduate School of Bioagricultural Sciences,

Nagoya University

Table of contents

(page)

Abbreviations

5-α-Glc-gingerol,
(*S*)-5-(*O*-α-D-glucopyranosyl)-1-(4-hydroxy-3-methoxyphenyl)decan-3-one
5-α-Mal-gingerol,
(*S*)-5-[*O*-α-(4-*O*-α-D-glucopyranosyl-D-glucopyranosyl)]-1-(4-hydroxy-3-methoxyphenyl)decan-3-one
AGE, *N*-acylglucosamine 2-epimerase
AnG, α-glucosidase from *Aspergillus niger*
AKI, aldose-ketose isomerase
BfCE, CE from *Bacteroides fragilis* NCTC9343
BSA, Bivine Sereum Albumin
CE, cellobiose 2-epimerase
CGTase, cyclodextrin glucanotransferase
CpCE, CE from *Chitinophaga pinensis* NBRC 15968
CsCE, CE from *Caldicellulosiruptor saccharolyticus*
DfCE, CE from *Dyadobacter fermentans* ATCC700827
EcCE, CE from *Eubacterium cellulosolvens* NE13
FjCE, CE from *Flavobacterium johnsoniae* NBRC 14942
Glc-Man, 4-*O*-β-D-mannnosyl-D-glucose
GlcNAC, *N*-acetyl- D –glucosamine
HaCE, CE from *Herpetosiphon aurantiacus* ATCC23779
HaG, α-glucosidase from *Halomonas* sp. H11
HH-COSY, HH-correlation spectroscopy
HMBC, heteronuclear multiple-bond connectivity
HSQC, heteronuclear single-quantum coherence
IPTG, isopropyl-l-thio-β-D-galactoside
MALDI-TOFMS, matrix assisted laser desorption ionization-time of flight mass spectrometry
Man-Glc, 4-*O*-β-D-glucosyl-D-mannose
ManNAC, *n*-acetyl- D –mannosamine
MGP, 4-*O*-β-D-mannosyl-D-glucose phosphorylase
MS, mass spectrometry;
NMR, nuclear magnetic resonance;
PhCE, CE from *Pedobacter heparinus* NBRC 12017
PMI, mannose 6-phosphate isomerase
*p*NPG, *p*-nitrophenyl α-D-glucoside

PVDF, poly vinylidene difluoride
RaCE, CE from *Ruminococcus albus*
RmCE, CE from *Rhodothermus marinus* JCM9785
SdCE, CE from *Saccharophagus degradans* ATCC43961
SDS-PAGE, sodium dodecyl sulfate-polyacrylamide gel electrophoresis
SlCE, CE from *Spirosoma linguale* ATCC33905
TFA, trifluoroacetic acid
TLC, thin-layer chromatography
TtCE, CE from *Teredinibacter turnerae* ATCC39867
X-gal, 5-Bromo-4-Chloro-3-Indolyl-β-D-Galactoside

Chapter 1. General introduction

1.1. Enzymatic synthesis of sugars

The synthesis and degradation of sugar, which is an essential energy source for all living cells, are undertaken by enzymatic reaction in cells. To date, carbohydrate related enzymes, for example α-amylase (EC 3.2.1.1) and xylose isomerase (EC 5.3.1.5), have long been applied as robust biocatalysts in the sugar industry for the production of maltooligosaccharide and fructose, respectively. Since the production of sugars as sweetners or energy source in food industry has almost saturated, a demand for enzymes that are capable of synthesizing value added sugars is expanding.

1.2. Value added sugars

Value added sugars are sometimes called as functional sugars that are expected to show some beneficial properties for human healthcare. In this study, the author focuses on two types of enzymes, namely α-glucosidase (EC 3.2.1.20, α-D-glucosideglucohydrolase) and cellobiose 2-epimerase (CE; EC 5.1.3.11) because they have potential to synthesize functional sugars such as glucosides and 4-*O*-β-D-galactosyl-D-mannose (epilactose) from low-priced sugars at a low cost. The details of each will be described in the followings.

1.3. α-Glucosidase and glucoside

1.3.1 α-Glucosidase

α-Glucosidase is a ubiquitous enzyme, widely distributed in

microorganisms, plants, and animals. It catalyzes liberation of α-glucose from the non-reducing ends of α-glucosides such as maltooligosaccharides and sucrose. Its substrate specificity is significantly diverse, depending on the enzyme origins, and the enzymes are classified into three groups based on their substrate specificities (Chiba 1988). Group I enzymes are more active toward 'heterogeneous' substrates, represented by sucrose and synthetic glucosides such as *p*-nitrophenyl α-D-glucoside (*p*NPG) and phenyl α-D-glucoside than toward 'homogeneous' substrates such as maltose. Group II enzymes, known as maltases, prefer homogeneous substrates to heterogeneous substrates. Like group II enzymes, group III enzymes mainly hydrolyze homogeneous substrates but have a high activity toward long-chain substrates like glycogen and soluble starch.

According to the sequence-based classification of glycoside hydrolase (GH), α-glucosidases are generally classified into two families, GH families 13 (subfamily 30) and 31 (Cantarel 2008). Enzymes from bacteria, some yeast such as *Saccharomyces cerevisiae*, and insects are mainly classified into the former family, and those from plants, animals, some yeast such as *Schizosaccharomyces pombe*, and fungi are in the latter.

Enzymes of both families catalyze hydrolysis of α-glucosides, with net retention of the anomeric configuration, through a double displacement mechanism, where two acidic amino acid residues act as a catalytic nucleophile and a general acid/base catalyst (McCarter 1996, Fig. 1-1). The general acid/base catalyst donates a proton to the glucosidic oxygen, and the catalytic nucleophile simultaneously attacks the anomeric carbon to form a β-glucosyl

enzyme intermediate. Consequently, the general acid/base catalyst activates a water molecule as a general base catalyst to stimulate nucleophilic attack of the water molecule at the anomeric carbon of the glucosyl–enzyme intermediate. Transglucosylation can occur if a free OH group of an acceptor molecule such as sugar or alcohol, in place of water, nucleophilically attacks the glucosyl–enzyme intermediate.

1.3.2. Industrial application of α-glucosidase

In the food and pharmaceutical industries, α-glucosidases play essential roles in the production of various types of oligosaccharides such as isomaltooligosaccharides, nigerooligosaccharides (Takaku 1988, Yamamoto 1999), and some glucosides such as α-D-glucosyl vitamin E (Murase 1997), α-D-glucosylglycerol (αGG) (Takenaka 2000a) and menthyl α-D-glucoside (Nakagawa 2000). Glucosylation of non-sugar compounds is a useful and important technique for improving their physicochemical properties, such as stability and water solubility (Murase 1997, Yamamoto 1992, Suzuki 1991, Kurosu 2002).

For example, αGG, a collective term for 2-*O*-αGG, (2*R*)-1-*O*-αGG, and (2*S*)-1-*O*-αGG, is one of the active glucosides observed in some osmotolerant bacteria and plants (Hincha 2004) and is also found in traditional Japanese liquors produced from rice (Takenaka 2000b) (Fig. 1-2). αGG has been reported to have some beneficial functions as a moisturizing agent in cosmetics (Yoshida 2007) and potential as health food material and therapeutic agent because it stimulates insulin-like growth factor behavior (Harada 2010) and has antitumor

effects (Nitta 2007).

1.3.3. Enzymatic synthesis of glucosides

α-Glucosidases and some other enzymes catalyzing transglycosylation, e.g., cyclodextrin glucanotransferases (CGTase, EC. 2.4.1.19), and sucrose phosphorylases (EC. 2.4.1.7), are attractive biocatalysts for the synthesis of various kinds of glycosides because each of these enzymes has potential for the specific glycosylation of various structural classes of acceptors (Luley-Goedl 2010, Aerts 2011). Basically CGTase catalyzes the intramolecular (cyclization) and intermolecular (coupling and disproportionation) transglucosylations from starch and related polysaccharides, and hydrolysis, and sucrose phosphorylase catalyzes reversible phosphorolysis of sucrose to α-D-glucose 1-phosphate and D-fructose. These enzymes follow a double-displacement mechanism described above (McCarter 1994).

Among these enzymes, α-glucosidases and CGTases have already widely been used for the industrial productions of glucosides because they had long achievements in the oligosaccharide production so that they can be avairable at a low cost. Of course, the synthesized glucosides are much more valuable than the original materials.

1.3.4. Problems in the synthesis of glucoside

As mentioned above, various kinds of glucosides are enzymatically synthesized by transglycosylation reaction in the mixture of acceptor possessing OH group and α-glucoside (donor substrate) in the industrial scale. However it

remains difficult to eliminate or prevent the byproducts produced by the additional transglucosylation and hydrolysis towards the target product and the glycosyl donor substrate.

For example, αGG is synthesized enzymatically from maltooligosaccharides and glycerol with fungal *α*-glucosidase (Takenaka 2000a) or bacterial CGTase (Nakano 2003). However, the yield of the production has been lowered by accumulation of byproducts such as maltooligosaccharides and di- or higher glucosylated glycerols which was unavoidable as a result of the enzymes nature. In contrast, sucrose phosphorylase has been reported to produce 2-*O*-αGG regioselectively from sucrose and glycerol in a high yield (Goedl 2008). Although sucrose phosphorylase is an attractive biocatalyst for the production of glucosides (Luley-Goedl 2010), not all types of glucosides can be synthesized using it. Consequently, research on its use for the production of various kinds of glucosides is still under development (Aerts 2011).

Recently, a new approach for the synthesis of glucosides using glycosynthase and glycosyl fluoride has been developed (Shaikh 2008). Glycosynthase, a mutant enzyme of glycosidase lacking the catalytic nucleophile, can transfer glycosyl residue to appropriate acceptors from glycosyl fluoride that have incorrect anomeric configuration. Glycosynthase does not hydrolyze the formed products, thus very high yields are achieved. However there are some drawbakcs in the practical use of glycosyl fluoride as a donor, because it is more expensive than the natural glycosyl donors, and the byproduct of the reaction, hydroxyl fluoride, is harmful.

1.4. Cellobiose 2-epimerase and epilactose

1.4.1. Research history of cellobiose 2-epimerase

Cellobiose 2-epimerase (CE) reversibly converts glucose residue to mannose residue at the reducing end of β-1,4-linked oligosaccharides such as cellobiose (4-*O*-β-D-glucosyl-D-glucose) and lactose (4-*O*-β-D-galactosyl-D-glucose) to produce 4-*O*-β-D-glucosyl-D-mannose (Glc-Man) and epilactose (4-*O*-β-D-galactosyl-D-mannose) respectively. It was first found in the culture fluid of an anaerobic ruminal bacterium, *Ruminococcus albus* (Tyler and Leatherwood 1967). It is a unique enzyme that catalyzes hydroxy-stereoisomerism at the C-2 position of a non-modified sugar through a proton abstraction/addition mechanism (Amein and Leatherwood 1969), because almost all carbohydrate epimerases act on activated sugars bearing nucleotidyl, phosphoryl, or acyl groups.

The gene of CE had been isolated from *R. albus* NE1 (Ito 2007), and the enzymatic characteristics of *R. albus* CE (RaCE) were investigated with a recombinant enzyme produced in *Escherichia coli* (Ito 2008). RaCE is most active at neutral pH values and relatively low temperature (30ºC). It epimerizes not only cellobiose but also lactose, cellotriose, and cellotetoraose, although it strictly recognizes the β-1,4-glycosidic linkage at the reducing end of substrates.

Since the amino acid sequence of RaCE was elucidated, three other CE genes from anaerobic bacteria, *Bacteroides fragilis* NCTC9343 (BfCE), *Eubacterium cellulosolvens* NE13 (EcCE) and *Caldicellulosiruptor saccharolyticus* (CsCE), have been identified (Senoura 2009, Taguchi 2008, Park 2011). The BfCE gene comprises the operon along with the genes

encoding β-mannanase and 4-*O*-β-D-mannosyl-D-glucose phosphorylase (MGP), which specifically phosphorolyzes 4-*O*-β-D-mannosyl-D-glucose (Man-Glc) to α-D-mannosyl phosphate and D-glucose (Senoura et al., 2011), implying that the physiological role of CE is to convert β-1,4-mannobiose to Man-Glc for further phosphorolysis.

The amino acid sequence RaCE shows relatively weak similarity to *N*-acylglucosamine 2-epimerases (AGEs) from porcine kidney and *Anabaena* sp. CH1, whose three-dimensional structures are available (Ito 2007). AGEs catalyze the interconversion of *N*-acetyl-D-glucosamine (GlcNAC) and *N*-acetyl-D-mannosamine (ManNAC). AGEs are dimeric enzymes, while CE is monomeric. Each monomer of the AGE is composed of an $(\alpha/\alpha)_6$ barrel fold (Itoh 2000, Lee 2007). A soaking study of porcine AGE crystal with GlcNAC revealed that His382, His248, Glu251, and Arg60 are situated at the nearest position to bound GlcNAC or a mixture of GlcNAC and ManNAC (Itoh 2000). The two corresponding His residues of *Anabaena* AGE were envisaged to serve as the general acid and the general base catalysts in proton abstraction/addition at the C2 position (Lee 2007). Secondary structure prediction suggested that RaCE is also formed by an $(\alpha/\alpha)_6$ barrel as AGEs, and two putative catalytic His residues are observed at the equivalent positions. These conserved His residues of RaCE were confirmed to be essential for the catalytic activity by site-directed mutagenesis (Ito 2009), suggesting that CE and AGE shall share the common structure at the active site, including catalytic amino acids.

In an available database in National Center for Biotechnology Information, many CE-like genes have been assigned as AGEs; however, the

deduced amino acid sequences of these CE-like proteins align more closely to CEs than to AGEs.

1.4.2. Enzymatic synthesis of epilactose

Epilactose, a rare sugar found in alkaline-treated or heated milk (Martinez-Castro 1980, Martinez-Castro 1981), has beneficial potential for use as a prebiotic food material, because it is highly resistant to rat intestinal enzymes and strongly proliferates human bifidobacteria (Ito 2008). Additionally, epilactose significantly promotes calcium and iron adsorption in the small intestine of rats (Nishimukai 2008, Suzuki 2010a, Suzuki 2010b).

Epilactose can be enzymatically synthesized from lactose and CE. In spite of the beneficial biological functions of epilactose, utilization of CE for the industrial production of epilactose is significantly limited due to the low thermal stability of known CEs (around 30˚C; Ito 2008, Senoura 2009, Taguchi 2008). Low temperature condition causes not only deterioration but also precipitation of lactose.

1.5. The scope of this study

In this work, the author focuses on α-glucosidase as a biocatalyst for the efficient production of various glucosides, and on CE for the purpose of the practical synthesis of epilactose. First, α-glucosidase showing high transglucosylation activity towards glycerol is screened and an enzyme with the desired properties is successfully obtained from a moderate halophilic marine bacterium, *Halomonas* sp. H11 strain, isolated from coral. In addition to its high

transglucosylation activity, the enzyme has several unique properties; first, significant stimulation by monovalent cations such as NH_4^+, K^+, Rb^+, and Cs^+, second, very narrow specificity for substrate chain-length and glucosidic bonds, and third, more feasible to synthesize some glucoside rather than the other α-glucosidase or CGTases.

On the other hand, CE-like genes with unknown function from various aerobic bacteria are cloned based on the genomic information. Total of nine CEs are obtained and their characteristics are determined using recombinant proteins expressed by *E. coli*. Among them, CE from *Rhodothermus marinus* JCM9785 (RmCE) shows the optimum reaction at 80˚C at pH 6.3, and stable at a range of pH 3.2-10.8 and below 80˚C. These properties of RmCE are desirable for the production of epilactose because the reaction should be carried out at a high temperature to make the substrate concentration high. Furthermore at acidic pH, non enzymatic alkaline epimerization of lactose to accumulate a byproduct, lactulose, can be avoided.

In the first half of this manuscript, screening of α-glucosidase, enzymatic properties of α-glucosidase from *Halomonas* sp. H11 (HaG), and its application for the synthesis of glucosides are described. The details are as follows; the screening of α-glucosidase and characterization of the selected bacterium, *Halomonas* sp. H11, are described in Chapter 2. Next, the purification and characterization of α-glucosidase, and cloning and sequence analysis are in Chapter 3 and Chapter 4, respectively. Finally, enzymatic synthesis of a novel glucoside, α-glucosylated 6-gingerol, and its basic physical properties are in Chapter 5.

In the latter half of the manuscript, cloning and characterization of CEs from nine aerobic bacteria are described. The cloning and characterization of CEs from genome sequenced aerobic bacteria are in Chapter 6. In Chapter 7, identification, cloning and characterization of CE from thermophilic aerobic bacterium, *R. marinus* JCM9785 whose genome is not available, are described.

Figures

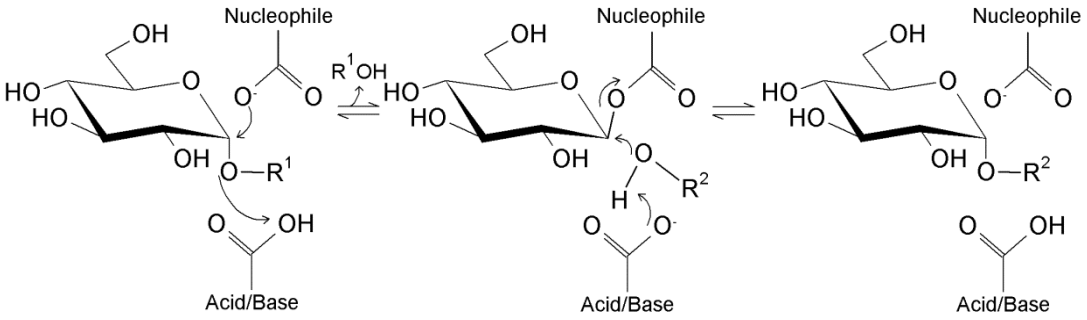

Fig. 1-1. Hydrolysis and transglucosylation reaction of α-glucosidase with double displacement mechanism.

Hydrolysis (R^1 = saccharide, R^2 = H)

Transglucosylation (R^1 = saccharide, R^2 = saccharide or aglycone)

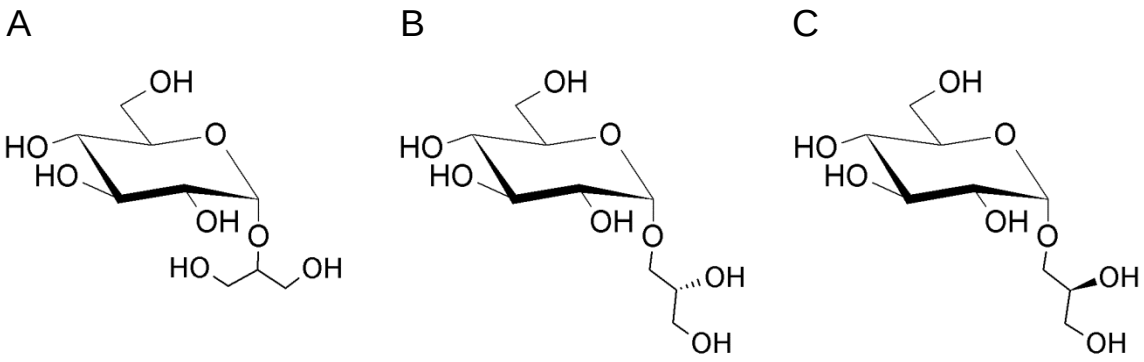

Fig. 1-2. The chemical structures of αGG.

A, 2-*O*-αGG; B, (2*R*)-1-*O*-αGG; and C, (2*S*)-1-*O*-αGG.

Chapter 2. Screening of α-glucosidase

2.1. Introduction

First of all, to obtain α-glucosidase that can be capable of synthesizing α-glucosylglycerol (αGG) efficiently, α-glucosidase is screened from marine bacteria using maltose and glycerol as donor and acceptor substrates, respectively. In this screening approach, α-glucosidase with higher transglucosylation activity toward glycerol than maltose or water molecule can preferentially synthesize αGG rather than producing maltotriose or glucose. Maltose is chosen as a glycosyl donor because it can be obtained by degradation of starch at a low cost. As the screening source, bacteria from marine environment are selected because there have been only a few reports about α-glucosidase or glycosides synthesis using marine bacteria. In this chapter, screening of α-glucosidase and identification of the bacterial strain selected are described.

2.2. Materials and methods

2.2.1. Isolation of bacterial strain

Bacterial strains from coral, collected in the sea near Okinawa, Japan, were propagated in a culture medium consisting of 10 g/L Na arginate (Wako Pure Chemical Industries, Osaka, Japan), 5 g/L peptone (Becton Dickinson, Franklin Lakes, NJ, USA), 5 g/L yeast extract (Becton Dickinson), 1 g/L KH_2PO_4 (Kanto Chemical, Tokyo, Japan), 0.2 g/L $MgSO_4 \cdot 7H_2O$ (Kanto Chemical), and 100 g/L NaCl; the pH was adjusted to 10 with separately sterilized 10 g/L

Na_2CO_3 (Kanto Chemical). The culture medium was incubated at 30°C for 2 weeks, and a single colony was isolated from the resulting culture fluid on the same medium containing 20 g/L agar.

2.2.2. Screening of α-glucosidase

2.2.2.1. Culture of the bacterial strain and preparation of cell-free extract

The single colony of each strain was separately inoculated to Marine Broth 2216 (Becton Dickinson) or liquid medium consisting of 10 g/L soluble starch (Kanto Chemical), 5 g/L polypeptone (Wako Pure Chemical Industries), 5 g/L yeast extract, 35 g/L NaCl, 0.1 g/L KH_2PO_4, and 0.2 g/L $MgSO_4 \cdot 7H_2O$; the pH was adjusted to 7.0 with 2 *N* NaOH, and aerobically cultivated at 30°C for 24 h. Cells were harvested by centrifugation, and disrupted by sonication using an Astrason ultrasonic processor XL (Misonix, Farmingdale, NY, USA) in 20 mM HEPES–NaOH buffer (pH 7.0) (the volume was equal to the culture medium). The resulting cell debris was removed by centrifugation, and the supernatant was regarded as the cell-free extract.

2.2.2.2. Reaction conditions for screening of α-glucosidase

A mixture consisting of 100 g/L maltose (Nihon Shokuhin Kako, Tokyo, Japan) and 100 g/L glycerol (Nacalai Tesque, Kyoto, Japan), pH of which was adjusted to 7.0 with 2 *N* HCl or NaOH, were used as screening substrates. Two hundreds μL of the substrate solutions and 5 μL of the cell-free extract prepared as described above were mixed and incubated at 40°C for 72 h. The resulting mixture was boiled to terminate the reaction.

2.2.2.3. Analysis of the reaction mixtures

The sugar components of the reaction mixtures were analyzed by the high performance liquid chromatography (HPLC) as the following condition: column, Ultron PS-80 N. L (ϕ8.0 x 500 mm, Shinwa Chemical Industries, Kyoto); Eluent, water; flow rate; 0.8 mL/min; column temperature, 60°C; detector, refractive index. The samples were appropriately diluted with water and filtrated with 0.45 μm filter (Millex HP, Millipore). The integral intensities by the detector were simply considered as the sugar content (w/w).

2.2.3. Identification of bacterial strain

Chromosomal DNA of the obtained bacterium was extracted using an Instragene matrix (Bio-Rad, Hercules, CA, USA) and used as the template in PCR. Primestar HS DNA polymerase (Takara Bio, Otsu, Japan) and a primer set of 9F and 1510R (Nakagawa 2001) were used to amplify a region of 16S rRNA (Table 2-1). A Bigdye Terminator v3.1 cycle-sequencing kit (Applied Biosystems, Foster City, CA, USA) and primers 9F, 785F, 802R, and 1510R (Nakagawa 2001) were used in sequence analysis (Table 2-1). An automatic DNA sequencer, ABI PRISM 3130 xl Genetic Analyzer System (Applied Biosystems), and the software Chromaspro 1.4 (Technelysium Pty, Tewantin, Australia) were used. Sequence similarity searches and phylogenetic classifications were performed using the software Basic Local Alignment Search Tool (http://blast.ncbi.nlm.nih.gov/Blast.cgi) and Aporon 2.0 (Techno Suruga Laboratory, Shizuoka, Japan), with the database Aporon DB-BA 6.0 (Techno Suruga Laboratory), the GenBank, DNA databank of Japan (DDBJ), and the EMBL Nucleotide Sequence Database. The cells grown on Marine Broth 2216

containing 20 g/L agar were used for following tests. Morphological observations were carried out using an optical microscope, BX50F4 (Olympus, Tokyo, Japan). Cells were stained with Feyber G Nissui (Nissui Seiyaku, Tokyo, Japan) in a Gram-staining test. Other physiological tests were performed by the methods described by Barrow (Barrow 1993) and using a kit, API20NE (bioMérieux, Lyon, France).

2.3. Results

2.3.1. Selection of bacterial strain

A bacterial strain, H11 was selected as the enzyme source because significant transglucosylation activitiy toward glycerol was observed (Fig. 2-1). In other words, the quantity of produced αGG was greater than that of glucose or maltotriose. Any other strains (about 80 bacteria isolated from marine) did not give such a result in the preliminary screening (data not shown). The glucosylation was observed only when the reaction was carried out with the cell extract of the strain H11 which were cultivated with the medium containing soluble starch. No transglucosylation occurred when using the cell extract of the strain cultivated in Marine Broth 2216 (data not shown).

2.3.2. Identification of bacterial strain

The sequence of 16S rRNA of strain H11 strain is shown in Fig. 2-2. A phylogenetic tree constructed with this sequence showed that the H11 strain is closely related to *Halomonas aquamarina*, *Halomonas meridiana*, and *Halomona saxialensis*, and is likely to be categorized into the *Halomonas* genus (Fig. 2-3, Table 2-2). Its 16S rRNA sequence showed 99.5% identities to those of

both *H. aquamarina* DMS 30161 and *H. meridiana* DMS 5425. Physiological tests revealed that the H11 strain is rod-shaped (0.7–0.8 × 1.2–2.0 μm), pale yellow, smooth-surfaced, Gram-negative, mobile, and capable of growing at 4–45°C. It showed catalase, oxidase, urease, and cytochrome oxidase activities. Otherwise, all of the following were negative: nitrate reduction; production of indole; glucose oxidation; arginine dihydrolase and β-galactosidase activities; lipase activity for Tween 80; hydrolysis of esculin, gelatin, starch and casein; and use of glucose, L-arabinose, D-mannose, D-mannitol, *N*-acetylglucosamine, maltose, potassium gluconate, *n*-capric acid, adipic acid, DL-malic acid, Na citrate, and phenyl acetate. These features were not totally identical to those of any *Halomonas* species reported so far (Kaye 2004, Vreeland 2005). Therefore, the H11 strain was named *Halomonas* sp. H11, and deposited at the National Biological Resource Center (Chiba, Japan) as NBRC 108813.

2.4. Discussion

In this chapter, enzymes showing higher transglucosylation activity toward glycerol than maltose or water were screened from marine bacteria using maltose and glycerol as donor and acceptor substrates, respectively. Successfully α-glucosidase with an ideal transglucosylation capability that synthesize a larger amount of αGG than maltotriose or glucose was obtained from the cell extract of *Halomonas* sp. H11 strain, which was isolated from coral near Okinawa (Fig. 2-1). The less quantity of glucose and maltotriose which are generated by α-glucosidase reactions of hydrolyzing maltose or transfer of glucosyl residue to maltose, strongly suggests that the cell-free extract of

Halomonas sp. H11 strain contains α-glucosidase that may synthesize glucoside efficiently by preventing generations of such extra byproducts.

The H11 strain is likely moderate halophilic marine bacterium, whose related species are distributed in the saline environment (Kaye 2004, Vreeland 2005). To our knowledge, there have been no reports related to α-glucosidases or such enzymes having transglucosylation activity in *Halomonas* sp., so that the putative enzyme appears to be a novel one.

Halomonas sp. H11 had neither hydrolysis activity of starch nor utilization of maltose or glucose in the condition of physiological tests. However it could utilize starch when soluble starch was contained in the culture medium. α-Glucosidase activity was detected only in the cell-free extract obtained from the cells cultivated with the starch medium, implying that the expression of the gene encoding the enzyme is induced by starch or degradation products of starch.

Figures and Tables

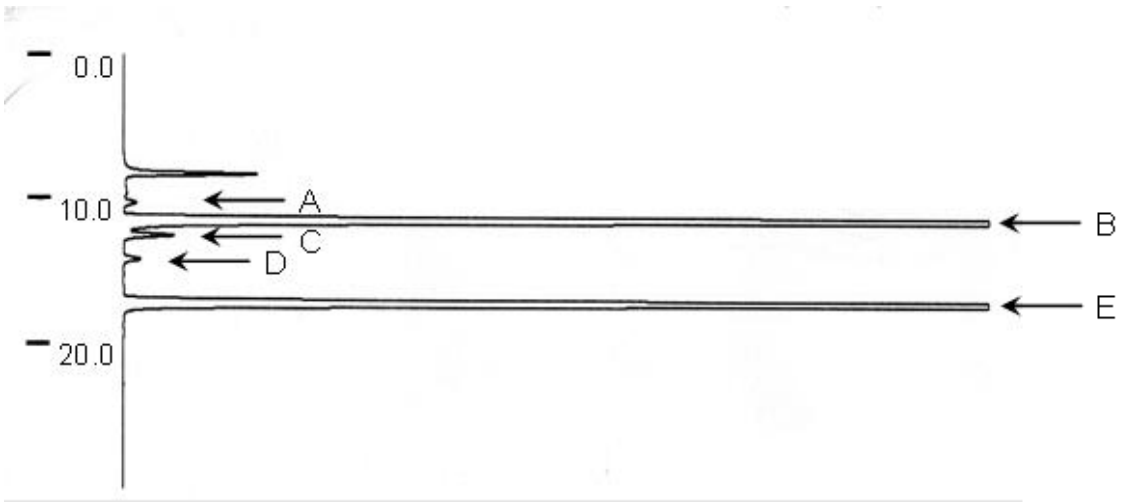

Fig. 2-1. HPLC chromatogram of the reaction mixture of the strain H11.

A reaction mixture consisting of maltose (glycosyl donor) and glycerol (glycosyl acceptor), and the cell-free extract of the strain H11 was incubated at 40°C at pH 7.0 for 72 h, and analyzed by HPLC. A, maltotriose; B, maltose; C, αGG; D, glucose; E, glycerol; and the others are unknown component derived from the cell extract.

```
   1  GAGTTTGATC CTGGCTCAGA TTGAACGCTG GCGGCAGGCC TAACACATGC
  51  AAGTCGAGCG GTAACAGATC CAGCTTGCTG GATGCTGACG AGCGGCGGAC
 101  GGGTGAGTAA TGCATAGGAA TCTGCCCGGT AGTGGGGGAT AACCTGGGGA
 151  AACCCAGGCT AATACCGCAT ACGTCCTACG GGAGAAAGGG GGCTTCGGCT
 201  CCCGCTATCG GATGAGCCTA TGTCGGATTA GCTAGTTGGT GAGGTAACGG
 251  CTCACCAAGG CCACGATCCG TAGCTGGTCT GAGAGGATGA TCAGCCACAT
 301  CGGGACTGAG ACACGGCCCG AACTCCTACG GGAGGCAGCA GTGGGGAATA
 351  TTGGACAATG GGGGGAACCC TGATCCAGCC ATGCCGCGTG TGTGAAGAAG
 401  GCCCTCGGGT TGTAAAGCAC TTTCAGCGAG GAAGAACGCC TAGCGGTTAA
 451  TACCCGCTAG GAAAGACATC ACTCGCAGAA GAAGCACCGG CTAACTCCGT
 501  GCCAGCAGCC GCGGTAATAC GGAGGGTGCA AGCGTTAATC GGAATTACTG
 551  GGCGTAAAGC GCGCGTAGGT GGCTTGATAA GCCGGTTGTG AAAGCCCCGG
 601  GCTCAACCTG GGAACGGCAT CCGGAACTGT CAAGCTAGAG TGCAGGAGAG
 651  GAAGGTAGAA TTCCCGGTGT AGCGGTGAAA TGCGTAGAGA TCGGGAGGAA
 701  TACCAGTGGC GAAGGCGGCC TTCTGGACTG ACACTGACAC TGAGGTGCGA
 751  AAGCGTGGGT AGCAAACAGG ATTAGATACC CTGGTAGTCC ACGCCGTAAA
 801  CGATGTCGAC CAGCCGTTGG GTGCCTAGCG CACTTTGTGG CGAAGTTAAC
 851  GCGATAAGTC GACCGCCTGG GGAGTACGGC CGCAAGGTTA AAACTCAAAT
 901  GAATTGACGG GGGCCCGCAC AAGCGGTGGA GCATGTGGTT TAATTCGATG
 951  CAACGCGAAG AACCTTACCT ACTCTTGACA TCCTGCGAAT TYGGTAGARA
1001  TACCTTAGTG CCTTCGGGAA CGCAGAGACA GGTGCTGCAT GGCTGTCGTC
1051  AGCTCGTGTT GTGAAATGTT GGGTTAAGTC CCGTAACGAG CGCAACCCTT
1101  GTCCTTATTT GCCAGCGCGT AATGGCGGGA ACTCTAAGGA GACTGCCGGT
1151  GACAAACCGG AGGAAGGTGG GGACGACGTC AAGTCATCAT GGCCCTTACG
1201  AGTAGGGCTA CACACGTGCT ACAATGGTCG GTACAAAGGG TTGCCAACTC
1251  GCGAGAGTGA GCCAATCCCG AAAAGCCGAT CTCAGTCCGG ATCGGAGTCT
1301  GCAACTCGAC TCCGTGAAGT CGGAATCGCT AGTAATCGTA GATCAGAATG
1351  CTACGGTGAA TACGTTCCCG GGCCTTGTAC ACACCGCCCG TCACACCATG
1401  GGAGTGGACT GCACCAGAAG TGGTTAGCCT AACGCAAGAG GGCGATCACC
1451  ACGGTGTGGT TCATGACTGG GGTGAAGTCG TAACAAGGTA GCC
```

Fig. 2-2. 16S rRNA sequence of *Halomonas* sp. H11 strain.

Length: 1493

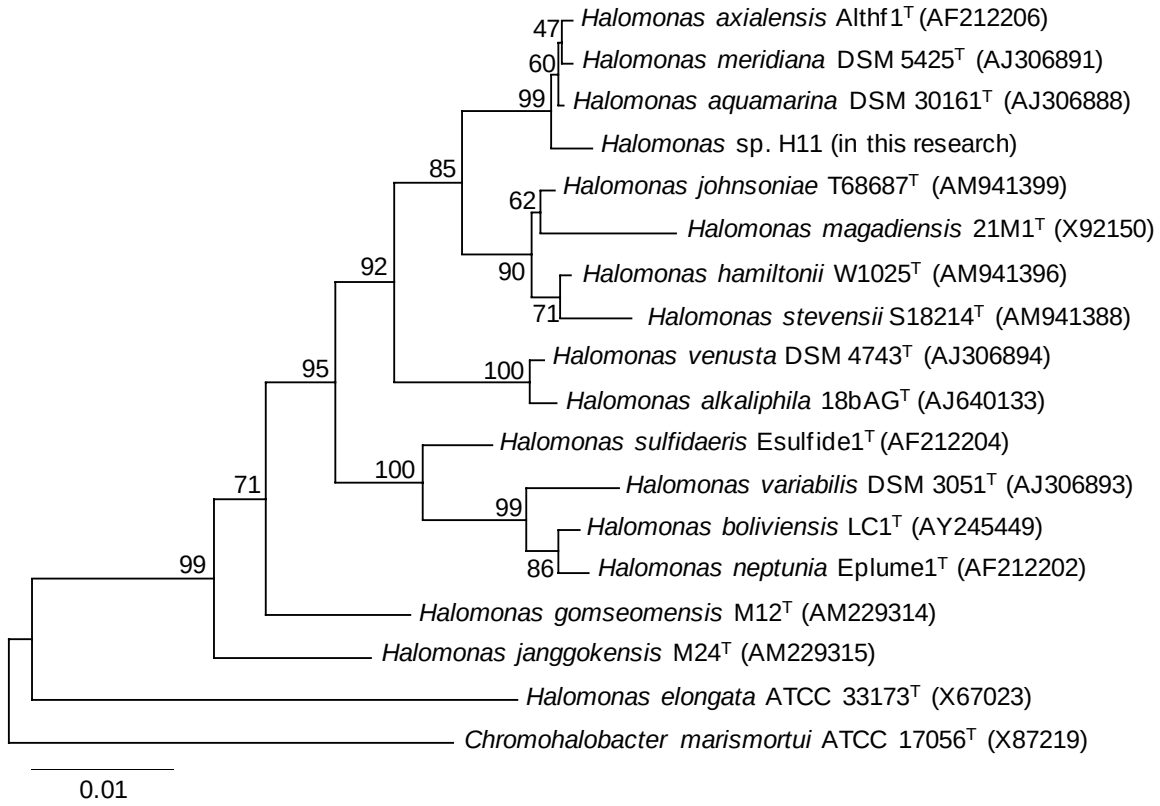

Fig. 2-3. Phylogenetic analysis of *Halomonas* sp. H11 strain based on 16S rRNA sequence.

The indicator beneath the tree is a scale bar representing 0.01 inferred substitutions per nucleotide portion. The numbers shown in the branch mean bootstrap values. Type strains are indicated as 'T' at the end of strain name. Accession number of 16S rRNA sequence is denoted by parenthesis.

Table 2-1. Primers used to identify the 16S rRNA sequence.

Primer	Sequence (5′-3′)
9F	GAGTTTGATCCTGGCTCAG
785F	GGATTAGATACCCTGGTAGTC
802R	TACCAGGGTATCTAATCC
1510R	GGCTACCTTGTTACGA

Table 2-2. Top 30 sequences showing higher identities with 16S rRNA sequence of the strain H11 by BLAST search.

Organism	Strain	Accession No.	Identity
Halomonas aquamarina	2PR52-11	EU440965	99.9%
Halomonas sp.	EP34	AM403725	99.9%
Halomonas sp.	es12	AJ551131	99.9%
Halomonas sp.	wp19	AJ551099	99.9%
Halomonas sp.	WT111	GQ152138	99.8%
Halomonas sp.	68(18zx)	AM403654	99.8%
Halomonas sp.	ws25	AJ551136	99.7%
Halomonas sp.	NTN12	AB166968	99.8%
Halomonas aquamarina	WP02-1-58	EF143425	99.7%
Halomonas sp.	69(20zx)	AM409192	99.7%
Halomonas sp.	ws31	AJ551141	99.9%
Halomonas sp.	LY054	FJ907960	99.6%
Halomonas aquamarina	WP02-1-81	EF143431	99.6%
Halomonas sp.	EP35	AM403726	99.6%
Halomonas sp.	EP13	AM398222	99.6%
Halomonas sp.	NTN93	AB167016	99.8%
Halomonas sp.	ws21	AJ551134	99.6%
Halomonas sp.	3029	AM110984	99.4%
Halomonas sp.	ws28	AJ551139	99.6%
Halomonas sp.	es11	AJ551130	99.6%
Halomonas aquamarina	DSM 30161	NR_042063	99.5%
Bacterium	L188S.606	EU935274	99.5%
Bacterium	L188S.607	EU935272	99.5%
Bacterium	L188S.603	EU935268	99.5%
Halomonas sp.	BCw166	FJ889608	99.5%
Halomonas sp.	SCSWB19	FJ461439	99.5%
Halomonas meridiana	PR51-13	EU441001	99.5%
uncultured bacterium		EF574488	99.5%
uncultured *Halomonas* sp.		AY588954	99.5%
Halomonas meridiana	DSM 5425	NR_042066	99.5%

Chapter 3. Isolation and characterization of α-glucosidase from *Halomonas* sp. H11

3.1. Introduction

In Chapter 2, α-glucosidase that had a higher transglucosylation activity toward glycerol than water or maltose when maltose and glycerol were used as donor and acceptor substrates, respectively, was found in the cell extract of *Halomonas* sp. H11. It seemed that this α-glucosidase was novel and suitable for the synthesis of α-glucosylglycerol (αGG). In this chapter, to identify the enzyme α-glucosidase from *Halomonas* sp. H11 (HaG) is purified and enzymatic properties are evaluated in details. Interestingly, HaG has several notable properties; first, significant stimulation by monovalent cations such as NH_4^+, K^+, Rb^+, and Cs^+, second, very narrow specificity for substrate chain-length and glucosidic bonds, and third, high transglucosylation capability toward the small molecular weight alcohols. The purification, basic enzymatic properties of effect of pH and temperatures, the effects of various salts on HaG activity, detailed kinetic analysis based on non-essential activator model, and evaluation of transglucosylation ability of HaG for glucosides synthesis are described in this chapter. To evaluate the capability of HaG to synthesize αGG, HaG and the previously reported *A. niger* α-glucosidase (AnG) are compared.

3.2. Materials and methods

3.2.1. Purification of α-glucosidase from *Halomonas* sp. H11 strain

Halomonas sp. H11 was cultured aerobically at 37°C for 24 h with rotary shaking at 150 rpm in 2 L of a medium consisting of 10g/L soluble starch (Kanto Chemical), 5 g/L polypeptone (Wako Pure Chemical Industries), 5 g/L yeast extract, 35 g/L NaCl, 0.1 g/L KH_2PO_4, and 0.2 g/L $MgSO_4 \cdot 7H_2O$; the pH was adjusted to 7.0 with 2 *N* NaOH. Bacterial cells were harvested by centrifugation, and disrupted by sonication in 50 mL of 20 mM HEPES–NaOH buffer (pH 7.0). The resulting cell debris was removed by centrifugation, and the supernatant was regarded as the crude extract. The pH of the crude extract was adjusted to 5.0 with 20 mM Na-acetate buffer (pH 5.0) and applied to a Toyopearl DEAE-650M column (ϕ16 × 170 mm; Tosoh, Tokyo, Japan) equilibrated with 20 mM Na-acetate buffer (pH 5.0). After washing with the same buffer, the adsorbed protein was eluted using a linear gradient of NaCl (0–0.5 M; total volume, 60 mL; flow rate, 2 mL/min). The active fractions eluted at about 0.1 M NaCl were collected, and $(NH_4)_2SO_4$ was added to the solution to give a final concentration of 1.5 M. This was loaded on a Toyopearl Butyl-650M column (ϕ16 × 200 mm, Tosoh) equilibrated with 20 mM HEPES–NaOH buffer containing 1.5 M ammonium sulfate (pH 7.0). The adsorbed protein was eluted using a descending linear gradient of ammonium sulfate (1.5–0 M; total volume, 120 mL; flow rate, 2 mL/min). The active fractions eluted at about 1.0 M ammonium sulfate were collected and desalted by repeated dilution and concentration. The sample was concentrated by ultracentrifugation using an Amicon Ultra-15 Centrifugal Unit (nominal molecular weight limit, 10 kDa; Millipore), and the

resulting concentrate was diluted with 20 mM HEPES–NaOH buffer (pH 7.0). Finally, the sample was concentrated to about 5 mL and applied to a Resource Q column (1 mL, GE Healthcare, Uppsala, Sweden) equilibrated with 20 mM HEPES–NaOH buffer (pH 7.0). After washing with 4 mL of the same buffer, the adsorbed protein was eluted using a linear gradient of NaCl (0–1.0 M; total volume, 30 mL; flow rate, 3 mL/min). The active fractions eluted at about 0.1 M NaCl were collected and desalted as described above.

To confirm the purity of the enzyme preparation, SDS-PAGE was carried out on 12.5% polyacrylamide gel, according to Laemmli (Laemmli 1970). A molecular size marker, Mark12 unstained standard (Invitrogen, Carlsbad, CA, USA), was used. The gel was stained with Rapid CBB Kanto (Kanto Chemical). Protein concentration was determined with a DC protein assay kit (Bio-Rad). Bovine serum albumin (BSA, Bio-Rad) was used as a standard protein. Since the enzyme activity was not affected by freezing–thawing, the enzyme preparation was frozen for long-term storage. The purified HaG was used for the following experiments.

3.2.2. Enzyme activity assay

For the standard assay, maltase activity was measured. A reaction mixture (0.1 mL), consisting of appropriate concentration of enzyme, 20 g/L maltose, and 40 mM HEPES–NaOH buffer (pH 7.0) was incubated at 30°C for 10 min. The reaction was terminated by adding twice the volume of 2 M Tris-HCl buffer (pH 7.0), and the liberated glucose was measured using the glucose oxidase–peroxidase method (Miwa 1972) with a Glucose C II-Test kit (Wako

Pure Chemical Industries). One unit of α-glucosidase activity was defined as the amount of enzyme that hydrolyzes 1 μmol of maltose per minute.

3.2.3. Effects of pH and temperature on activity and stability

The optimum pH and temperature were examined by measuring enzyme activities at given pH values and temperatures, respectively. The reaction pH was adjusted with 40 mM Britton–Robinson buffer (pH 3.0–12.0, composed of a mixture of 40 mM acetic acid, 40 mM phosphoric acid, and 40 mM glycine; the pH value was adjusted with NaOH) as the reaction buffer. The pH stability was determined based on the residual activity after incubation of 0.36 μg/mL of enzyme solutions in 10 mM Britton–Robinson buffer at various pH values at 4°C for 24 h. The temperature stability was evaluated from the residual activity after incubating the enzyme in 20 mM HEPES–NaOH (pH 7.0) at given temperatures for 15 min. The activity before treatment was considered as 100% of the residual activity.

3.2.4. Substrate specificity

The initial hydrolytic rates for following substrates were measured: maltose, maltotriose, (Nihon Shokuhin Kako), maltotetraose (Seikagaku, Tokyo, Japan), maltopentaose (Seikagaku), maltohexaose (Seikagaku), isomaltose (Tokyo Chemical Industry, Tokyo, Japan), trehalose (Wako Pure Chemical Industries), nigerose (Wako Pure Chemical Industries), kojibiose (Wako Pure Chemical Industries), sucrose (Kanto Chemical), methyl α-D-glucoside (Taoka Chemical, Osaka, Japan), and soluble starch (Nacalai Tesque). A reaction

mixture (0.1 mL) consisting of 7.2 μg/mL enzyme, 4 mM substrate (soluble starch, 2 g/L), and 40 mM HEPES–NaOH buffer (pH 7.0) was incubated at 30°C for 10 min. The liberated glucose was determined as described above. The enzyme reaction toward *p*NPG (Sigma-Aldrich, St. Louis, MO, USA) was performed by incubating 0.1 mL of a mixture consisting of 4 mM substrate and 7.2 μg/mL of enzyme in the same buffer. The reaction was stopped by adding twice the volume of 1 M Na_2CO_3. The absorbance at 405 nm was measured to determine the amount of *p*-nitrophenol (*p*NP) released. *p*NP (Wako Pure Chemical Industries) was used as a standard.

3.2.5. Effects of various salts on enzyme activity and stability

Enzyme activities in the presence of 10 mM solutions of various salts (LiCl, NaCl, MgCl, KCl, $CaCl_2$, $MnCl_2$, $FeCl_2$, $CoCl_2$, CuCl, $ZnCl_2$, $AgNO_3$, CsCl, and NH_4Cl) and 5 mM $(NH_4)_2SO_4$ were assayed. The effects of ammonium ions on the temperature–activity profile were investigated by measuring the activity at various temperatures in the presence or absence of 10 mM NH_4Cl. The thermal stability of HaG in the presence of 10 mM NH_4Cl was evaluated as described above.

3.2.6. Kinetic parameters for maltose and *p*NPG in the presence of monovalent cations

To evaluate the effects of monovalent cations on the kinetic parameters for maltose and *p*NPG, the apparent kinetic parameters for these substrates in the presence of 10 mM activators were determined from the initial rates of

hydrolysis at various substrate concentrations (2–20 mM for maltose and 0.001–8 mM for *p*NPG) by regressing to the Michaelis–Menten equation. Activations for hydrolysis of maltose by monovalent cations were kinetically analyzed in detail, based on a non-essential activator model (Dixon 1979). The reaction scheme for a reaction activated by a non-essential activator is shown in Fig. 3-1. In this model, rate equations 1 and 2 below were given under the assumption of rapid equilibration of reaction:

Equation 1

$$v = \frac{K_{\mathrm{A}}(k_{\mathrm{cat1}} \cdot K_{\mathrm{AS}} + k_{\mathrm{cat2}} \cdot \mathrm{A})\mathrm{S}}{K_{\mathrm{m}} \cdot K_{\mathrm{AS}}(K_{\mathrm{A}} + \mathrm{A}) + K_{\mathrm{A}}(K_{\mathrm{AS}} + \mathrm{A})\mathrm{S}}$$

where *v* is the initial hydrolysis rate, while A and S indicate concentration of activator and substrate, respectively. The four dissociation constants in this equation are related as shown in Equation 2.

Equation 2

$$K_{\mathrm{mA}} \cdot K_{\mathrm{A}} = K_{\mathrm{AS}} \cdot K_{\mathrm{m}}$$

The individual constants were determined as follows. First, the initial hydrolytic rates were measured at various concentrations of maltose (2–20 mM), without an activator, to obtain k_{cat1} and K_{m}. The values were calculated by fitting the experimental data to Equation 1 at A = 0 by non-linear regression. Next, the hydrolytic rates were measured at a substrate concentration much higher than that for K_{m} in the presence of various concentrations of activators (0.001–100 mM). The k_{cat2} and K_{AS} values were calculated from the concentration in the

activator–rate plot. Finally, the enzyme assay was carried out with maltose at the same concentration as that for K_m in the presence of various concentrations of activators (0.001–100 mM). K_A was determined from the concentration of the activator–hydrolytic rate plot as described above. Then K_{mA} was obtained by substituting the other parameters for Equation 2. To verify the calculated parameters, the experimental hydrolytic rates for 4.5 mM or 50 mM maltose in the presence of various concentrations of activators were compared with the theoretical values calculated from the obtained parameters.

3.2.7. Transglucosylation activity toward various alcohols

The transglucosylation activities toward ethanol, glycerol, propylene glycol, 1-propanol, 2-propanol, 1-butanol and benzyl alcohol (All reagents were purchased from Kanto Chemical) were qualitatively analyzed by thin-layer chromatography (TLC). Reaction mixtures (10 μL) containing 5% v/v alcohols, 100 g/L maltose, 50 mM HEPES–NaOH buffer (pH 7.0), 5 mM $(NH_4)_2SO_4$, and 0.18 μg/μL of HaG were incubated at 37°C for 24 h. A 10-fold diluted sample (1 μL) was analyzed by TLC (Silica gel 60 F_{254}; Merck, Darmstadt, Germany) with a solvent system consisting of 2-propanol:1-butanol:water = 2:2:1, v/v/v. Glucose and maltose (each 10 g/L) were used as standards. The chromatograms were visualized by spraying with a solvent consisting of 1.8 M sulfuric acid in methanol and heating.

3.2.8. Enzymatic synthesis of α-glucosylglycerol

The production efficiencies of αGG by HaG and *Aspergillus niger* α-glucosidase (AnG) were compared; AnG has been reported to produce

α–glucosylglycerol (αGG) efficiently (Takenaka 2000a). A reaction mixture (1 mL) containing 200 g/L maltose, 200 g/L glycerol, 0.04 U/mL of purified HaG or AnG, 40 mM reaction buffer (HEPES–NaOH buffer, pH 7.0, for HaG, and Na-acetate buffer, pH 5.0, for AnG) was incubated at 37°C. To investigate the effect of activator, the reactions in the presence of 5 mM $(NH_4)_2SO_4$ were also performed. AnG was purchased from Amano Enzymes (Nagoya, Japan), and the activity was assayed using the same method as that used for HaG except for the reaction buffer, which was 40 mM Na-acetate buffer (pH 5.0). The total αGG was quantified by HPLC under the same conditions described in chapter 2. To determine the ratio of stereoisomers of the product, αGG was purified with HPLC. αGG (5 mg) was trimethylsilylated using TMSI–C (GL Science, Tokyo, Japan) and analyzed by gas chromatography as described elsewhere (Takenaka 2000b).

3.3. Results

3.3.1. Purification of α-glucosidase from *Halomonas* sp. H11

α-Glucosidase from Halomonas sp. H11 (HaG) was purified from a cell-free extract to homogeneity by several types of column chromatography (Table 3-1). After hydrophobic column chromatography with Toyopearl Butyl 650M, the total enzyme activity significantly increased because of activation by NH_4^+, described in detail later. The purified enzyme showed a single band in SDS-PAGE (Fig. 3-2), and its molecular mass was estimated to be 58 kDa. It showed 50.9-fold higher specific activity than that of the crude extract.

3.3.2. Effects of pH and temperature

The effects of pH and temperature on enzyme activity and stability were investigated and these are summarized in Fig. 3-3. The maximum activity was observed at pH 6.5 when 20 mM Britton–Robinson buffer was used as the reaction buffer. In 40 mM HEPES–NaOH (pH 7.0), the optimum temperature for HaG was 30°C, and interestingly it exhibited more than 50% of the maximum activity even at 4°C. As will be mentioned in detail later, the monovalent cation in the buffer used was important for both pH–activity and temperature–activity. HaG was stable in the range from medium pH to the alkaline side at 4°C for 24 h. After treatment at 4–60°C for 15 min, the original activity was retained below 45°C, but abruptly decreased above 50°C.

3.3.3. Substrate specificity

The hydrolytic rates for various substrates were measured (Table 3-2). HaG showed high activity for maltose, *p*NPG, and sucrose, in this order. The hydrolytic rates for isomaltose, trehalose, nigerose, and maltotriose were negligible, and kojibiose was not hydrolyzed at all. Maltooligosaccharides longer than maltotriose, starch, and methyl α-D-glucoside were rarely hydrolyzed.

3.3.4. Effects of various salts on enzyme activity

The effects of various salts on HaG activity were investigated. The relative activities in the presence of 10 mM salt concentration, where the activity with no salt was regarded as 100%, were summarized in Table 3-3. In addition to the activation by KCl, RbCl, CsCl and $(NH_4)Cl$, 5 mM $(NH_4)_2SO_4$ also activated HaG as the same level of 10 mM $(NH_4)Cl$, obviously indicates that activation

factors are monovalent cations. On the other hand, HaG activity was inhibited by divalent cations such as Mg^{2+} and Ca^{2+}.

3.3.5. Kinetic analysis for activation of the enzyme by monovalent cations

The results described above showed that monovalent cations, particularly K^+, Rb^+, NH_4^+, and Cs^+, were strong activators for HaG. To clarify the effects of these monovalent cations, the apparent kinetic parameters for maltose and *p*NPG in the absence or presence of 10 mM concentration of activators were measured (Table 3-4). The K_{mapp} and k_{catapp} values for maltose in the absence of monovalent cations were 4.5 mM and 0.80 s^{-1}, respectively. These values were most improved to 1.45 mM and 7.43 s^{-1} by NH_4^+ and K^+, respectively. The k_{catapp}/K_{mapp} value was increased 22.4-fold by NH_4^+ relative to that without any monovalent cations. For *p*NPG, K_{mapp} and k_{catapp} were 4.6 mM and 1.0 s^{-1}, respectively, in the absence of an activator. They were almost same as those for maltose. On the other hand, K_{mapp} was significantly improved to about 0.02 mM in the presence of all the monovalent cations tested. Although the changes were less, k_{catapp} values were also improved, to 4.36 s^{-1}, 3.29 s^{-1}, 1.55 s^{-1}, and 3.59 s^{-1} by K^+, Rb^+, Cs^+, and NH_4^+, respectively. The k_{catapp}/K_{mapp} values were increased 969-fold, 893-fold, 372-fold, and 929-fold by K^+, Rb^+, Cs^+, and NH_4^+, respectively.

Next, the kinetic parameters for hydrolysis of maltose in a non-essential activation model were measured to evaluate the activation by K^+, Rb^+, NH_4^+, and Cs^+ (Table 3-5). The measured reaction rates towards 4.5 mM or 50 mM maltose with various concentrations of activators fitted well to the theoretical lines,

indicating that activation by monovalent cations was explained well by a non-essential activation model (Fig. 3-4). The activation degree reached almost maximum at 10 mM of each activator, and even at the range of 10–100 mM. The actual hydrolytic rates for 4.5 mM and 50 mM maltose in the absence of an activator were 0.71 s^{-1} and 1.53 s^{-1}, respectively, whereas those for 4.5 mM maltose increased 8.3-fold, 5.9-fold, 5.0-fold, and 7.1-fold in the presence of 50 mM K^+, Rb^+, Cs^+, and NH_4^+, respectively. Similarly, the rates for 50 mM maltose were increased 5.7-fold, 4.0-fold, 2.7-fold, and 4.3-fold by the same concentration of the respective monovalent cations.

The K_A and K_{AS} values for NH_4^+, which mirror the affinity of the activator with the enzyme and the enzyme–substrate complex respectively, were the lowest among the monovalent cations tested, followed by Rb^+, K^+, and Cs^+, in this order. The K_{mA} values were as follows: Cs^+, 1.19 mM; NH_4^+, 1.86 mM; Rb^+, 2.88 mM; and K^+, 3.52 mM. The k_{cat2} value for the hydrolysis of maltose in the presence of K^+ was the best of those for the monovalent cations tested, and those with Rb^+, NH_4^+, and Cs^+ followed in this order.

3.3.6. Effects of monovalent cations on pH–activity and temperature–activity

The effects of monovalent cations on enzyme activity at various pH values and temperatures were evaluated. As shown in Fig. 3-5, the activities at all pH values were raised by monovalent cations in the following order: K^+, Rb^+, NH_4^+, and Cs^+. These ions shifted the bell-shaped pH–activity curve to the alkaline side. The optimum pH in the absence of monovalent cations was 6.5, and those in the presence of 10 mM K^+, Rb^+, and NH_4^+ were 7.0, and 7.5 in the

presence of Cs^+. NH_4^+ was most effective in increasing the activity around the alkaline side. Interestingly, the optimum temperature for HaG activity was shifted from 30°C to 40°C in the presence of 10 mM NH_4^+ (Fig. 3-6), although stability was not affected (data not shown). The actual activity in the presence of NH_4^+ at 40°C was 11.6-fold higher than that in its absence.

3.3.7. Transglucosylation toward various alcohols

The transglucosylation activities toward various alcohols, i.e., ethanol, glycerol, propylene glycol, 1-propanol, 2-propanol, 1-butanol and benzyl alcohol were investigated. Transglucosylation products were detected in the reactions other than 1-butanol and benzyl alcohol (Fig. 3-7). As expected from the results on substrate specificity, no oligosaccharides were produced by transglucosylation.

3.3.8. Enzymatic synthesis of α-D-glucosylglycerol

The efficiencies of the syntheses of αGG by HaG and AnG were compared in the absence and presence of 10 mM NH_4^+. The time-course of αGG production is shown in Fig. 3-8 a. The production rate and yield of αGG by HaG in the presence of NH_4^+ were the highest among the four cases tested. The carbohydrate contents (%, w/w) of the reaction mixture at 816 h are summarized in Fig. 3-8 b. In the reaction of HaG in the presence of NH_4^+, the content of αGG represented 29.4% w/w of the total carbohydrates (the molar yield of αGG from converted maltose was 92.7%), and the αGG content for the reaction of AnG was around 8% w/w, independent of NH_4^+. The accumulations of glucose and trisaccharides (G3) were considerably less in the reaction with HaG than in that

with AnG. The compositions of the stereoisomers of αGG at 816 h were analyzed by gas chromatography, revealing that the ratios of the constituent isomers 2-*O*-αGG:(2*R*)-1-*O*-αGG:(2*S*)-1-*O*-αGG were 10:52:38 for HaG, and 7:73:20 for AnG.

3.4. Discussion

In this work, the author describes a unique α-glucosidase, which exhibits strong transglucosylation activity toward glycerol rather than hydrolyzing maltose, and has additional remarkable features, namely stimulation by monovalent cations and narrow substrate specificity. The enzyme is probably psychrophilic and prefers a moderate pH (Fig. 3-3, Fig. 3-5). These conditions are well suited to the marine environment where *Halomonas* sp. H11 was isolated.

HaG was found to be specific to maltose, sucrose, and *p*NPG, and rarely acted toward longer maltooligosaccharides, or disaccharides other than maltose (Table 3-2). Such a narrow specificity for the substrate chain-length by HaG is remarkable characteristic because bacterial α-glucosidases generally hydrolyze not only maltose but also longer maltooligosaccharides (Kelly 1983, Nakano 1994, Hung 2005). Based on the molecular mass of the purified protein, HaG seems to be classified into GH-family 13 (Cantarel 2009).

HaG was greatly stimulated by monovalent cations, namely K^+, Rb^+, NH_4^+, and Cs^+. Although numerous enzymes have been documented to be activated by monovalent cations in the plant and animal world (Shulter 1970), most types of known α-glucosidases in GH-family 13 are not activated by monovalent cations. There have been only two reports documenting stimulation

of α-glucosidase activity by monovalent cations. Crude α-glucosidases from fast-growing rhizobia and *Agrobacterium tumefaciens* were reported to be stimulated by K^+, NH_4^+, and Rb^+ (Hoelzle 1989), and purified α-glucosidase from *Rhizobium* sp. USDA 4280 was reported to be stimulated to 141% and 207% by addition of 10 mM K^+ and NH_4^+, respectively (Berthelot 1999). However such α-glucosidases have as yet rarely been investigated in detail.

The activation kinetics and enzymatic properties of HaG were determined. The monovalent cation activators, K^+, Rb^+, NH_4^+, and Cs^+, for HaG have similar ionic diameters. In particular, the ionic diameters of Rb^+ and NH_4^+ are almost the same (Rb^+, 1.48 Å; NH_4^+, 1.43 Å). These ions gave almost the same K_A and K_{AS} values for HaG (Table 3-5). In addition, the k_{cat2} values for hydrolysis of maltose in the presence of these ions were also similar. The K_A and K_{AS} values for Cs^+, which has an ionic diameter of 1.70 Å, were higher than those for the other ions. The k_{cat2} value was highest with the smallest ion, K^+, whose diameter is 1.33 Å. These results imply that the activator binding site of HaG is suitable for binding to monovalent ions with ionic diameters of around 1.4 Å.

The K_{mapp} and k_{catapp} values for maltose and *p*NPG were improved by the addition of K^+, Rb^+, Cs^+, and NH_4^+ (Table 3-4). In particular, the K_{mapp} values for *p*NPG were significantly improved, regardless of the type of monovalent cation. Enzyme–*p*NPG complexes might be stabilized by interaction between the negative charge of the nitrate group of *p*NP and a monovalent cation bound to the substrate binding site of the enzyme. Monovalent cation activators may therefore be involved in the formation of the substrate binding sites of HaG.

While only small portion of α-glucosidases are stimulated by monovalent cations, one major group of α-amylases classified in the same GH-family 13, i.e., α-amylases from mammals and *Pseudoalteromonas haloplanktis*,are allosterically activated by chloride ions (Maurus 2005, D'Amico 2000). In all chloride-dependent α-amylases whose crystal structures have been solved (Nakao 1994, Larson 1994, Qian 1993, Brayer 1995, Strobl 1998, Aghajari 1998a, Aghajari 1998b), Cl^- binds to a common site, close to the center of the catalytic barrel in the vicinity of the active site. Some of these amylases have been further investigated by structural and kinetic analyses with mutant enzymes (Maurus 2005, Aghajari 2002); Cl^- may play a role by polarizing the catalytic water molecule and interacting with the general acid/base catalyst to elevate the acid dissociation constant (pK_a) value of Glu residue (Feller 1996). In the case of HaG, the enzyme activity at the alkaline side was enhanced by the addition of monovalent cations (Fig. 3-5). This indicates that the pK_a value of the acid/base catalyst is increased, as observed in chloride-dependent α-amylases. Monovalent cations might interact with the second catalytic Asp, which is situated at the conserved region IV and forms hydrogen-bonding interactions with the general acid/base catalyst, thereby increasing the pK_a value of the acid/base (Maurus 2005).

It is notable that monovalent cations increases the optimum temperature of HaG (Fig. 3-6), but as yet I have no explanation for this phenomenon. The temperature–activity profiles in the absence and presence of NH_4^+ are similar to those of psychrophilic and mesophilic α-amylases (Feller 1994). A study of the interactions of monovalent cations and HaG will provide some insights to aid

understanding of the environmental adaptation of the enzyme.

HaG efficiently transferred glucosyl residues to some alcohols (Fig. 3-7). The precise structures of these products were not analyzed, but based on the properties of HaG, they were thought to be α-glucosides linked to the OH groups of alcohols. The glucosylation efficiency toward glycerol to produce αGG is superior to that of AnG when their hydrolytic activities towards maltose are compared (Fig. 3-8), implying that HaG has stronger transglucosylation activity than does AnG. The synthesis of αGG is more efficient in the presence of NH_4^+, suggesting that a monovalent cation stimulates not only hydrolysis but also the transglucosylation activity of HaG. As deduced from the substrate specificity (Table 3-2), smaller amounts of trisaccharides were produced in the reaction with HaG than in that with AnG (Fig. 3-8b). Such an efficient production rate and yield of αGG, with few byproducts, is a very attractive property of HaG. The transglucosylation reaction for glycerol was carried out with the enzymes considerably small amount (0.04 U/mL) to distinguish the effects of activator and the differences of HaG and AnG. It should be noted that the length of reaction time can be shortened if the amount of enzymes is increased (data not shown).

Figures and Tables

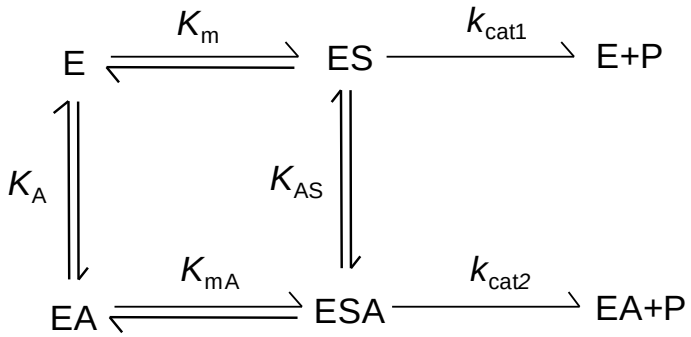

Fig. 3-1. Kinetic model for the reaction activated by a non-essential activator.

E, S, P, and A indicate enzyme, substrate, product, and activator, respectively. K_m and K_{mA} denote the dissociation constants for the ES complex and ESA ternary complex, respectively, to EA. K_A and K_{AS} are the dissociation constants for the EA complex and ESA ternary complex, respectively, to ES. k_{cat1} and k_{cat2} are rate constants in the absence and presence, respectively, of an activator.

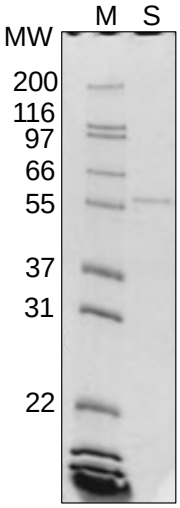

Fig. 3-2. SDS-PAGE of purified HaG.

M, size marker; S, purified HaG (58 kDa).

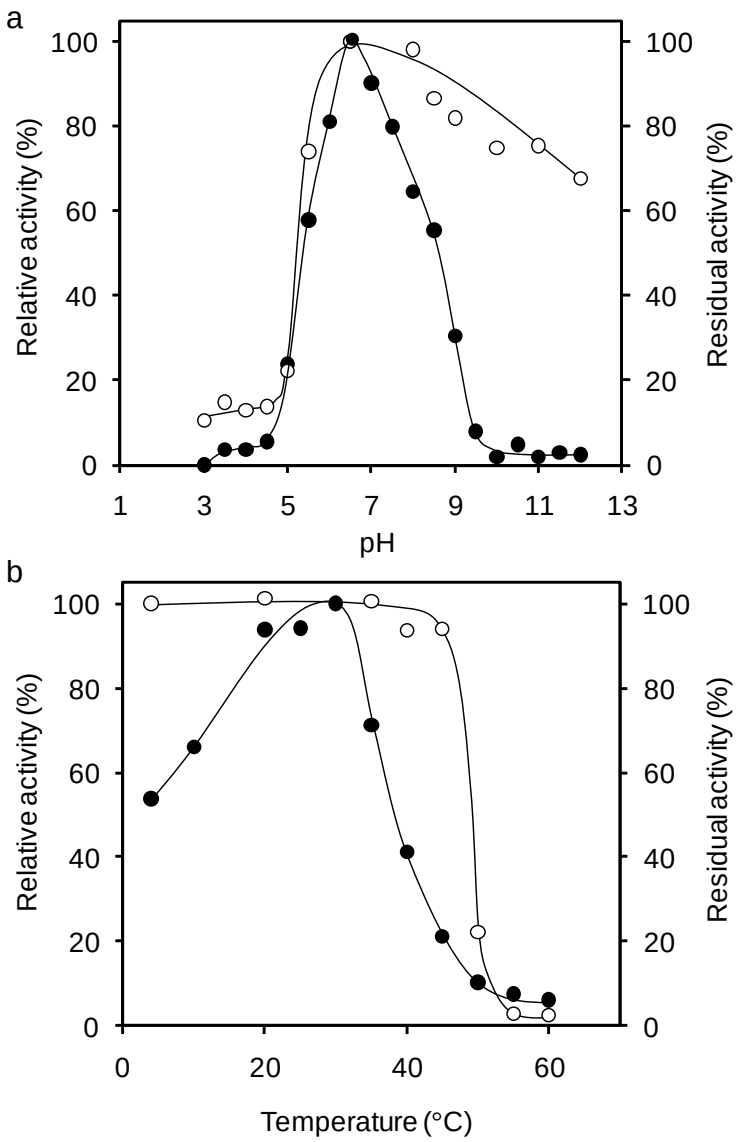

Fig. 3-3. Effects of pH and temperature on activity and stability of HaG.

a, Effects of pH. Solid and open circles indicate relative activity and residual activity after 24 h treatment at 4ºC, respectively. The activity at pH 6.5 was regarded to be 100% in relative activity. The activity before pH treatment was 100% in residual activity.

b, Effects of temperature. Solid and open circles indicate the relative activity and residual activity after heat treatment for 15 min at pH 7.0, respectively. The activity at 30˚C was regarded to be 100% in relative activity. The activity before heat treatment was 100% in residual activity.

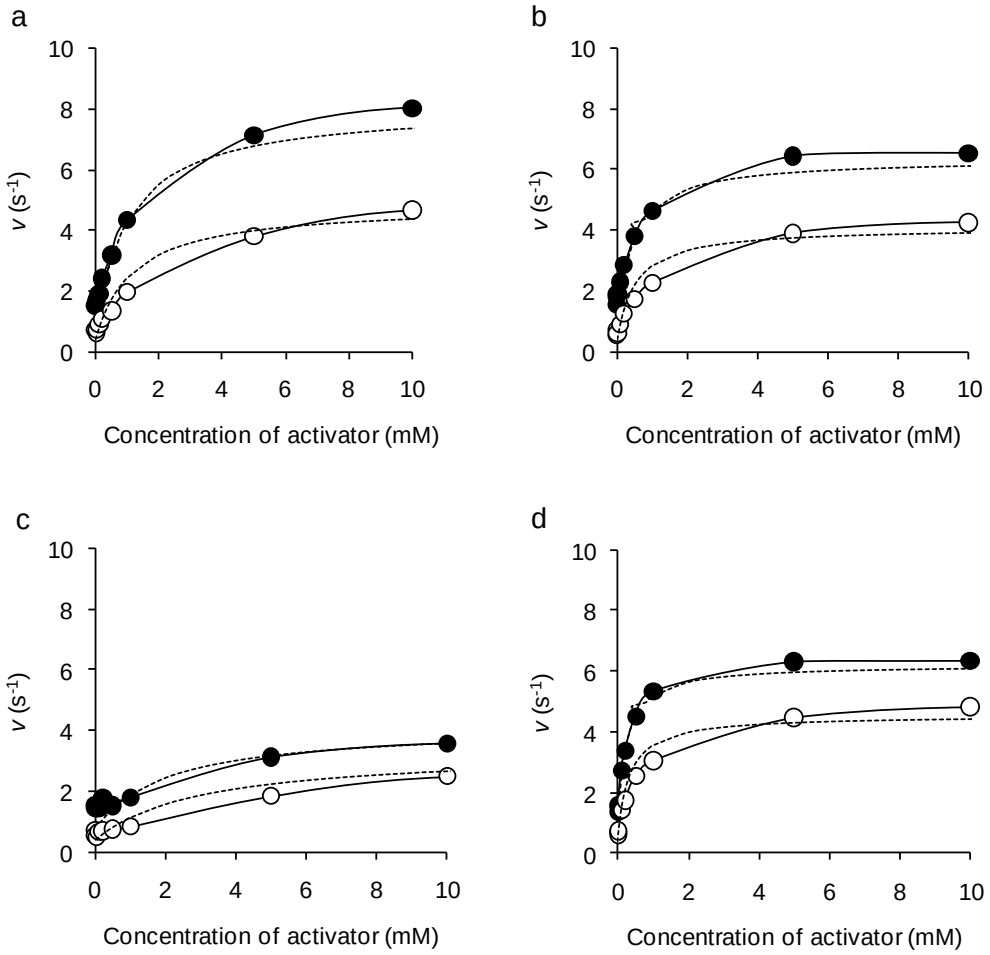

Fig. 3-4. Activator–reaction rate plots for hydrolysis of maltose.
Reaction rates for 4.5 mM (open circle) and 50 mM (solid circle) maltose were measured in the presence of various concentrations of monovalent cations. The averages of at least two measurements less than 5% standard deviation were shown. Theoretical lines (dotted line) were drawn based on Equation 1 and measured kinetic parameters. a, K^+; b, Rb^+; c, Cs^+, and d, NH_4^+.

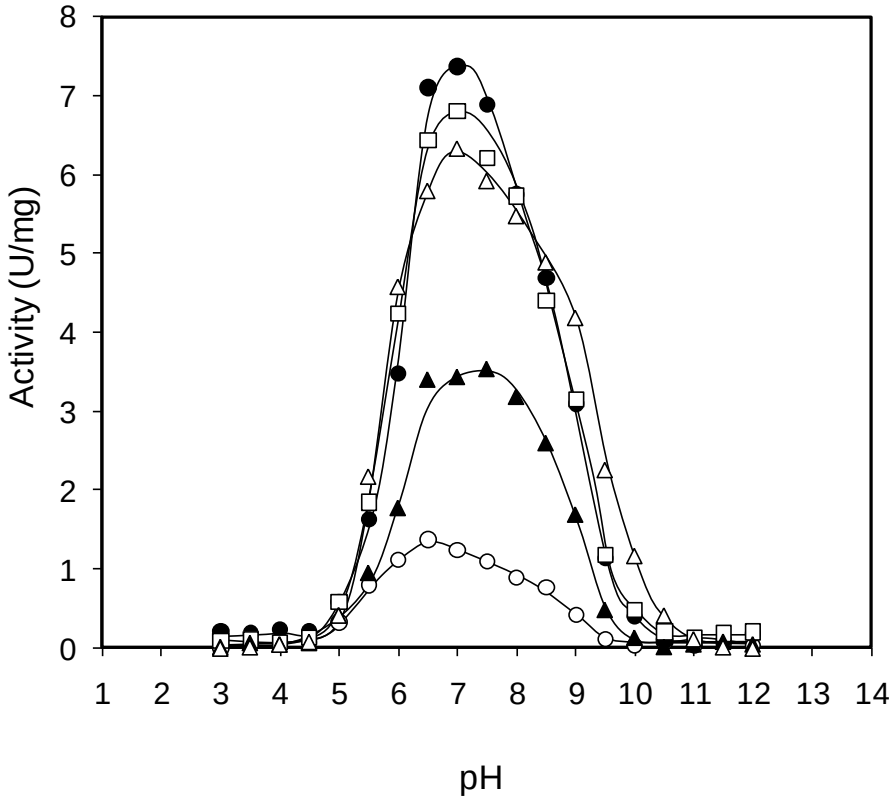

Fig. 3-5. pH–activity profiles of HaG in the presence of 10 mM monovalent cations.

Enzyme activity was assayed at various pH values. The averages of at least two measurements less than 5% standard deviation were shown. Open circle, no monovalent cation; solid circle, K^+; open triangle, Rb^+ ; solid triangle, Cs^+; and open square, NH_4^+.

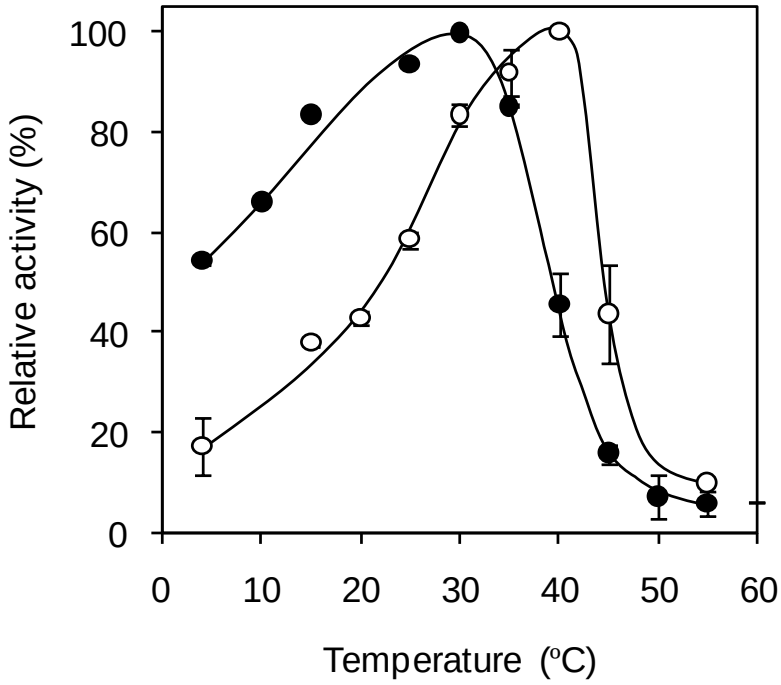

Fig.3-6. NH_4^+ effect on temperature–activity curve of HaG.
Enzyme activity was measured at various temperatures in the absence or presence of 10 mM NH_4^+. The activities at 30°C and 40°C in the presence and absence, respectively, of NH_4^+were regarded as 100%. The averages on at least two measurements were shown. Solid and open circles indicate HaG activity measured in the presence of 0 and 10 mM NH_4^+, respectively.

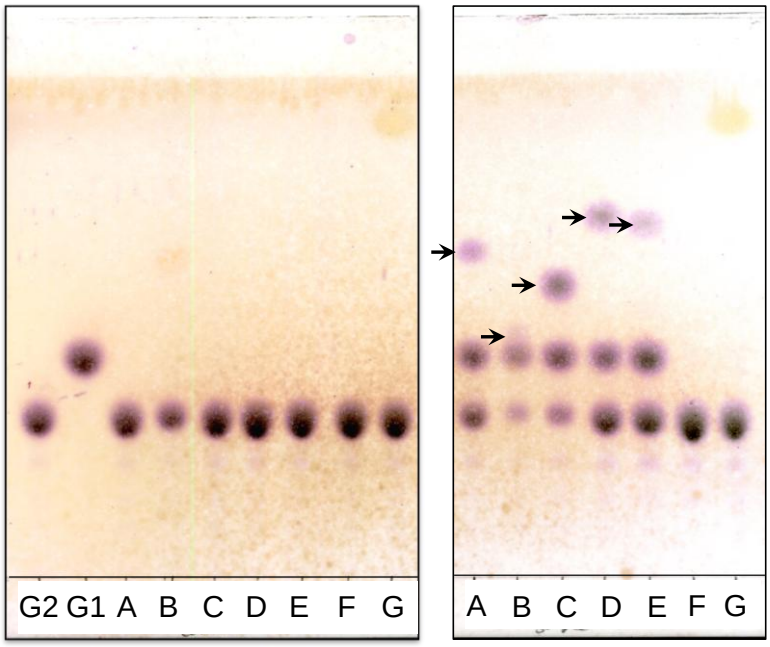

Fig. 3-7. Transglucosylate reaction by HaG towards various alcohols.
The 10-fold diluted mixtures before and after reaction (left and right, respectively) were analyzed. The enzymatic products are indicated by arrows. G2 and G1 denote maltose and glucose standard respectively. A, ethanol; B, glycerol; C, propylene glycol; D, 1-propanol; E, 2-propanol; F, 1-butanol; G, benzyl alcohol

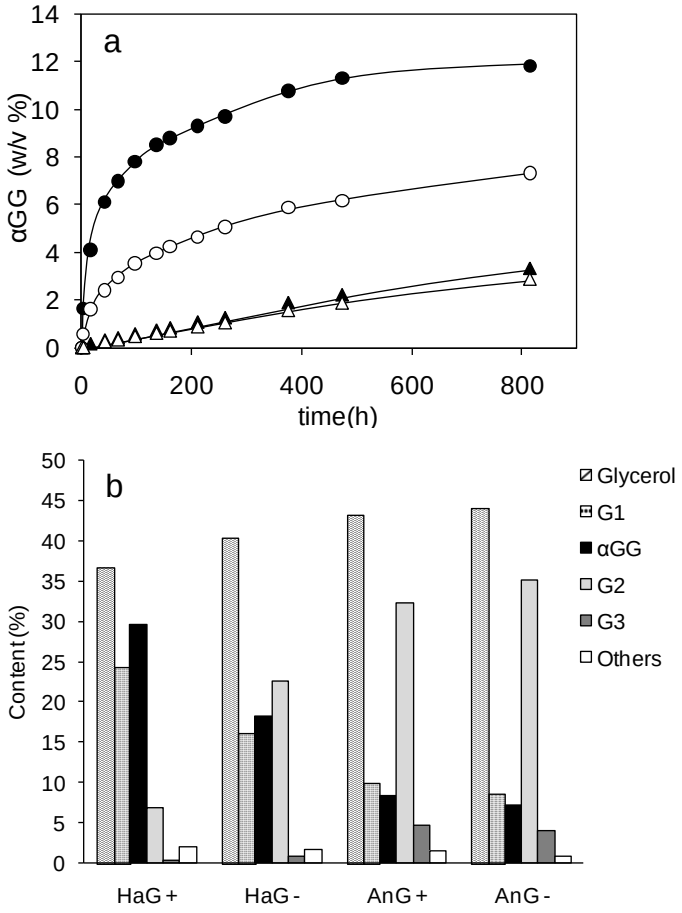

Fig. 3-8. Enzymatic synthesis of αGG.

a, Time-course of production of αGG. αGG (%, w/v) produced in the reaction mixture with 200 g/L maltose, 200 g/L glycerol, and 0.04 U/mL enzymes. Open and solid circles indicate the reaction with purified HaG in the absence and presence of 10 mM NH_4^+, respectively. Open and solid triangles are those with α-glucosidase from *A. niger* (AnG).

b, Content (%, w/w) of carbohydrates at reaction time 816 h. Plus and minus denote the presence and absence of NH_4^+, respectively. The carbohydrate content is equivalent to the area percentage of the detector, i.e., the refractive index response, in HPLC analysis. G1: glucose, αGG, α-glucosylglycerol; G2: disaccharides; G3: trisaccharides.

Table 3-1. Summary of HaG purification steps.

Procedures	Total protein (mg)	Total activity (U)	Specific activity (U/mg)	Yield (%)	Purification (-fold)
Cell free extract	833	19.4	0.0234	100	1.00
DEAE-650M	24.8	2.21	0.0893	11.4	3.82
Butyl-650M	7.90	19.7	2.49	101	106
Ultrafiltration	6.54	7.07	1.08	36.4	46.2
Resource Q	0.922	1.09	1.19	5.63	50.9

Table 3-2. Hydrolytic rates of HaG for various substrates.

Substrate	Hydrolytic rate (s^{-1})	Relative hydrolytic activity (%)
Maltose	0.763	100
Isomaltose	0.016	1.1
Trehalose	0.024	2.6
Nigerose	0.032	4.2
Kojibiose	N. D.	N. D.
Maltotriose	0.040	5.3
Maltotetraose	N. D.	N. D.
Maltopentaose	N. D.	N. D.
Maltohexaose	N. D.	N. D.
Sucrose	0.253	33
Methyl-α-D-glucoside	N. D.	N. D.
Soluble starch	N. D.	N. D.
*p*NPG	0.439	57.5

N. D., not detectable

Reaction rates on 4 mM of each substrate (expect soluble starch was 0.2% w/v) is shown, where the activity to maltose is 100 for calculating relative activity.

Table 3-3. Effect of salts for the hydrolytic activity of HaG.

Salt	Relative activity (%)
LiCl	151
NaCl	116
KCl	601
RbCl	579
CsCl	332
NH_4Cl	548
$MgCl_2$	30
$CaCl_2$	20
$CoCl_2$	1
$ZnCl_2$	N.D.
$MnCl_2$	N.D.
$FeCl_2$	N.D.
CuCl	N.D.
$AgNO_3$	N.D.
$(NH_4)_2SO_4$*	545

The relative activities in the presence of 10 mM salts were shown. The hydrolytic activity towards maltose in the non-additive of any salt was considered as 100% of the relative activity.

N. D., not detectable; *, Concentration was adjusted 5 mM to make the molar concentration of NH_4^+ equal to that of NH_4Cl.

Table 3-4. Apparent kinetic parameters for maltose and *p*NPG in the absence or presence of monovalent cations.

Activator	Maltose				*p*NPG			
	k_{catapp} (s^{-1})	K_{mspp} (mM)	k_{catapp}/K_{mapp} (s^{-1} mM^{-1})	k_{catapp}/K_{mapp} (-fold)	k_{catapp} (s^{-1})	K_{mspp} (mM)	k_{catapp}/K_{mapp} (s^{-1} mM^{-1})	k_{catapp}/K_{mapp} (-fold)
None	0.80	4.50	0.18	1	1.00	4.64	0.22	1
K^+	7.43	2.06	3.61	20.3	4.36	0.021	209	969
Rb^+	6.73	1.92	3.51	19.7	3.29	0.017	193	893
Cs^+	5.23	2.88	1.82	10.2	1.55	0.019	80.2	372
NH_4^+	5.77	1.45	3.98	22.4	3.59	0.018	200	929

The hydrolysis rate was assayed in the presence of 10 mM activator (cation) at various substrate concentrations. Parameters were calculated by regressing the experimental data to Michaelis–Menten equation.

Table 3-5. Kinetic parameters for hydrolysis of maltose in non-essential activator model.

Activator	k_{cat1} (s^{-1})	k_{cat2} (s^{-1})	K_m (mM)	K_{mA} (mM)	K_A (mM)	K_{AS} (mM)
K^+	0.8	8.6	4.5	3.52	1.35	1.06
Rb^+	0.8	6.7	4.5	2.88	0.66	0.42
Cs^+	0.8	4.2	4.5	1.19	7.14	1.88
NH_4^+	0.8	6.4	4.5	1.86	0.54	0.22

Non-essential activator model is shown in Fig. 3-1.

Chapter 4. Cloning and sequence analysis of α-glucosidase from *Halomonas* sp. H11

4.1. Introduction

α-glucosidase from *Halomonas* sp. H11 (HaG) is a novel α-glucosidase that is capable of utilizing maltose and short chain alcohols, i. e., glycerol, ethanol, propylene glycol, 1-propanol and 2-propanol, as a glycosyl donor and acceptor, respectively, in transglucosylation (Chapter 3). In addition to the high transglucosylation ability, biochemical properties of HaG such as great stimulation by monovalent cations and extremely narrow hydrolyzing specificity for maltose or *p*NPG, are worth further researching. In this chapter, the cloning of the HaG gene and comparison of the amino acid sequence of HaG with the related enzymes are described.

4.2. Materials and methods

4.2.1. Analysis of N-terminal amino acid sequence

Purified α-glucosidase from *Halomonas* sp. H11 (HaG) on polyacrylamide gel was transferred to a poly vinylidene difluoride (PVDF) membrane (Immobilon-P^{SQ}, Millipore) using a semi-dry electroblotting apparatus (Bio-Rad). The protein band detected with Coomassie Brilliant Blue R-250 (Wako Pure Chemical Industries) was cut off and analyzed using a protein sequencer Procise 492cLC (Applied Biosystems).

4.2.2. Analysis of internal amino acid sequence

To determine the internal amino acid sequence, purified HaG was

digested by lysylendopeptidase as follows. The purified enzyme (55 μg) was dissolved in 100 μL of 20 mM Tris-HCl (pH 8.0) containing 8 M urea. Then 3 μL of 0.02% w/v lysylendopeptidase (Wako Pure Chemical Industries) was added, followed by incubating at 37°C overnight. The resultant peptides were separated by reverse-phase HPLC under the following conditions: column, ODS AS-303 (YMC, Kyoto, Japan); flow rate, 1 mL/min; column temperature, 40°C; detection, UV 215 nm; elution, linear gradient of 0–100% acetonitrile in 0.1% trifluoroacetic acid (TFA) for 60 min. Then the resulting peptides were sequenced with the protein sequencer as described above.

4.2.3. Cloning of the gene encoding α-glucosidase from *Halomonas* sp. H11

4.2.3.1. Cassette PCR

The cassette PCR protocol was adopted to obtain the HaG gene (Isegawa 1992). Chromosomal DNA of *Halomonas* sp. H11 was prepared using a previously described method (Sambrook 2001) and digested with *Sal*I or *Pst*I (Takara Bio) to connect cassette DNA fragments supplied by an LA PCR^{TM} *in vitro* cloning kit (Takara Bio). The resulting DNA fragments were used as a template in the PCR to amplify the regions including HaG gene. All the primers used in this section are listed in Table 4-1. *Ex*Taq polymerase (Takara Bio) and a set of primers, HAG-N1, designed on the basis of the N-terminal amino acid sequence of HaG, and primer CS1 corresponding to the cassette sequence, were used. To amplify the desired region specifically, nested PCR was performed with primers HAG-N2 and CS2. The amplified DNA fragment was

cloned into a pGEMT-Easy vector (Promega, Madison, WI, USA) with a Ligation Mighty Mix (Takara Bio) and the construction was introduced into *E. coli* DH5α by heat-shock. The white colonies grown on LB medium containing 100 μg/mL ampicillin, 0.1 mM isopropyl-l-thio-β-D-galactoside (IPTG), and 2 μg/ml X-gal (5-Bromo-4-Chloro-3-Indolyl-β-D-Galactoside) were separately examined by colony-directed PCR as described below. The PCR products were sequenced with primers HAG-F′3, HAG-F′4, HAG-F′5, HAG-F′6, HAG-R′1, HAG-R′4, pGEM-up-F, and pGEM-dn-R. Sequence analyses were performed using a dye terminator cycle-sequencing with quick start kit (Beckman Coulter, Inc., Brea, CA, USA) and a DNA sequencer, CEQ2000XL (Beckman Coulter). To obtain the remaining regions of the HaG gene, PCR was performed with two primer sets designed on the basis of the analyzed DNA sequence, HAG-I1 and CS1, and HAG-I2 and CSI. Nested PCR was followed by HAG-F′1 and CS2, and HAG-I3 and CS2, respectively. A homology search of complete HaG sequence was performed using the BLAST program (Altschul 1990). The predicted pI was calculated by the program of Compute pI of ExPASy Proteomics (http://ca.expasy.org/).

4.2.3.2. Colony directed PCR

E. coli transformant colony, picked by the tip of the toothpick and dissolved in 30 μL of sterilized water, was used as the PCR template. Reaction condition was as follows; A reaction mixture: template; 1 μL, 10x Ex Taq buffer; 2 μL, 2.5 mM dNTPs; 1.6 μL, 20 mM primers (pGEM-up-F and pGEM-dn-R) each; 0.4 μL, *Ex* Taq; 0.05 μL, and water; 15 μL, PCR program: first 94°C for 2 min,

and 30 cycles of 94°C for 30 s, 55°C for 30 s and 72°C for 2 min, then finally hold at 72°C for 3 min.

4.2.4. Recombinant expression in *E. coli*

Recombinant HaG was overexpressed by *E. coli* BL 21 (DE3) Codonplus™ RIL (Stratagene; La Jolla, CA, USA). HaG gene amplified with a set of primers, 5'-AAACATATGCAAGACAACATGATGTGGTG-3' (forward, *Nde*I site underlined) and 5'-AAACTCGAGTTAGGCAACCTGCATAAAGG-3' (reverse, *Xho*I site underlined), designed according to the determined HaG sequence, was cloned into an expression plasmid, pET22b (Merck, Darmstadt, Germany) via *Nde*I and *Xho*1 sites. The sequence was confirmed by the some primers corresponding to the verified HaG gene (Table 4-1), and primers 5'-ATATAGGCGCCAGCAACCGCACCTGT-3' and 5'-TAACCACCACACCCGCCGCGCTTAAT-3' which are complement to the vector sites. *E. coli* BL21 (DE3) – Codonplus™ RIL was transformed using the constructed expression plasmid, and the transformant was cultured in 3 mL of LB medium, supplemented with 100 μg/mL ampicillin, at 30 °C for 15 h. The resulting culture fluid (0.5 mL) was inoculated into 500 mL of the same medium. When A_{600} reached 0.5, 0.1 M IPTG (0.5 mL) was added to the culture (final concentration, 0.1 mM), and it was further incubated at 16 °C for 24 h. The cells were collected by centrifugation and disrupted by sonication in 20 mM HEPES-NaOH buffer (pH 7.0, buffer A), followed by centrifugation to remove the cell debris.

The recombinant HaG was purified by two-step column chromatography

of the crude extract. First, a DEAE 650M Toyopearl (Tosoh, Tokyo, Japan) column chromatograph (2.6 cm × 20 cm, 106 mL) was used; the adsorbed protein was eluted with a linear gradient of 0–0.5 M NaCl after elution of non-adsorbed protein with buffer A. Second, chromatography was carried out on a Buthyl 650M Toyopearl (Tosoh) column chromatograph (ϕ1.6 cm × 15 cm, 30 mL). Ammonium sulfate was added to the sample to give a final concentration of 1.5 M, and the sample was loaded onto the column. Non-adsorbed protein was eluted with buffer A containing 1.5 M ammonium sulfate, and adsorbed protein was eluted with a linear gradient of 1.5–0 M ammonium sulfate. The highly purified fractions were pooled and dialyzed against 5 mM HEPES-NaOH buffer (pH 7.0). The purity of the sample was checked by SDS-PAGE.

4.2.5. General properties of recombinant enzyme

Substrate specificity, temperature-activity and stimulation by 10 mM monovalent cations i. e., K, NH_4^+, Rb^+ and Cs^+ were evaluated by the same methods as described in the previous chapter.

4.3. Results

4.3.1. Amino acid sequence analysis

The N-terminal amino acid sequence of purified HaG was MQDNM MWWRGGVIYQIYPRS. For the analysis of the internal amino acid sequence, 5 peptides were separately collected by reverse phase HPLC. Each of peptide had following N-terminal amino acid sequence; TLGAPEANPY, SVREIWMYIR, ALISMRQMLD, NHXVVMPDAN, and TLPDAEGEVG.

4.3.2. DNA sequence analysis

A whole HaG gene was obtained by the cassette PCR method with the primers designed based on the N-terminal amino acid sequences. The HaG gene consisted of 1617 bases and encoded 538 amino acids (Fig. 4-1). The theoretical molecular mass and pI were 61,139 Da and 4.75, respectively. The partial internal peptide sequence, TLGAPEANPY, was found in this sequence but not the other peptides. Four regions, I, II, III, and IV, conserved in the GH-family 13 enzymes, were found in the deduced amino acid sequence of HaG, namely, DQVISH, GFRLDTVNF, EIGD, and ATSNHD. HaG was therefore obviously classified into the GH-family 13. The sequence data for HaG is available from the DDBJ, with accession number AB663683. The amino acid sequence of HaG exhibited high identities, of the order of 87%, 79%, 78%, 69%, and 68%, to those of putative α-amylases (provably α-glucosidase) from *Halomonas*. sp. TD01 (GenBank ID, EGP19311), *Chromohalobacter salexigens* DSM 3043 (GenBank ID, ABE57826), *Halomona selongata* DSM 2581 (GenBank ID, CBV43561), *Marinomonas posidonica* IVIA-Po-181 (GenBank ID, AEF56441), and *Marinomonas* sp. MED121 (GenBank ID, EAQ64921), respectively (Table 4-3). Targeting to the validated proteins, HaG showed 60%, 58%, 57%, and 56% identities to α-glucosidase from *Xanthomonas campestris* WU-9701 (GenBank ID, BAC87873), oligo-1,6-glucosidase from *X. campestris* pv. raphani 756C (GenBank ID, AEL07660), oligo-1,6-glucosidase from *Pseudomonas stutzeri* DSM4166 (GenBank ID, AEA85435), and α-glucosidase from *Agrobacterium tumefaciens* F2 (GenBank ID, EGP58908), respectively. Identities to α-glucosidase from *Geobacillus* sp. HTA-462 (PDB code: 2ZE0)

(Shirai 2008), trehalulose synthase from *Pseudomonas mesoacidophia* (PDB code: 2PWH), oligo-1,6-glucosidase from *Bacillus cereus* (PDB code: 1UOK) (Watanabe 1997), and dextran glucosidase from *Streptococcus mutans* (PDB code: 2ZIC) (Hondoh 2008), all of whose crystal structures have been solved, were 36%, 35%, 33%, and 31%, respectively.

4.3.3. Expression, purification and characterization of recombinant enzyme

HaG was sufficiently expressed by *E. coli* in a soluble fraction and purified with the two step column chromatography (Table 4-2, Fig. 4-2). Using purified recombinant HaG, the substrate specificity, temperature-activity and effects of monovalent cations were determined. All of these properties matched those of the non-recombinant one (data not shown).

4.4. Discussion

In this chapter, the author determined the gene encoding HaG. Amino acid sequence of HaG contains the 4 conserved regions characteristic to GH-family 13 enzymes, thus it is obvious that HaG is classified into GH-family 13 like as many other bacterial α-glucosidases.

Based on multiple alignment, HaG was predicted to have a longer β → α loop 4, which is connecting β-strand 4 and α-helix 4, than other enzymes (Fig. 4-1). The length of the β → α loop 4 is the determinant of the specificity for substrate chain-length in GH-family 13 α-glucosidases and related enzymes such as oligo-1,6 glucosidase and dextran glucosidase (Saburi 2006). The shorter loop of dextran glucosidase, which forms open substrate binding sites to

accommodate long-chain substrates, has been shown to be associated with a high preference for long-chain substrates. Compared with the other α-glucosidases and oligo-1,6-glucosidase, HaG has an even longer β → α loop 4. The length of the putative β → α loop 4 of α-glucosidase from *X. campestris*WU-9701 (BAC87873), which hydrolyzes almost only maltose among maltooligosaccharide, as does HaG (Usami 2001), is the same as that of HaG. Such an unusually long β → α loop 4 might contribute to the narrow specificity for substrate chain-length in HaG.

HaG exhibited relatively high sequence identity (56%) to α-glucosidase from *A. tumefaciens* F2 (GenBank ID, EGP58908) which is stimulated by K^+, NH_4^+ and Rb^+, implying that these enzymes share a monovalent cation binding site structure and activation mechanism.

A sequence similarity search by BLAST showed that putative proteins with high similarities to HaG are distributed in moderate halophilic, marine (*Halomonas* sp. and *Marinomonas* sp.) and plant-pathogen-related (*Agrobacterium* sp. and *Xanthomonas* sp.) bacteria (Table 4-3, Fig. 4-1). In fact, all of these bacteria listed in table 4-3 are known to adapt to saline environment.

Some kinds of *Halomonas* sp. have been reported to exist at extreme ocean depths (Tamegai 2006, Sánchez-Porro 2010, Kaye 2004), and *Halomonas elongata* DMS 3043 is known to accumulate compatible solutes such as ectoine and betaine to balance high osmotic pressure (Wohlfarth 1990). αGG is also known to be accumulated as a compatible solute in cyanobacteria and some osmotolerant bacteria to adopt a high osmotic pressure. In cyanobacteria, the synthesis of αGG is carried out by two enzymes,

GG-phosphate synthase (EC 2.4.1.213) and GG-phosphate phosphatase (EC. 3.1.3.69), with glycerol 3-phosphate and ADP-glucose (Klähn 2011). As there is no report that α-glucosidases might be involved in the formation of αGG in any living organisms, and general task of α-glucosidase is producing glucose from α-glucoside for carbon source, I have yet no idea why HaG hydrolyzes maltose specifically and exhibits strong transglucosylation activity towards glycerol and some other alcohols. At least, the condition in which maltose and glycerol are each 200 g/L, as demonstrated for αGG synthesis in previous chapter, will be improbable in living cells. The physiological role of HaG should be investigated precisely. α-Glucosidases similar to HaG in marine bacteria are expected to have similar properties to HaG. Further investigation of the relations between enzymes and their environment is also required.

Figures and Tables

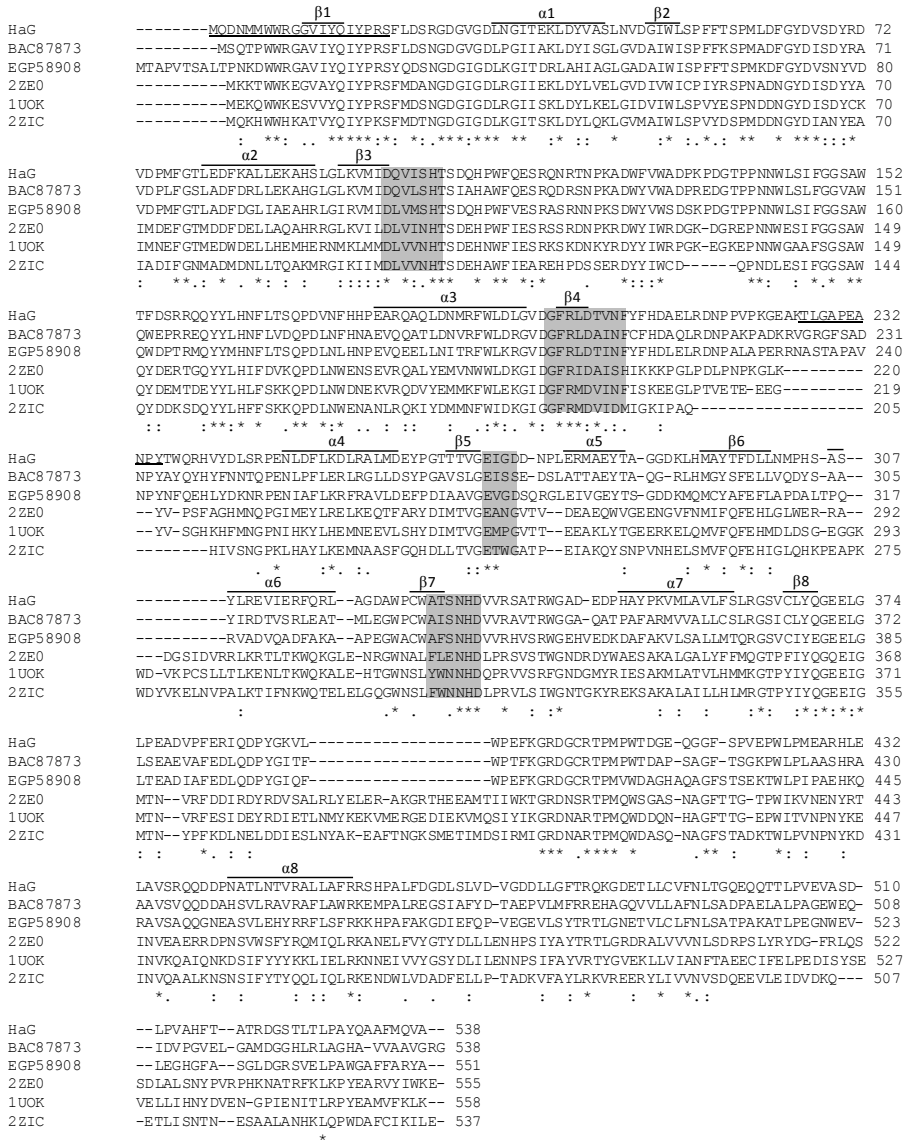

Fig. 4-1. Multiple alignment of amino acid sequence of HaG and some α-glucosidases.

Amino acid sequences of HaG and α-glucosidases from *Xanthomonas campestris* WU-9701 (Genbank ID: BAC87873), *Agrobacterium tumefaciens*F2 (Genbank ID: EGP58908), and *Geobacillus* sp. HTA-462 (PDB code: 2ZE0), oligo-1,6-glucosidase from *Bacillus cereus* (PDB code: 1UOK), and dextran glucosidase from *Streptococcus mutans*(PDB code: 2ZIC) were aligned using the Clustal Omega program (Sievers 2011, Goujon 2010). Asterisk, colon, and period indicate completely conserved, strongly similar, and weakly similar residues, respectively, as mentioned on the website (http://www.ebi.ac.uk/Tools/msa/clustalo/help/faq.html#23). α and β above the sequence represent the predicted α-helices and β-strand, respectively. Four conserved regions I, II, III, and IV, common in GH-family 13 are shaded. N-terminal and partial internal amino acid sequences analyzed by Edman degradation are underlined.

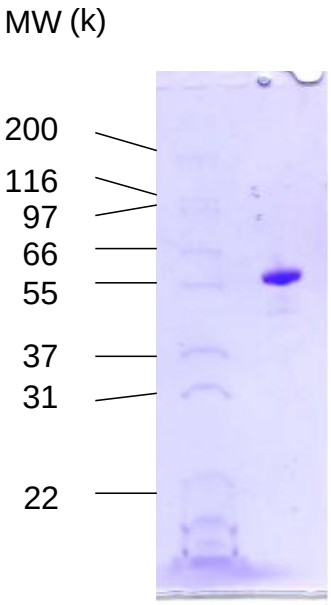

Fig. 4-2. Purified recombinant HaG.

Left, size marker; Right, purified recombinant HaG 1 μg.

Table 4-1. Primers used to identify HaG gene.

Primer	Sequence (5′-3′)
HAG-N1	ATGCARGAYAAYATGATGTGGTGG
CS1	GTTCATTTTTCATTCTCACA
HAG-I1	ACCAAGTGATCAGCCATACCTC
HAG-I2	TACGTCGCGGTAGTCACTCAC
HAG-N2	ATGATGTGGTGGCGNGGNGG
CS2	GTAATACGACTCACTATAGGG
HAG-F′1	AATCCTAAAGCCGACTGGTTCG
HAG-I3	ATAGCCAGATGCCGTCCAC
HAG-F′3	TACTATCTGCACAACTTCCTG
HAG-F′4	TCGACCTGCTCAACATGC
HAG-F′5	AACGCTTGGCAGGTGACG
HAG-F′6	TGGCGGTGCTGTTCTCACTG
HAG-R′1	ATGCCGTTCAGATCGCCTAC
HAG-R′4	TCGCTTCCGGTGCACCCAG
pGEM-up-F	TCCATTCGCCATTCAGGCTG
pGEM-dn-R	TTCCGGCTCGTATGTTGTGTG

Table 4-2. Purification steps of the recombinant HaG.

Step	Total protein (mg)	Total activity (U)	Specific activity (U/mg)	Yield (%)	Purification (-fold)
Cell extract	89.1	83.3	0.93	100	1.00
DEAE 650M	54.0	374	6.93	60.6	7.41
Buthyl 650M	17.8	67.5*	3.79	20.0	4.06

*The activity was measured after dialyzation against 5 mM HEPES-NaOH buffer.

Table 4-3. The result of BLAST search for amino acid sequence of HaG.

Accession	Description	Identities (%)
---------	alpha-glucosidase [*Halomonas* sp. H11]	---
ZP_08637456.1	alpha amylase, catalytic region [*Halomonas* sp. TD01]	87
YP_572324.1	alpha amylase [*Chromohalobacter salexigens* DSM 3043]	79
YP_003898746.1	alpha amylase, catalytic region [*Halomonas elongata* DSM 2581]	78
YP_004483360.1	alpha amylase catalytic subunit [*Marinomonas posidonica* IVIA-Po-181]	69
ZP_01077046.1	alpha-glucosidase [*Marinomonas* sp. MED121]	68
YP_004315080.1	alpha amylase catalytic region [*Marinomonas mediterranea* MMB-1]	68
YP_001343171.1	alpha amylase catalytic subunit [*Marinomonas* sp. MWYL1] >	68
ZP_06053150.1	alpha amylase [*Grimontia hollisae* CIP 101886]	64
YP_431546.1	alpha-glucosidase [*Hahella chejuensis* KCTC 2396]	60
ZP_01116520.1	probable alpha-glucosidase [*Reinekea* sp. MED297]	64

Top 10 sequences with high identities to HaG are shown

Chapter 5. Enzymatic synthesis of α-glucosylated 6-gingerol

5.1. Introduction

To evaluate the utility of α-glucosidase from Halomonas sp. H11 (HaG), avairable α-glucosidases and CGTases, namely α-glucosidases from *Aspergillus niger*, *Aspergillus nidulans* ABPU1, *Acremonium strictum* and *Saccharomyces cerevisiae,* and cyclodextrin glucanotransferases (CGTases) from *Geobacillus stearothermophilus, Bacillus coagulans*, *Bacillus* sp. No. 38-2, and *Bacillus clarkii* 7364 are compared from the point of transglucosylation ability. Here, 6-gingerol is selected as a candidate for glucosylation acceptor as the following reasons.

Ginger (*Zingiber officinale*) is used worldwide as a spice, flavoring agent, and herbal medicine. The rhizome of ginger is known to be a rich source of biologically active compounds, including the main pungent principles, gingerols, which exist as a series of derivatives with alkyl chains of various lengths, of six to ten carbons. Gingerols have been identified as the major bioactive components in a fresh ginger rhizome. Among the various types of gingerols, 6-gingerol [(*S*)-5-hydroxy-1-(4-hydroxy-3-methoxyphenyl)decan-3-one] is one of the most active and abundant ingredient (Baranowski 1985, Govindarajan 1982), and its biological functions have been most investigated to date. It shows various pharmacological effects; e. g., promoting adiponectin expression and antitumor promotion (Isa 2008, Ju 2011). Thus, 6-gingerol has great potential for functional food and pharmaceutical applications. However, at acidic pHs and temperatures

above 60°C, 6-gingerol is reversibly dehydrated to form 6-shogaol, which is more lipophilic and pungent than 6-gingerol (Fig. 5-1). The presence of a β-hydroxy keto group in the structure makes 6-gingerol thermally labile and easy to dehydrate (Bhattarai 2001).

In this chapter, HaG, another four types of α-glucosidases and four CGTases from various microorganisms are evaluated as the biocatalysts for glucosylation of 6-gingerol. Surprisingly, a novel glucoside, α-glucosylated 6-gingerol is successfully synthesized only by using HaG. The synthesis, chemical structure and physical properties of glucosylated 6-gingerol are described.

5.2. Materials and methods

5.2.1. Enzymes

α-Glucosidases from *A. niger*, *A. strictum*, and *S. cerevisiae* were purchased from Amano Enzyme, Kirin Kyowa Foods (Tokyo, Japan), and Oriental Yeast (Tokyo, Japan), respectively. α-Glucosidase B from *A. nidulans* ABPU1, a kind gift from Dr. Kobayashi (Nagoya University), was prepared by a previously reported method (Kato 2002). The purified HaG expressed by *E. coli* was prepared as described previous chapter.

CGTase from *G. stearothermophilus* was supplied by Novozymes Japan (Chiba, Japan), and those from *B. coagulans*, *Bacillus* sp. No. 38-2, and *B. clarkii* 7364 were from Nihon Shokuhin Kako.

5.2.2. Enzyme assays

5.2.2.1. α-Glucosidase

The activity of α-glucosidases was measured as described in section 3.2.2. The buffers used were HEPES-NaOH buffer (pH 7.0) for HaG and α-glucosidases from *A. strictum*, and *S. cerevisiae*; Na-acetate buffer (pH 5.0) for those from *A. niger* and *A. nidulans*.

5.2.2.2. CGTase

A reaction mixture (1 mL) containing 9 mg/mL soluble starch (Nakalai Tesque, Kyoto, Japan), 50 mM K-phosphate buffer (pH 6.0), and an appropriate concentration of enzyme was incubated at 40°C for 10 min, and 2.5 mL of 40 mM NaOH was added to terminate the reaction. Then, an aliquot (0.3 mL) consisting of 250 μM Na_2CO_3 and 0.32 mM phenolphthalein was added to the mixture, and A_{550} was measured to determine the concentration of β-cyclodextrin produced. One unit of CGTase was defined as the amount of enzyme that produces 1 mg of β-cyclodextrin per minute.

5.2.3. Screening of enzymes for glucosylation of 6-gingerol

A reaction mixture (10 μL) containing 100 mg/mL donor substrate, 25 mg/mL 6-gingerol (Nakalai Tesque), 50 mM of the reaction buffer for optimum pH described above, and enzyme was incubated at 40°C for 24 h. The donor substrates for α-glucosidase and CGTase were maltose and a commercial dextrin, Pinedex #100 (dextrose equivalent, 4, Matsutani Chemical Industry, Hyogo, Japan), respectively. The amounts of enzymes added were 1.5 mU (α-glucosidase) and 5.0 mU (CGTase). The reaction product was assessed by

TLC. The reaction mixture was 10-fold diluted with methanol, and 1 µL of the obtained solution was spotted on a TLC plate. Development and visualization of the chromatogram were performed with the same method described in section 3.2.7.

5.2.4. Purification of 5-α-Glc-gingerol and 5-α-Mal-gingerol

The transglucosylation products were purified from 1 mL of HaG reaction mixture, of maltose (0.1 g, 0.3 mmol), 6-gingerol (25 mg, 0.085 mmol), 20 mM HEPES-NaOH (pH 7.0) and 0.15 U of HaG, using preparative TLC glass plates ($60F_{254}$, 2 mm, 200 mm × 200 mm, Merck). The amount of reaction mixture applied per plate was 0.5 mL. A solvent of chloroform:methanol:acetic acid = 80:20:5 (v/v/v) was used for purification of 5-α-Glc-gingerol, and 1-butanol:2-propanol:water = 2:2:1 (v/v/v) was used for 5-α-Mal-gingerol. The glucosylated products were extracted from the scraped silica using MeOH:water = 1:1 (v/v), and concentrated *in vacuo*. The sample, dissolved in water, was filtered with a 0.45 µm filter, and freeze-dried.

5.2.5. Structural analysis of glucosylated 6-gingerol

5.2.5.1. Mass Spectrometry

Mass analyses of 5-α-Glc-gingerol and 5-α-Mal-gingerol were performed by electro-spray ionization (ESI) in positive mode using an LCQ (Thermo Fisher Scientific, Waltham, MA, USA). The sample dissolved in 50% v/v MeOH (0.1 mg/mL) was injected directly into the instrument.

5.2.5.2. NMR

The ^{1}H- and ^{13}C-NMR spectra for 5-α-Glc-gingerol were recorded at

30°C using an AV400M digital NMR spectrometer (Bruker Biospin, Karlsruhe, Germany) in several modes, namely ^{1}H (400 MHz), ^{13}C (100 MHz), HH-COSY, HSQC, and HMBC. The sample was dissolved in D_2O (Nacalai Tesque) with 2,2,3,3-d_4-3-(trimethylsilyl)propionic acid sodium salt (Wako Pure Chemical Industries) as an internal reference.

5.2.5.3. Glucoamylase treatment

5-α-Mal-gingerol was treated with glucoamylase from *Rhizopus* sp. (Seikagaku) to presume the glucosidic linkages between the two glucose moieties linked to 6-gingerol. The reaction was carried out under the following conditions: 1 mg of freeze-dried sample with 40 mU glucoamylase, and 4 mM Na-acetate buffer (pH 5.0) (total 10 μL) were incubated at 40°C for 24 h, and a 1 μL aliquot was analyzed by TLC, as described in section 5.2.3. The enzymatic activity of glucoamylase was determined according to the manufacturer's instructions.

5.2.6. Time-course of production of 5-α-Glc-gingerol by α-Glucosidase from *Halomonas* sp. H11

A mixture (0.1 mL) of 1 M maltose, 0.1 M 6-gingerol, 20 mM HEPES-NaOH buffer (pH 7.0), and 0.18 U of HaG was incubated at 40°C. To activate the HaG, 5 mM $(NH_4)_2SO_4$ was included. The time-course of 6-gingerol consumption and 5-α-Glc-gingerol production was monitored by HPLC under the following conditions: column, YMC Pack Pro C18 AS-303 (4.6 mm × 250 mm, YMC, Kyoto, Japan); eluent, acetonitrile:water = 7:3 (v/v); column temperature, 30°C; flow rate, 1 mL/min; detection, A_{280}. The retention times for main analytes

were as follows; 5-α-Glc-gingerol, 2.6 min; 5-α-Glc-gingerol, 3.0 min; 6-gingerol, 4.6 min; and 6-shogaol, 7.8 min. The tentative concentration for each compound was determined from the A_{280} intensity ratios.

5.2.7. Determination of physical properties of 5-α-Glc-gingerol

5.2.7.1. UV-vis spectrum

Absorption UV-vis spectrum of 5-α-Glc-gingerol was measured by scanning the absorbance from 200 nm to 600 nm with a spectrophotometer (U-2900, Hitachi, Tokyo, Japan). A sample was dissolved (4.4 mM) in water.

5.2.7.2. Stability assay

To assess the stability of 5-α-Glc-gingerol under acidic and high temperature conditions, 1 mg of purified 5-α-Glc-gingerol was dissolved in 1 mL of a solution consisting of 0.1 M HCl and 50% v/v methanol, and incubated at 60°C or 80°C for 7 h. As a control, 6-gingerol was also treated by the same conditions. The decrease in the amount of each compound was measured by HPLC, as described in section 5.2.6. The standard of dehydration product of 6-gingerol, 6-shogaol, was purchased from Wako Pure Chemical Industries.

5.2.7.3. Digestibility assay of 5-α-Glc-gingerol

The digestibility of 5-α-Glc-gingerol by rat intestinal extract was evaluated. Rat intestinal acetone powder (Sigma-Aldrich; 50 mg) was suspended in 1 mL of water, and the resulting supernatant was used as the enzyme solution. 5-α-Glc-gingerol (1 mg, 2.0 μmol) dissolved in 10 μL of 0.5 M Na-phosphate buffer (pH 7.0) was mixed with 90 μL of enzyme solution and

incubated at 37°C. Then 1 μL of the reaction mixture was applied to a TLC plate and immediately dried to terminate the reaction. The TLC analysis was performed as described in section 5.2.3. The decrease in the amount of 5-α-Glc-gingerol was evaluated from the intensity of the spot.

5.3. Results

5.3.1. Glucosylation of 6-gingerol with various α-glucosidases and CGTases

The transglucosylation activities toward 6-gingerol of five kinds of α-glucosidases, namely from *Aspergillus niger*, *Aspergillus nidulans* ABPU1 (Kato 2002), *Acremonium strictum*, *Halomonas* sp. H11, and *Saccharomyces cerevisiae*, and four kinds of CGTases, namely from *Bacillus coagulans*, *Bacillus* sp. No. 38-2, *Bacillus clarkii* 7364 and *Geobacillus stearothermophilus*, were evaluated. Since 6-gingerol is water-insoluble and is an oil at the reaction temperature (40°C), addition of water-miscible co-solvents such as ethanol and methanol might facilitate solubilization of 6-gingerol in the reaction mixture (Bertrand 2006). However, some α-glucosidases are known to transfer glucosidic residues to alcohols to produce alkyl α-glucosides, so any co-solvents were not added to the reaction mixture. To assist the enzymatic reaction at the water/lipid interface, the solution was thoroughly mixed by vortex during the reaction. As shown by TLC analysis (Fig. 5-2), a spot with lower mobility than that of 6-gingerol, predicted to be a glucosylated 6-gingerol, was detected only in the reaction with HaG. In contrast to HaG, α-glucosidases from other origins produced oligosaccharides longer than trisaccharides, though 6-gingerol derivatives were not detected. Similarly, no glucosylated compounds derived

from 6-gingerol were observed in the reactions with CGTases. Among the nine enzymes tested, only HaG appeared to be applicable to the glucosylation of 6-gingerol.

5.3.2. Chemoenzymatic synthesis of glucosylated 6-gingerol by α-Glucosidase from *Halomonas* sp. H11

5.3.2.1. Structural analysis of the main product

The main product was purified to give a single spot on TLC analysis (Fig. 5-3). In mass spectrometry, a peak at $[M + Na]^+$ *m/z* 479.2 that corresponding to mono-glucosylated 6-gingerol: Calcd for $[C_{29}H_{46}O_{14}]$: *m/z* 479.5 $[M + Na]^+$, was found (Fig. 5-4 a). ^{1}H- and ^{13}C-NMR analyses, namely ^{1}H, ^{13}C, HH-COSY, HSQC, and HMBC, were performed to determine the pattern and the position of glucosylation of 6-gingerol. The chemical shifts of the product are listed in Table 5-1. The raw spectrum chromatograms for NMR are shown in supplemental Fig. 1. The proton intensities in the sugar and the 6-gingerol were consistent with a conjugated product, with one glucose per 6-gingerol molecule. In the ^{1}H-NMR data, a doublet signal at δ_H 5.00 was assignable as an anomeric proton of glucose. Its small coupling constant (J = 3.84 Hz) also suggested an α-glucosyl linkage to 6-gingerol. As correlations between H1'–C6 and H6–C1' were observed in HMBC, the glucosylated 6-gingerol produced by HaG was identified as a novel chemical compound, (*S*)-5-(*O*-α-d-glucopyranosyl)-1-(4-hydroxy-3-methoxyphenyl)decan-3-one (5-α-Glc-gingerol, Fig. 5-5).

No correlations of H1'–C14 or H14–C1' were detected by HMBC,

implying that HaG selectively transferred a glucosyl moiety to the 5-OH group, i.e., the OH of the β-hydroxy keto group, in 6-gingerol.

5.3.2.2. Time-course of production of 5-α-Glc-gingerol

The time-course of the transglucosylation to 6-gingerol by HaG was investigated using HPLC. As shown in Fig. 5-6, the production of 5-α-Glc-gingerol reached the maximum (yield based on 6-gingerol, 60%) at 6 h. The yield was not changed even if the reaction time was extended or the initial concentration of maltose or 6-gingerol was changed (data not shown).

5.3.2.3. Structural analysis of the minor product

An unknown product, which was predicted to be more hydrophilic than 5-α-Glc-gingerol, was detected by HPLC, although its production level was much lower than that of 5-α-Glc-gingerol (yield based on 6-gingerol, 10%, Fig. 5-6, square). It was purified with very small quantity and TLC showed the presence of a single component, R_f 0.67 [1-butanol:2-propanol:water = 2:2:1 (v/v/v)] (Fig. 5-7). In mass spectrometry, a peak at $[M + Na]^+$ *m/z* 641.2 that corresponding to di-glucosylated 6-gingerol: Calcd for $[C_{29}H_{46}O_{14}]$: *m/z* 641.7 $[M + Na]^+$, was found (Fig. 5-4 b).

As a result of glucoamylase treatment, glucose and putative 5-α-Glc-gingerol were detected by TLC analysis (Fig. 5-7). This suggested that the unknown product was (*S*)-5-[*O*-α-(4-*O*-α-D-glucopyranosyl-D-glucopyranosyl)]-1-(4-hydroxy-3-methoxy phenyl)decan-3-one (5-α-Mal-gingerol), namely the conjugate of maltose and

6-gingerol. Because glucoamylase efficiently digests α-1,4-glucosidic linkages almost exclusively, and HaG is highly specific for α-1,4-glucosidic linkages (Chapter 3).

5.3.3. Properties of 5-α-Glc-gingerol

5.3.3.1. Basic properties of 5-α-Glc-gingerol

5-α-Glc-gingerol was hydrophilic than 6-gingerol as its R_f value was 0.84 [1-butanol:2-propanol:water = 2:2:1 (v/v/v)] (Fig. 5-2). Purified, freeze-dried 5-α-Glc-gingerol was an orange powder (18 mg, 0.039 mmol, yield 46%, Fig. 5-8a), and this powder form was retained at least below 80°C, in contrast to 6-gingerol which is an oil above 30–32°C. 5-α-Glc-gingerol was water-soluble up to at least 43.8 mM, unlike 6-gingerol, which is essentially insoluble in water (Fig. 5-8b). The UV-vis spectrum of a 4.4 mM solution of 5-α-Glc-gingerol in water was measured. The λ_{max} 278 nm was almost the same as that of 6-gingerol (Fig. 5-9). The extinction coefficient was 231 mol^{-1} L cm^{-1}.

5.3.3.2. Stability for heat and acid

The stabilities of 6-gingerol and 5-α-Glc-gingerol at acidic pH and high temperature were compared. The remains of 6-gingerol and 5-α-Glc-gingerol after incubation in 0.1 M HCl (pH 1.2) were examined by HPLC. In the case of 5-α-Glc-gingerol, 82% remained even after incubation at 60°C for 7 h, whereas 47% of 6-gingerol was converted to a dehydration product, i.e., 6-shogaol, or degradation products (Fig. 5-10). After incubation at 80°C for 7 h, 11% of 6-gingerol and 26% of 5-α-Glc-gingerol remained. The main degradation

products of 5-α-Glc-gingerol were 6-gingerol and/or 6-shogaol, meant deglucosylation catalysed by acid (Fig. 5-11).

5.3.3.3. Stability for digestive enzymes

5-α-Glc-gingerol was not hydrolyzed by digestive enzymes from rat intestinal extract, suggesting that the glucosidic bond in 5-α-Glc-gingerol was resistant to rat intestinal α-glucosidase (Fig. 5-12).

5.4. Discussion

In this chapter, glucosylation of 6-gingerol using HaG and another four α-glucosidases and four CGTases from different sources were evaluated. Surprisingly only HaG could synthesize the glucosylated 6-gingerol among nine kinds of enzymes tested.

HaG has a very narrow hydrolytic specificity for smaller substrates such as maltose and *p*NPG, and does not react with maltooligosaccharides as an acceptor in transglucosylation (Chapter 3). In agreement with this observation, for the synthesis of glucoside of 6-gingerol in this chapter, HaG produced α-glucosylated 6-gingerol mainly but minimal quantities of maltooligosaccharides (Fig. 5-2); it was supposed that maltose could not serve as an acceptor molecule in transglucosylation, and only 6-gingerol could access the acceptor site of HaG to produce α-glucosylated 6-gingerol. It seems that the preference of HaG for small acceptor substrates may be one of the key factors in its efficient glucosylation of 6-gingerol.

In the TLC result of the other α-glucosidases tested, the existence of

maltooligosaccharides indicates that the all these enzymes were active and maltose was just preferred over 6-gingerol as an acceptor substrate for their transglucosylation (Fig. 5-2). Although the interaction between 6-gingerol and these enzymes has not been elucidated yet, 6-gingerol is expected to be a very poor acceptor because these α-glucosidases expect HaG favor the glucosyl framework at their acceptor pocket, subsite +1 and +2 (Chiba 1997, Chiba 1988). Of the enzymes used, HaG and α-glucosidases from *S. cerevisiae*, which have 37% amino acid sequence identity, are most similar genetically each other (Cantarel 2009). However, it was found that their transglucosylation abilities toward 6-gingerol are different. α-Glucosidase from *S. cerevisiae* mainly produced maltotrisaccharide sugars (Fig. 5-2), indicating that the enzyme tends to use maltose as a glucosyl donor but also as an acceptor, whereas HaG only uses maltose as a donor.

No glucosylated compounds derived from 6-gingerol were observed in the reactions with CGTases. This can also be explained by the precedence of acceptor substrates for CGTases. CGTases have +1 to +3 subsites for acceptor binding site which are preferable to the glucosyl framework (Leemhuis 2010). Dextrin used as a glucosyl donor substrate should be a significantly better acceptor than 6-gingerol is.

To our knowledge, the synthesized glucoside, 5-α-Glc-gingerol is a novel compound. It is noteworthy that regioisomers glucosylated at the phenolic OH of 6-gingerol were not synthesized using HaG, although α-glucosidase from *Xanthomonas campestris* WU9701 and related enzymes, which show high sequence-identity with HaG (around 60%), transfer a glucosyl residue to the

phenolic OH group of some chemical compounds such as benzene-1,4-diol (hydroquinone) and (2*R*,3*S*)-2-(3,4-dihydroxyphenyl)-3,4-dihydro-2*H*-chromene-3,5,7-triol [(+)-catechin] (Kurosu 2002, Sato 2000). In spite of their high sequence identity, recognition of the acceptor substrate in HaG and that in α-glucosidase from *X. campestris* WU9701 are obviously different in terms of the OH group to which the glucose residue is transferred. Three-dimensional structural analyses of these enzymes are required to obtain a more detailed understanding. 5-α-Glc-gingerol is a novel compound, and this is the first report of enzymatic glucosylation of 6-gingerol. In chapter 3, HaG was revealed to have strong glucosylation activity toward glycerol and some alcohols. It seems that the OH group in an alkyl chain is a good acceptor for HaG.

The minor product, 5-α-Mal-gingerol which is also a novel compound, might be generated by additional glucosylation of the dominant product, 5-α-Glc-gingerol. There is no room for the possibility that the maltose residue is linked to the phenolic OH of 6-gingerol because no glucosylation at the phenolic OH occurred with HaG. 5-α-Mal-gingerol can be digested to 5-α-Glc-gingerol and glucose by glucoamylase; therefore the yield of 5-α-Glc-gingerol can be improved by glucoamylase treatment.

The glucosylation of water-insoluble compounds is important as it significantly increases their solubility in water. Accordingly, 5-α-Glc-gingerol is water-soluble although the precise solubility could not be determined in this research due to very few yield of purified 5-α-Glc-gingerol (Fig. 5-8).

In stability test, 5-α-Glc-gingerol was predominantly stable against heat

and acid (Fig. 5-10, Fig. 5-11). The presence of a β-hydroxy keto group in 6-gingerol is thought to be the main cause of its thermal lability (Bhattarai 2001). Hence, glucosylation at the OH group of the β-hydroxy keto group in 6-gingerol prevents dehydration, resulting in higher stability against acid and heat.

5-α-Glc-gingerol appeared to be resistant to the digestive enzymes from rat intestine (Fig. 5-12). However, since this was just an *in vitro* examination, and did not take account of factors such as the effects of intestinal flora, precise digestibility evaluation should be undertaken *in vivo*. Additionally, it is not as yet certain whether 5-α-Glc-gingerol can fulfill the same physiological functions as 6-gingerol, so physiological functions of 5-α-Glc-gingerol should also be investigated and compared with those of 6-gingerol to evaluate improvements in the physiological functions of 6-gingerol as a result of glucosylation.

Figures and Tables

a

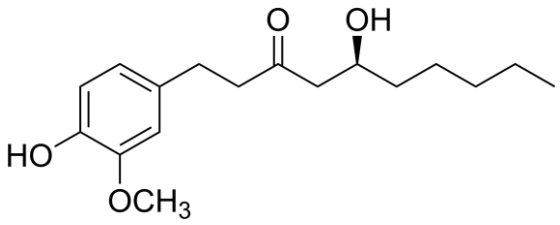

b

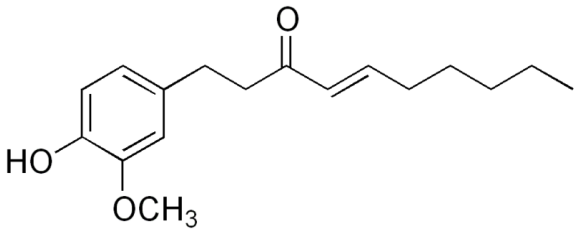

Fig. 5-1. Chemical structures of 6-gingerol (a) and 6-shogaol (b).

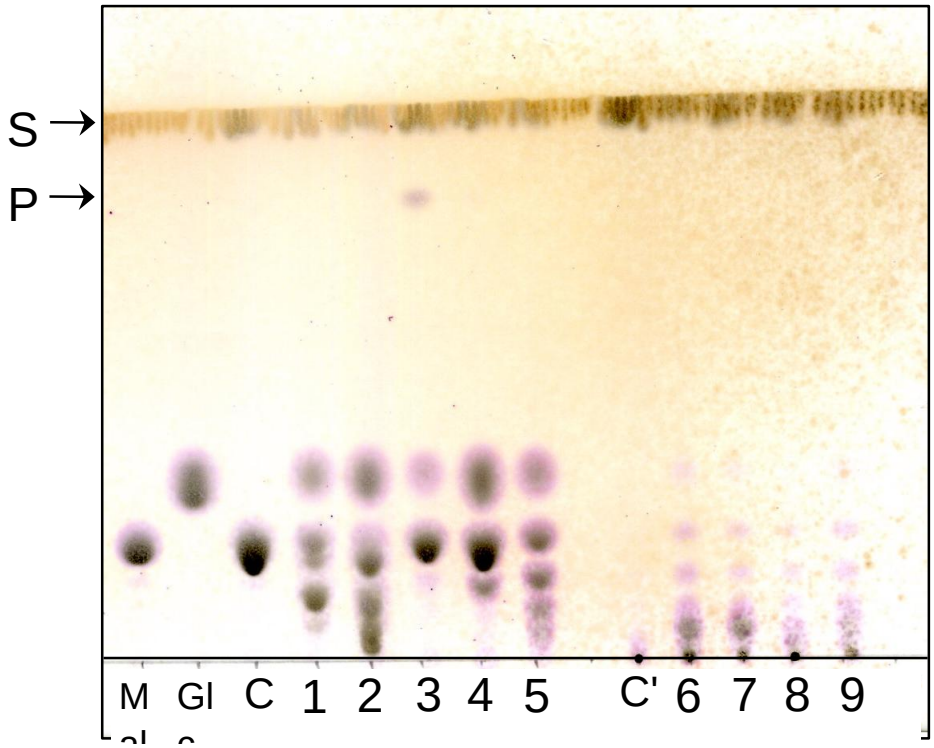

Fig. 5-2. Evaluation by thin-layer chromatography of transglucosylation abilities of various α-glucosidases and CGTases toward 6-gingerol.

Mal, maltose; Glc, glucose; C, α-glucosidases control. The reactions using α-glucosidases from 1, *A. niger*; 2, *A. nidulans*; 3, *Halomonas* sp. H11; 4, *S. cerevisiae*; and 5, *A. strictum.* C', CGTases control. The reactions using CGTases from 6, *B*. *coagulans*; 7, *Bacillus* sp. No. 38-2; 8, *B*. *clarkii* 7364; and 9, *G*. *stearothermophilus*.

S and P at the left indicate substrate (6-gingerol) and enzymatic product derived from 6-gingerol (5-α-Glc-gingerol), respectively. Spots of lower mobility than maltose indicate maltooligosaccharides.

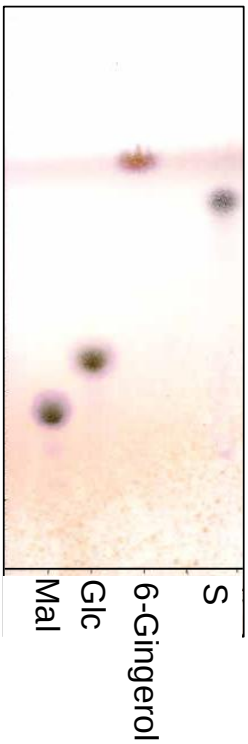

Fig. 5-3. TLC analysis of purified 5-α-Glc-gingerol.

Mal, Glc, and 6-gingerol indicate standard samples of glucose, maltose, and gingerol, respectively. S is purified 5-α-Glc-gingerol. The solvent system was 1-butanol:2-propanol:water = 2:2:1 (v/v/v).

a

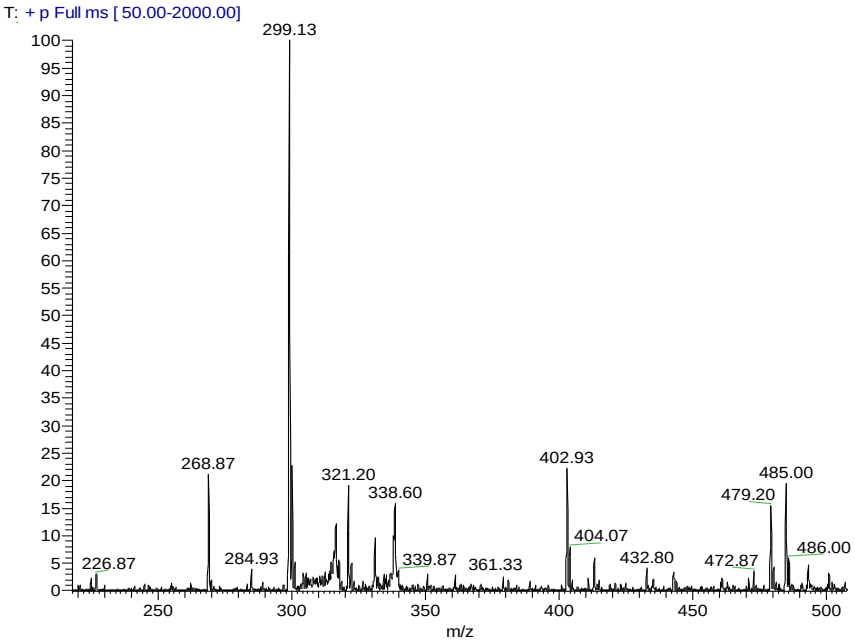

b

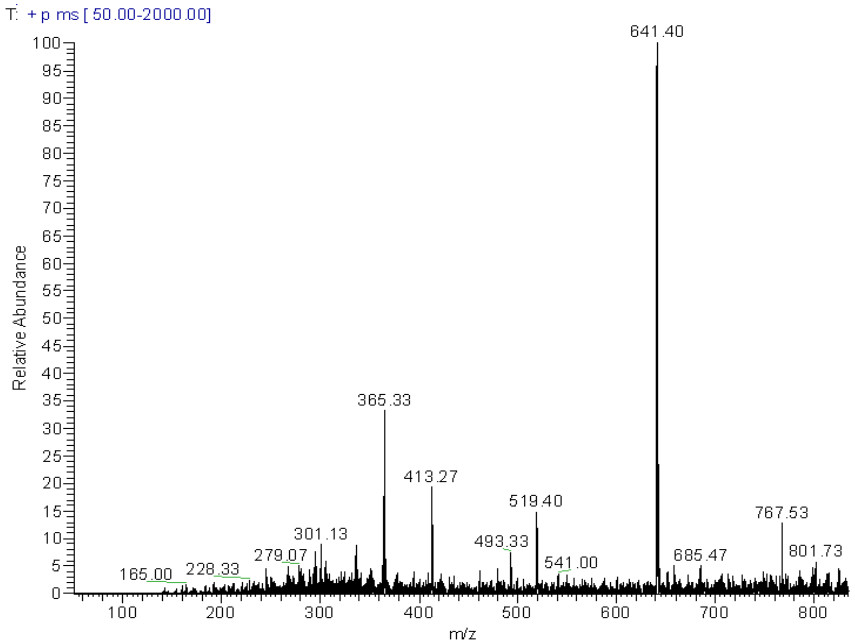

Fig. 5-4. Mass spectra of the products.

a) 5-α-Glc-gingerol. A peak at *m/z* 479.20 is correspond to the conjugate of glucose and 6-gingerol, b) The product predicted to be 5-α-Mal-gingerol (*m/z* 641.40)

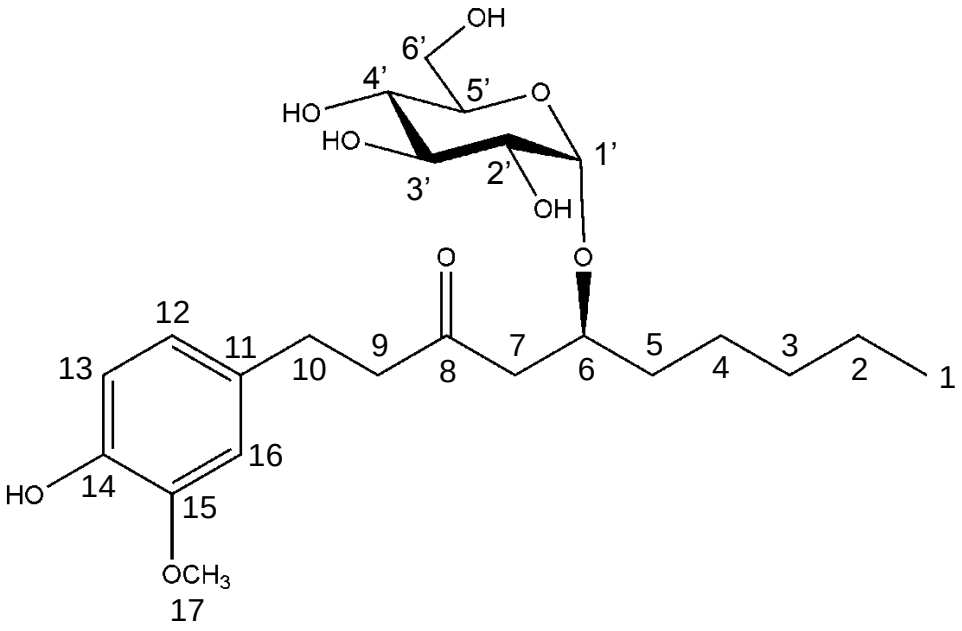

Fig. 5-5. Structure of the transglucosylated main product from 6-gingerol using HaG, (*S*)-5-(*O*-α-D-glucopyranosyl)-1-(4-hydroxy-3-methoxyphenyl)decan-3-one (5-α-Glc-gingerol).

The numbers shown correspond to the assigned NMR signals in Table 5-1.

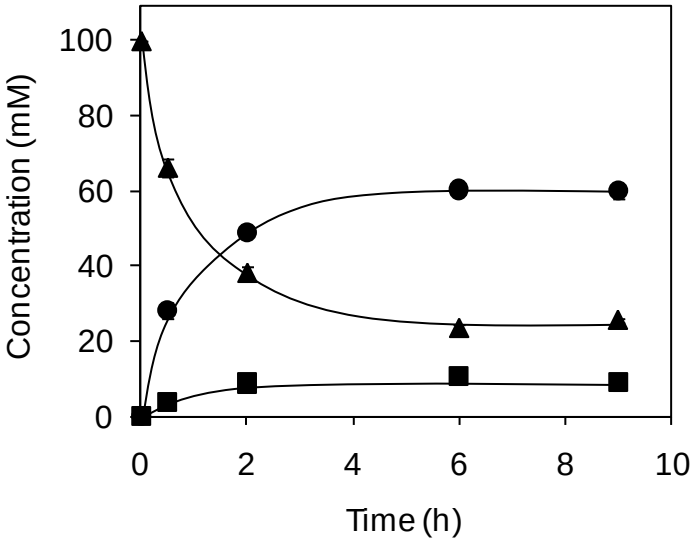

Fig. 5-6. Time-course of the production of 5-α-Glc-gingerol by HaG.
Circles, 5-α-Glc-gingerol; squares, 5-α-Mal-gingerol; and triangles, 6-gingerol. The temporary concentration was determined by HPLC from the A_{280} intensity ratios.

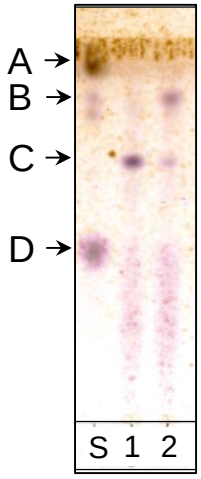

Fig. 5-7. TLC analysis of the minor product, 5-α-Mal-gingerol.

The minor product (5-α-Mal-gingerol) was treated with glucoamylase. S, standards of 6-gingerol (A), 5-α-Glc-gingerol (B), and glucose (D). 1, 5-α-Mal-gingerol (C) before glucoamylase treatment; 2, after the treatment.

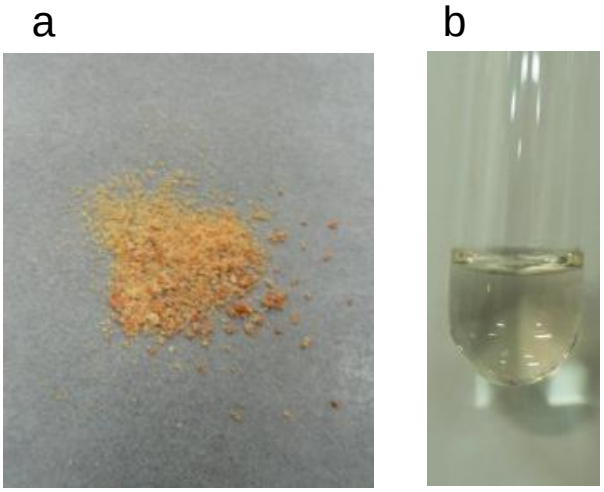

Fig. 5-8. Appearances of 5-α-Glc-gingerol.
a, Freeze-dried powder; b, 0.2% w/v solution in water

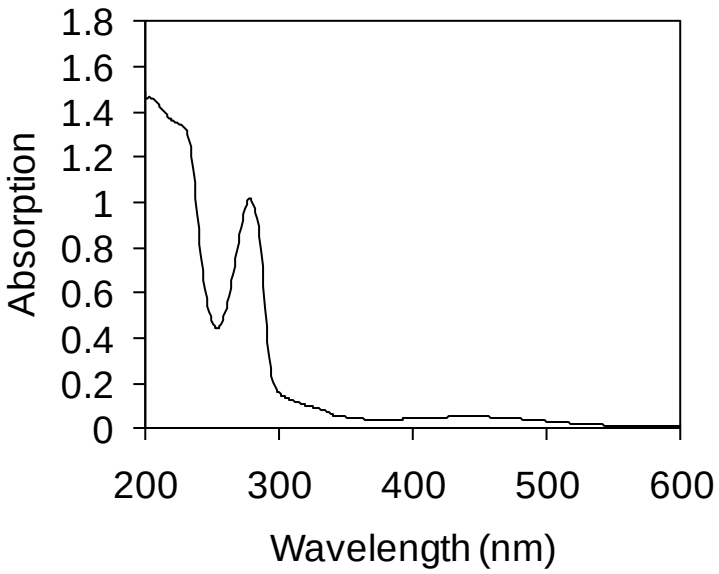

Fig. 5-9. UV-vis spectrum for 5-α-Glc-gingerol.

A sample was dissolved (4.4 mM) in water.

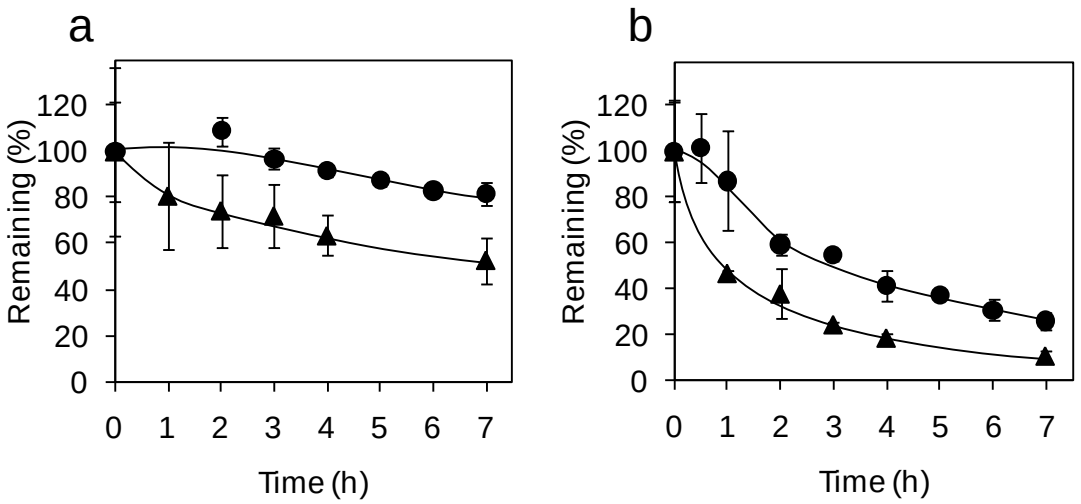

Fig. 5-10. Stability of 5-α-Glc-gingerol under acidic conditions and to heat. Stabilities of 5-α-Glc-gingerol and 6-gingerol in 0.1 M HCl were compared. Circles and triangles indicate 5-α-Glc-gingerol and 6-gingerol, respectively. a, 60°C and b, 80°C.

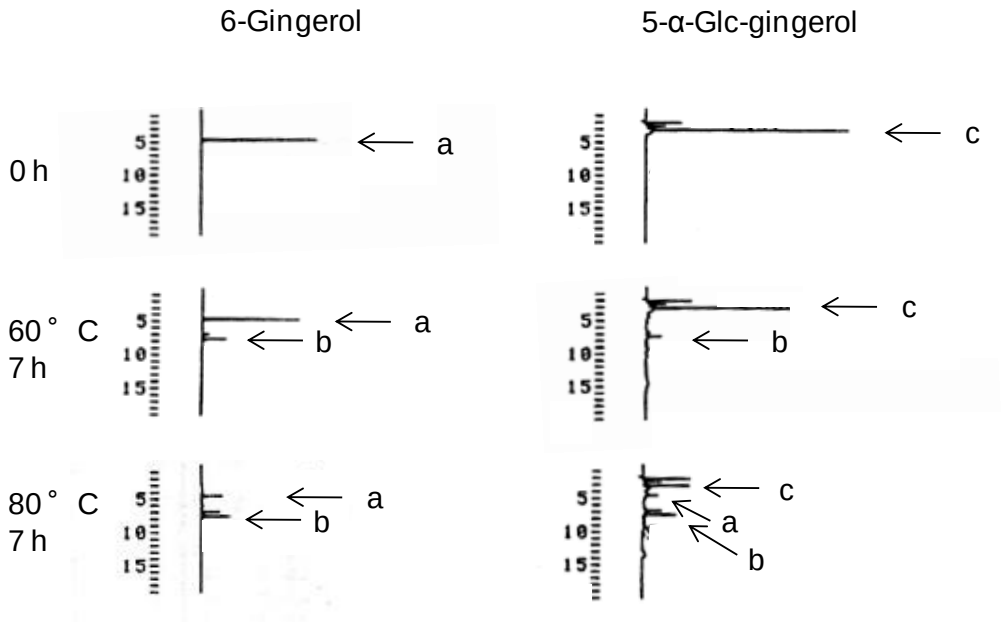

Fig. 5-11. HPLC chromatogram for the stability assay.
The traces of HPLC chromatograms are shown. 6-gingerol (a), 6-shogaol (b), and 5-α-Glc-gingerol (c) are indicated by arrows.

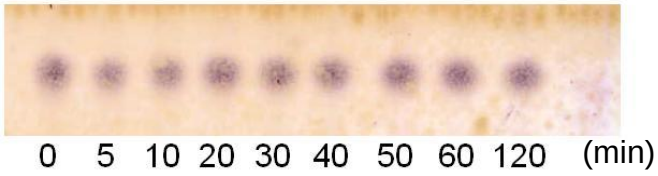

Fig. 5-12. Digestive test of 5-α-Glc-gingerol for rat intestinal enzymes.
The detected spots of 5-α-Glc-gingerol by TLC analysis were focused of which the same amounts of reaction samples were applied. The reaction time for digestion is indicated.

Table 5-1. ^{1}H- and ^{13}C-NMR spectral data for 5-α-Glc-gingerol.

No.	δ_C	δ_H (Mult. *J* Hz)
1	13.26	0.85 (3H, t, 6.90)
2	21.83	1.25 (2H, m)
3	23.55	1.22 (2H, t)
4	30.97	1.22 (2H, t)
5	32.41	1.53 (1H, m), 1.38 (1H, m)
6	74.16	4.05 (1H, m)
7	47.43	2.88 (1H, dd), 2.52 (1H, dd)
8	72.95	
9	44.66	2.95 (2H, d)
10	28.92	2.85 (2H, d)
11	133.56	
12	121.08	6.75 (1H, d, 8.04)
13	115.56	6.88 (1H, d, 8.04)
14	143.10	
15	147.36	
16	112.88	6.93 (1H, s)
17	56.01	3.85 (3H, s)
1′	96.57	5.00 (1H, d, 3.84)
2′	71.28	3.50 (1H, t)
3′	73.84	3.60 (1H, t)
4′	69.29	3.42 (1H, t)
5′	75.97	3.49 (1H, t)
6′	60.19	3.90 (1H, dd), 3.70 (1H, dd)

The spectrum was obtained in D_2O at 400 MHz (^{1}H-NMR) and 100 MHz (^{13}C-NMR).

J Values not listed in this table were not assignable owing to signal overlapping.

Chapter 6. Cloning and characterization of cellobiose 2-epimerases from aerobic bacteria

6.1. Introduction

Epilactose, a rare sugar found in alkaline-treated or heated milk (Martinez-Castro 1980, Martinez-Castro 1981), has beneficial potential for healthcare. Epilactose can be enzymatically synthesized from lactose by cellobiose 2-epimerase (CE). In spite of the beneficial biological functions of epilactose, utilization of CE for the industrial production of epilactose is significantly limited because known CEs are thermally unstable (around 30˚C; Ito 2008, Senoura 2009, Taguchi 2008). Additionally the reported CEs are all from unaerobic bacteria which are difficult to be cultured in a large scale.

In increasing genome information, many genes whose amino acid sequence similarities are around 40% to the reported CE from *Ruminococcus albus* (RaCE), but with unknown function, have been annotated as *N*-acylglucosamine 2-epimerase (AGE). In this chapter, such CE-like genes with unknown function, most of which are annotated as AGEs, are investigated. The author picks eight CE-like genes from aerobic bacteria, that is, *Chitinophaga pinensis* NBRC 15968, *Flavobacterium johnsoniae* NBRC 14942, *Pedobacter heparinus* NBRC 12017, *Dyadobacter fermentans* ATCC700827, *Herpetosiphon aurantiacus* ATCC23779, *Saccharophagus degradans* ATCC43961, *Spirosoma linguale* ATCC33905 and *Teredinibacter turnerae* ATCC39867. Each gene is cloned and recombinant proteins expressed by *E. coli* are characterized.

6.2. Materials and methods

6.2.1. Bacterial strains

C. pinensis NBRC 15968, *F. johnsoniae* NBRC 14942 and *P. heparinus* NBRC 12017 were provided by the National Institute of Technology and Evaluation Biological Resource Center (Chiba, Japan). *D. fermentans* ATCC700827, *H. aurantiacus* ATCC23779, *S. degradans* ATCC43961, *S. linguale* ATCC33905 and *T. turnerae* ATCC39867 were from the American Type Culture Collection. All the bacteria were aerobically cultured according to the supplier's instructions. *E. coli* DH5α and *E. coli* BL21 (DE3)-Codonplus-RIL were used for the preparation of expression plasmids and the production of recombinant proteins, respectively.

6.2.2. Construction of the expression plasmids

6.2.2.1. Genome sequenced strains

The following CE-like genes of the indicated bacteria whose genome sequences are available, were obtained by PCR: *C. pinensis*, NCBI reference sequence YP_003125030; *D. fermentans*, YP_003086363; *F. johnsoniae*, YP_001197274; *H. aurantiacus,* YP_001543663; *P. heparinus*, YP_003094236; *S. degradans*, YP_525984; *S. linguale*, YP_003385134; and *T. turnerae*, YP_003075376. Cells of each bacterium from 1 mL of culture fluid were suspended in 0.132 mL of 0.5 N NaOH and this was boiled for 10 min. Then the resulting mixture was neutralized by adding 32 μL of 2 M Tris-HCl buffer (pH 7.0) and used as the template in PCR to amplify the genes. PCR was performed using KOD Plus DNA polymerase (Toyobo). Primers used for cloning and

sequencing are listed in the Table 6-1. *Nde*I sites in the putative CE genes of *H. aurantiacus* and *T. turnerae* were deleted by the introduction of silent mutations by the overlapping PCR method (Ho et al., 1989). All target genes other than that of *T. turnerae* were cloned into *Nde*I and *Xho*I sites of the pET22b vector. The target gene of *T. turnerae* was cloned using the same vector, and the *Nde*I and *Eco*RI sites. Thirty-four nt in the CE-like genes of *T. turnerae* (nine amino acids in the deduced amino acid sequence) were different from the registered sequences. The sequence analyzed was deposited in the DNA Data Bank of Japan under the accession number AB719057.

6.2.3. Production and purification of the recombinant cellobiose 2-epimerase-like proteins

Transformants of *E. coli* BL21 (DE3)-Codonplus-RIL harboring each expression plasmid were cultured in 0.5 L of LB medium containing 100 μg/mL of ampicillin at 30°C until the A_{600} reached 0.5. One-hundred millimolar IPTG was added to a final concentration of 0.1 mM, and cell culturing was continued at 16°C for 24 h. Bacterial cells, harvested by centrifugation, were suspended in 20 mL of 20 mM Na-phosphate buffer (pH 7.0, buffer A) and disrupted by sonication. The cell-free extract was obtained by centrifugation. Each of extract was applied to a DEAE Toyopearl 650M column (ϕ1.6 × 15 cm, Tosoh, Tokyo), equilibrated with buffer A. Adsorbed protein was eluted by a linear gradient of 0–0.5 M NaCl (total elution volume, 120 mL). The pooled fractions were dialyzed against 5 mM Na-phosphate buffer (pH 7.0, buffer B), and applied to a hydroxyapatite Bio-Gel HT column (ϕ1.6 × 10 cm, Bio-rad) equilibrated with buffer B. Adsorbed protein was eluted by a linear gradient of sodium phosphate buffer (pH 7.0) of 5–200 mM

(total elution volume, 60 mL). The purity of each fraction was analyzed by SDS-PAGE. Active fractions were pooled and concentrated to several mg/mL by ultrafiltration using Amicon Ultra-15 Centrifugal Unit (nominal molecular weight limit, 10 000; Millipore). The protein concentration was determined by the Bradford method (Bradford, 1976), in which BSA was used as the standard. An equal volume of glycerol was added to the purified samples for storage at −20 °C.

6.2.4. Substrate specificity and structural analysis of the reaction products

A reaction mixture of 20 μL, consisting of 10 μg/mL enzymes, 100 mM substrates and buffer A, was incubated at 30°C for 24 h. Glucose, galactose, lactose, epilactose, cellobiose, sophorose, mannose, cellotriose, laminaribiose, β-1,4-mannobiose, gentiobiose, maltose, GlcNAC and ManNAC were tested as substrates. One microliter of the aliquot was analyzed by TLC (Silica gel 60 F_{254}, Merck), in which the solvent system of 1-butanol:2-propanol:water (2:2:1, v/v/v) was used. The chromatogram was visualized by spraying 1.8 M sulfuric acid in methanol and heating.

The reaction products from lactose, epilactose, cellobiose and β-1,4-mannobiose were characterized. A reaction mixture of 0.7 mL, consisting of 100 mg/mL substrate, 100 μg/mL of enzyme and buffer A, was incubated at 30°C for 24 h. The reaction was terminated by boiling for 3 min and the products were purified by HPLC, as the following condition; column, Sugar SP0810 (ϕ8.0 x 300 mm; Shodex, Tokyo); column temperature, 80°C; eluent, water; flow rate, 0.8 mL/min; detection, refractive index. Authentic epilactose (Sigma-Aldrich) was

used as standard.

Chemical structures of the products produced by the *F. johnsoniae* CE-like protein (FjCE) were determined by ESI-MS and ^{13}C-NMR. ESI-MS was performed using an LCT Premier XE (Waters, Milford, MA) with positive mode. ^{13}C-NMR spectra were recorded at 25°C in D_2O with an Inova500 (125 MHz, Agilent, Santa Clara, CA). The peak arising from dioxane at 67.40 ppm was standardized. The structures of the oligosaccharides produced by the other enzymes were confirmed by monosaccharide analysis as follows. A mixture of 50 μL consisting of 2 mg/mL of the product and 2 M TFA was kept at 100°C for 3 h. The material was dried *in vacuo* and the residue was dissolved in 20 μL of water. One microliter of aliquot was analyzed by TLC, as described above. Comprised carbohydrates were detected using a detection reagent consisting of EtOH:sulfuric acid:acetic acid:anisaldehyde (92:3:2:3, v/v/v/v).

6.2.5. Enzyme assay

A reaction mixture of 1 mL consisting of an appropriate concentration of enzyme, 100 mM lactose and buffer A was incubated at 30°C for 10 min. The enzymatic reaction was terminated by adding 0.2 mL of 0.1 *N* HCl and boiling the sample for 3 min. As an internal standard, 0.3 mL of 5 mg/mL sorbitol was added, and the epilactose produced was measured by HPLC, as described in section 6.2.4.

6.2.6. Effects of pH and temperature

Optimum pH and temperature were determined by measuring the activity at various pH values (pH 3–13) and temperatures (25–55°C),

respectively. The Britton-Robinson buffer was used as the reaction buffer to vary the reaction pH. Temperature and pH stabilities were evaluated by measuring the residual activity after temperature and pH treatments, respectively. As temperature treatment, the enzyme was incubated at 25–55°C for 15 min. For pH treatment, the enzyme was kept in 10 mM Britton-Robinson buffer (pH 3-13) at 4°C for 24 h. The ranges in which the enzyme retained more than 90% of the original activity were considered as a stable range.

6.2.7. Kinetic analysis

Kinetic parameters for epimerization of lactose and cellobiose were determined by measuring the initial reaction rates toward 10–350 mM of the substrates and fitting the results to the Michaelis-Menten equation.

6.2.8. Phylogenetic analysis

Amino acid sequences of CEs and related enzymes including putative proteins (336 sequences) were collected by a sequence similarity search of RaCE with the BLAST and a phylogenetic tree was constructed by the Neighbor-Joining method (Saitou & Nei, 1986) with ClustalW (Thompson et al., 1994). The graphic was illustrated by MEGA 5.05 (Tamura et al., 2011).

6.3. Results

6.3.1. Purification of cellobiose 2-epimerase-like proteins

Recombinant CE-like proteins produced in *E. coli* were purified to homogeneity (Fig. 6-1). The amount of purified enzymes from a 0.5 L culture was 5.1–75.9 mg.

6.3.2. Substrate specificity and structural analysis of the reaction products

All the recombinant proteins, except *C*. *pinensis*, acted on cellobiose, lactose, epilactose and β-1,4-mannobiose (Fig. 6-2), whereas GlcNAC, ManNAC, D-glucose and D-mannose did not serve as substrates. Those from *S*. *degradans* (SdCE), *S*. *linguale* (SlCE), *H*. *aurantiacus* (HaCE), *T*. *turnerae* (TtCE) and *D. fermentans* (DfCE) also acted on cellotriose (Fig. 6-2). The cell-free extract of the *E. coli* transformant producing the CE-like protein from *C*. *pinensis* (CpCE) showed epimerization activity to lactose (data not shown). Consequently, CpCE was likely to have been inactivated during the purification process, presumably because of its instability.

Structures of the oligosaccharides produced from lactose, epilactose, cellobiose and β-1,4-mannobiose by FjCE were determined by ESI-MS and ^{13}C-NMR. All of the products gave a signal at 365.1 *m/z* $[M + Na]^+$, corresponding to disaccharides. Chemical shifts in ^{13}C-NMR analysis of the products from epilactose, cellobiose and β-1,4-mannobiose were coincident with values reported for lactose, Glc-Man and Man-Glc, respectively (Bock et al, 1984), and chemical shifts of the product from lactose were identical to the chemical shifts of authentic epilactose (Table 6-1). These results clearly indicated that FjCE catalyzes 2-epimerization of glucose or mannose residues at the reducing end of the substrates. The structures of the oligosaccharides produced by the other CE-like proteins were confirmed by analysis of the monosaccharide components (Fig. 6-3), because all the oligosaccharides showed similar mobility to the corresponding oligosaccharides produced by FjCE (Fig. 6-1). The reaction products derived from cellobiose, lactose, epilactose and β-1,4-mannobiose

were revealed to be composed of glucose/mannose, galactose/mannose, galactose/glucose, and glucose/mannose, respectively, indicating that all the CE-like proteins examined are also CEs.

6.3.3. Effects of pH and temperature

All the CEs, except for the *P. heparinus* CE (PhCE), showed the highest activity at weakly alkaline pH values as observed in most known CEs. In contrast, the optimum pH of activity for PhCE was 6.3 (Table 6-3). All the CEs showed high stability at alkaline pH, and DfCE, SlCE and TtCE were more stable at acidic pH when compared with the other enzymes. DfCE, HaCE and SlCE showed relatively high optimum temperature and thermostability.

6.3.4. Kinetic analysis

DfCE, HaCE, SdCE and SlCE showed 2.5–4.8-fold higher k_{cat}/K_m to cellobiose than to lactose (Table 6-4); this observation is similar to that observed for RaCE, BfCE and EcCE. In contrast, the k_{cat}/K_m values towards both substrates for the enzymes FjCE, PhCE and TtCE were similar. DfCE, SlCE and TtCE showed significantly high k_{cat} and K_m values, which were not observed for the other enzymes examined herein or previously reported enzymes.

6.3.5. Phylogenetic analysis of CE and related proteins

A phylogenetic tree of CE and related proteins, AGEs, aldose-ketose isomerases (AKI), and mannose 6-phosphate isomerases(PMI) was constructed (Fig. 6-4). These proteins were divided into four groups. CE and AGE were clearly classified into different groups. All the CEs, characterized so far, are

found in the CE cluster. CsCE which also catalyzes monosaccharide isomerization and epimerization (Park et al., 2011) is closely related to RaCE.

6.4. Discussion

CE-like genes from various aerobic bacteria, namely *C. pinensis* NBRC 15968, *F. johnsoniae* NBRC 14942, *P. heparinus* NBRC 12017, *D. fermentans* ATCC700827, *H. aurantiacus* ATCC23779, *S. degradans* ATCC43961, *S. linguale* ATCC33905 and *T. turnerae* ATCC39867 were annotated as AGE based on the sequence information. In this study all of them have been revealed to be CE but not AGE. This is the first report documenting CE activity in aerobic bacteria.

Thermotolerant CE is attractive for the industrial production of epilactose from lactose. Some CEs in this study are stable at a moderate high temperature and a broad range of pH (Table 6-3). High k_{cat} is also convenient because it critically determine the reaction rate in the high concentration of substrate usually adopted in bioprocess. For these reasons, DfCE and SlCE are most suitable as the catalysts for the synthesis of epilactose. However their thermotolerance is even not enough to stand the industrial process in which the temperature is usually kept over 50°C.

The phylogenetic analysis of CEs and some related proteins was performed (Fig. 6-4). Interestingly, CmEpiA from *Cellvibrio mixtus*, which is an epimerase catalyzing epimerization of mannose/glucose (Centeno et al., 2006), is found in the CE cluster, and is closely related to CEs from aerobes rather than CsCE. It is possible that CmEpiA also works as CE. Bacterial phosphomannose

isomerases and the yihS protein, which is an aldose-ketose isomerase catalyzing specific interconversion of mannose, fructose and glucose (Ito 2008), are located to the other two groups. YihS from *E. coli* and *Salmonella enterica* (EcYihS and SeYihS, respectively) have been shown to be specific to monosaccharides and essentially different from CsCE in terms of epimerization activity toward cellobiose.

In *B. fragilis* NCTC9343, the physiological role of CE was predicted to supply Man-Glc from β-1,4-mannobiose for further phosphorolysis by MGP (Senoura 2011), which is classified into the glycoside hydrolase (GH) family 130 according to the sequence based classification (Cantarel 2009). As shown in Fig. 6-4, 66 of the106 proteins that belong to the CE cluster were from bacteria harboring GH130 proteins, regardless of anaerobes or aerobes. This implies that the metabolic pathway of β-1,4-mannobiose through epimerization and phosphorolysis is not limited to anaerobes and also distributes to various aerobes.

Figures and Tables

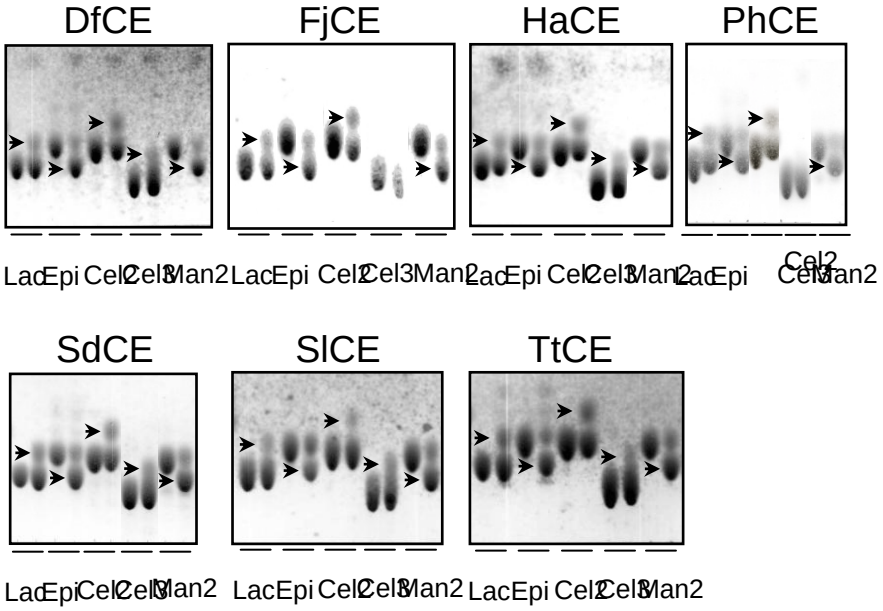

Fig. 6-1. Detection of epimerization activity of the CE-like protein from various aerobes.

Epimerization activity of CE-like proteins was detected by TLC. Left and right lanes of each substrate are before and after the reaction, respectively. The reaction products are indicated by arrows. Lac, lactose; Epi, epilactose; Cel2, cellobiose; Cel3, cellotriose; and Man2, β-1,4-mannobiose.

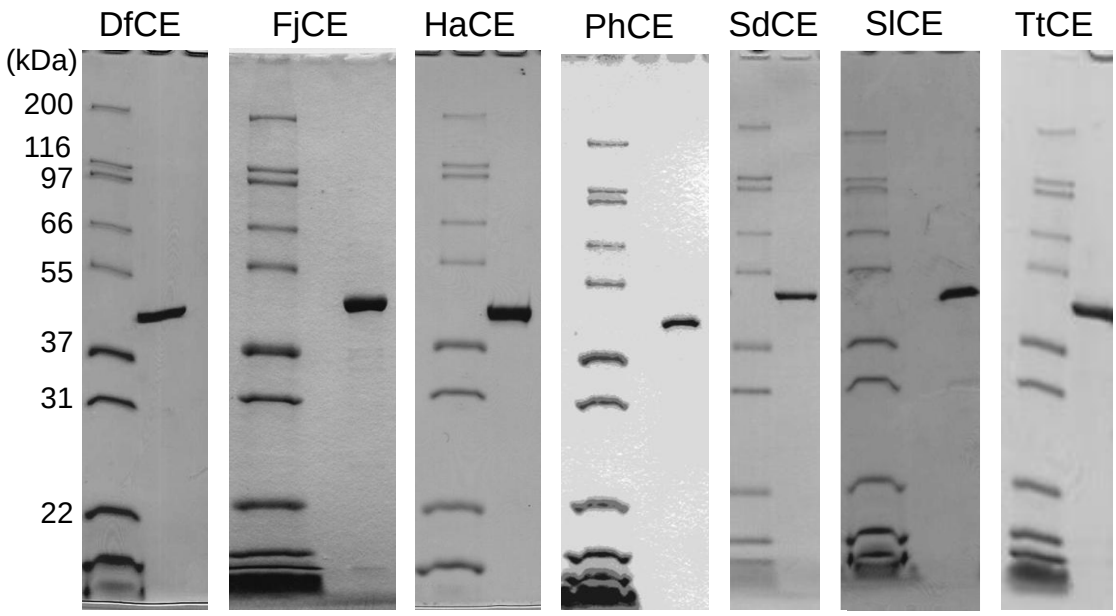

Fig. 6-2. SDS-PAGE of Purified CE-like Proteins.

One μg of the purified CE-like proteins was analyzed by SDS-PAGE followed by CBB staining. Molecular masses of standard proteins were shown on the left side.

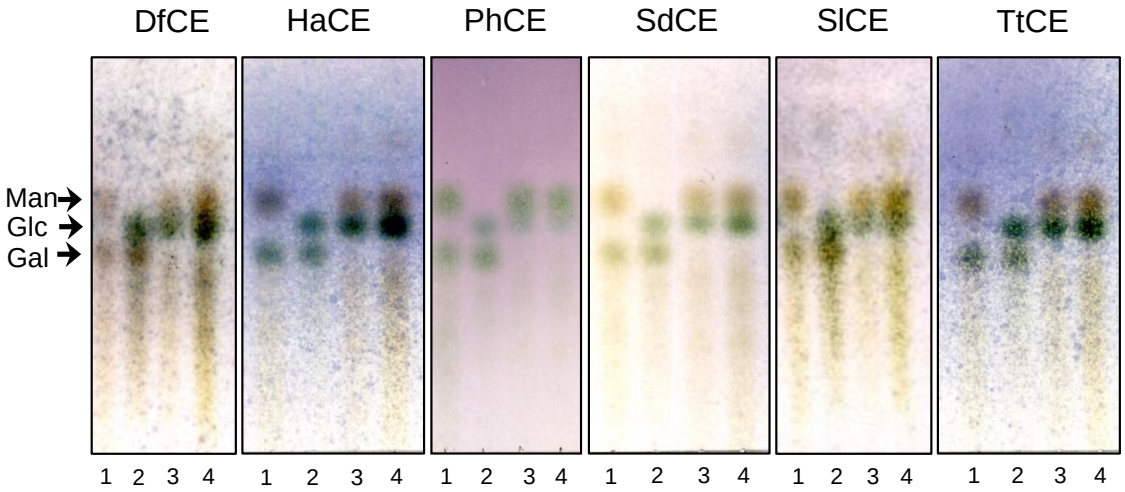

Fig. 6-3. Monosaccharide components of the reaction products of the recombinant CE-like proteins.

Reaction products from lactose (1), epilactose (2), cellobiose (3), and β-1,4-mannobiose (4) were hydrolyzed by TFA, and the resulting monosaccharides were analyzed by TLC. Mobility of mannose (Man), glucose (Glc), and galactose (Gal) was shown on the left.

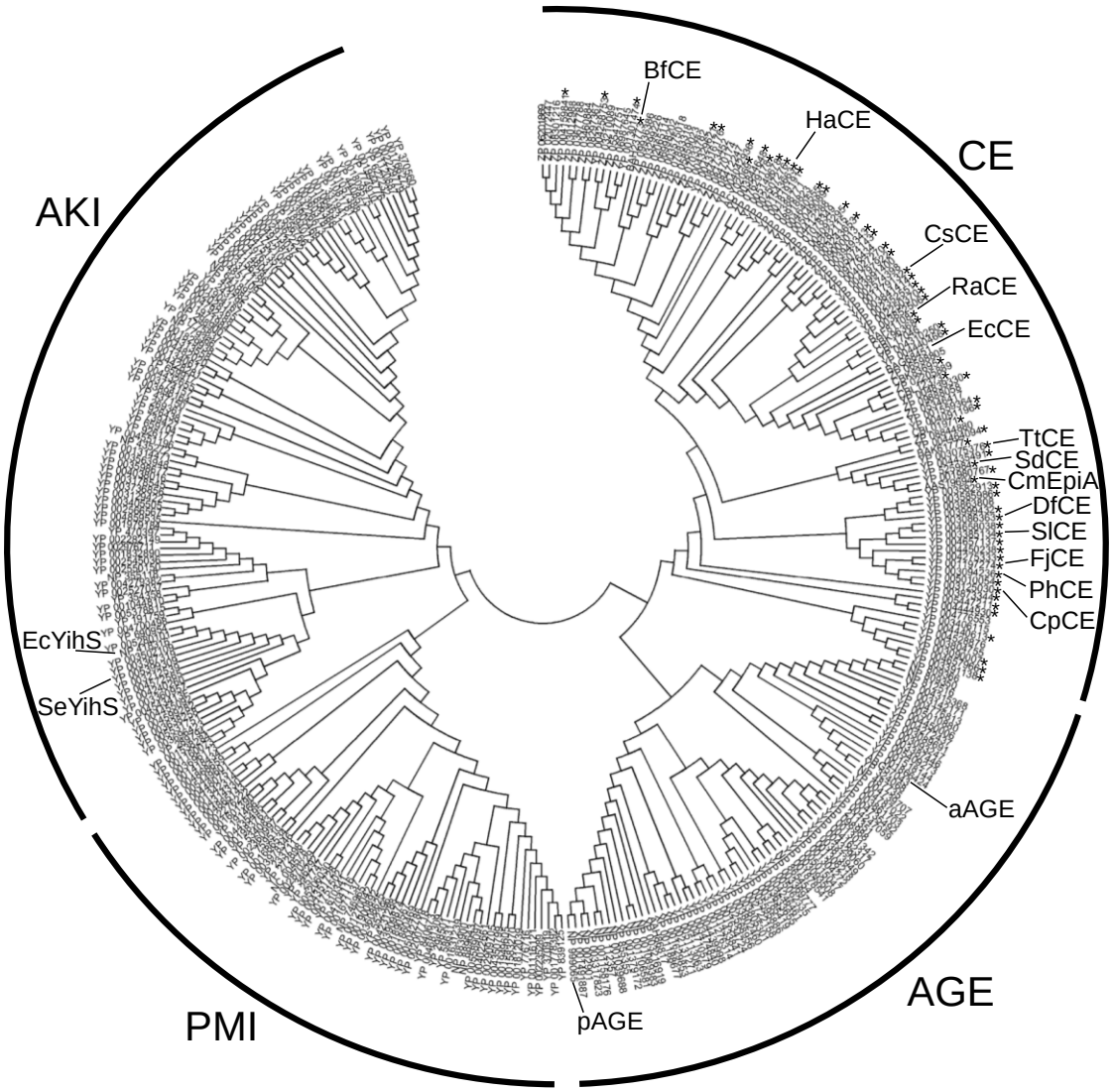

Fig. 6-4. The phylogenetic tree of CEs and related enzymes.

Accession number of Genbank or NCBI reference requence was shown. aAGE and pAGE are AGEs from *Anabaena* sp. CH1 and pig, respectively. EcYihS and SeYihS are aldose-ketose isomerases (AKIs) from *E. coli* and *Salmonella enterica*, respectively. PMI indicate mannose 6-phosphate isomerase. CEs from the bacteria harboring glycoside hydrolase family 130 enzymes were indicated by asterisks.

Table 6-1. Primers used for amplification and sequencing of CE-like genes.

Name	Sequence (5'-3')	Purpose
CpCE-R-NdeI	aaacatatgaattggacatcagacgaaaaac	Cloning of CpCE
CpCE-R-XhoI	aaactcgagtcacttcaaacgcttcacgacct	Cloning of CpCE
DfCE-F-NdeI	aaacatatggccgcatttacacccgaag	Cloning of DfCE
DFCE-R-XhoI	gaactcgagttacgctttgccggtcctg	Cloning of DfCE
FjCE-F-NdeI	aaacatatgccagcaaatctaaaacagctt	Cloning of FjCE
FjCE-R-XhoI	aaactcgagttaggttttaattcggttaataa	Cloning of FjCE
HaCE-F1-NdeI	aaacatatggcgaatctcgtagatgg	Cloning of HaCE
HaCE-R1-del NdeI	gcctccatcatgtgcaacatgg	Deletion of *Nde* I site in the HaCE gene
HaCE-F2-del NdeI	accatgttgcacatgatggag	Deletion of NdeI site in the HaCE gene
HaCE-R2-XhoI	aaactcgagttaccctcggatctgaacactc	Cloning of HaCE
PhCE-F-NdeI	aaacatatgagcgaaattcttatacaaga	Cloning of PhCE
PhCE-F-XhoI	aaactcgagtcaggaaaaatcgaaattgacac	Cloning of PhCE
SdCE-F-NdeI	aagggcatatgggtgtgccgcttaaaaaaa	Cloning of SdCE
SdCE-R-XhoI	gggctcgagttattcgttattaccaaatatttctc	Cloning of SdCE
SlCE-F-NdeI	aagggcatatggacttaaagcaacttcgcg	Cloning of SlCE
SlCE-R-XhoI	gggctcgagttatccatgcagatgatccagtcg	Cloning of SlCE
TtCE-NdeI	aaaccatatggaaactgaaacggatac	Cloning of TtCE
TtCE-R1-del NdeI	ttcataaacatgtgaacgtgcc	Deletion of *Nde* I site in the TtCE gene
TtCE-F2-del NdeI	acgttcacatgtttatgaatac	Deletion of *Nde* I site in the TtCE gene
TtCE-R2-EcoRI	aaagaattcctaacagtcgacattcaacac	Cloning of TtCE
CPCE300	ttattggacggtggactata	Sequence of CpCE
CPCE600	gcagatatcctggaattact	Sequence of CpCE
CPCE900	actggtcaatgcctgggaac	Sequence of CpCE
DFCE1	gcggatggctcgccgctgga	Sequencing of DfCE
DFCE2	gatgccagactcaaaaagcag	Sequencing of DfCE
FJCE300	accaaaagatactaaaaacc	Sequence of FjCE
FJCE600	aaacattttattaataccga	Sequence of FjCE
FJCE900	tgaagaatatctgaagattg	Sequence of FjCE
HACE1	atagaccgcatcggccatgc	Sequencing of HaCE
HACE2	ggccacatcccaaactcgcag	Sequencing of HaCE
PHCE300	agggcaaaccagcagatacc	Sequence of PhCE
PHCE600	aagattattgacagagatac	Sequence of PhCE
PHCE900	gaacagacctactacgataa	Sequence of PhCE
SDCE1	gaacatggcggtgtattttgg	Sequencing of SdCE
SDCE2	ctagaagcttataccgcattac	Sequencing of SdCE
SLCE1	ttcgtagttcattcccccgtc	Sequencing of SlCE
SLCE2	ctttatttcctgattatcgt	Sequencing of SlCE
TTCE1	ctgtttatcgaacacgtcgt	Sequencing of TtCE
TTCE2	atgcgtgttcatggttttgg	Sequencing of TtCE
pET22b_IC_S	atataggcgccagcaaccgcacctgt	Sequencing
pET22b_IC_anti	taaccaccacacccgccgcgcttaat	Sequencing

Sites of the restriction enzymes are underlined.

Table 6-2. Chemical shifts of the oligosaccharides produced by FjCE in ^{13}C -NMR.

Product from lactose			Product from cellobiose			Product from β-1,4-mannobiose			Product from epilactose		
Sample (ppm)	Epilactose (ppm)	Difference (ppm)	Sample (ppm)	Glc-Man (ppm)	Difference (ppm)	Sample (ppm)	Man-Glc (ppm)	Difference (ppm)	Sample (ppm)	Lactose (ppm)	Difference (ppm)
103.3	103.3	0	102.9	104.2	1.3	100.3	101.7	1.4	103.1	103	-0.1
94	94	0	94	95.3	1.3	96	97.5	1.5	96	95.8	-0.2
93.9	93.8	-0.1	77.1	78.5	1.4	78.9	80.5	1.6	78.6	78.4	-0.2
76.8	76.8	0	76.2	77.6	1.4	76.6	78.1	1.5	75.6	75.4	-0.2
76.4	76.4	0	75.7	77.1	1.4	74.8	76.2	1.4	75	74.9	-0.1
75.6	75.6	0	73.4	74.7	1.3	74.4	75.9	1.5	74.6	74.5	-0.1
75.2	75.2	0	71.2	72.6	1.4	74	75.6	1.6	74	73.9	-0.1
72.7	72.7	0	70.5	71.9	1.4	73	74.6	1.6	72.8	72.6	-0.2
72	72	0	69.7	71.2	1.5	70.8	72.3	1.5	71.2	71.1	-0.1
71.3	71.24	-0.06	69.2	70.6	1.4	66.9	68.4	1.5	68.8	68.6	-0.2
71.2	71.18	-0.02	60.9	62.2	1.3	61.2	62.4	1.2	61.2	61.1	-0.1
70.9	70.8	-0.1	60.5	62	1.5	60.5	62.2	1.7	60.3	60.2	-0.1
70.4	70.4	0									
69.2	69.2	0									
68.8	68.8	0									
61.3	61.3	0									
60.6	60.6	0									

Table 6-3. Effects of pH and temperature on CEs from various aerobes.

Enzyme	pH		temperature (°C)	
	Optimum	Stability	Optimum	Stability
DfCE	7.7	3.2 - 10.2	50	≤50
FjCE	8.4	4.7 - 9.8	35	≤30
HaCE	7.3	8.0 - 9.4	45	≤50
PhCE	6.3	5.3 - 11.8	35	≤30
SdCE	7.7	4.7 - 10.8	35	≤30
SlCE	7.7	2.2 - 9.5	45	≤50
TtCE	8.8	3.4 - 10.2	35	≤45

Table 6-4. Kinetic parameters of CEs from various aerobes.

Enzyme	Cellobiose			Lactose		
	k_{cat} (s^{-1})	K_m (mM)	k_{cat}/K_m (s^{-1} mM^{-1})	k_{cat} (s^{-1})	K_m (mM)	k_{cat}/K_m (s^{-1} mM^{-1})
DfCE	240 ± 39.8	179 ± 32	1.34	44.9 ± 4.9	95.7 ± 23.9	0.469
FjCE	39.9 ± 3.23	53.2 ± 7.3	0.750	17.5 ± 0.5	34.9 ± 4.3	0.501
HaCE	18.7 ± 0.45	28.2 ± 5.3	0.663	14.0 ± 1.8	51.9 ± 6.8	0.270
PhCE	7.02 ± 0.21	29.6 ± 5.8	0.237	5.43 ± 0.06	24.5 ± 0.9	0.222
SdCE	26.1 ± 1.83	22.6 ± 4.4	1.15	7.82 ± 0.42	29.2 ± 4.4	0.268
SlCE	222 ± 2.89	104 ± 9.4	2.13	92.1 ± 12.2	206 ± 40	0.447
TtCE	165 ± 6.56	198 ± 13	0.833	175 ± 31	238 ± 45	0.735
RaCE[1)]	63.8	13.8	4.62	52.1	33.0	1.58
BfCE[2)]	67.6	3.75	18.0	79.5	6.56	12.1
EcCE[3)]	28.5	11.3	2.52	32.5	72.0	0.451

Mean ± standard deviation of three independent experiments is shown. Kinetic parameters of CEs except for RmCE were determined at 30 °C. 1) Ito et al., 2008. 2) Senoura et al., 2009. 3) Taguchi et al., 2008.

Chapter 7. Cellobiose 2-epimerase from *Rhodothermus marinus* JCM9785

7.1. Introduction

In Chapter 6, cellobiose 2-epimerases (CEs) from various aerobic bacteria were identified. For the production of epilactose, the enzymatic reaction temperature should be above 50°C to increase solubility of lactose and avoid contamination of microorganisms, so that more thermotolerant and stable enzyme is required. In this chapter, the author focuses on thermophilic marine bacterium, *Rhodothermus marinus* for CE producer because CE-like gene is found in *R. marinus* DSM4252 whose genome is available. In this study, CE-like gene in another strain, *R. marinus* JCM9785 whose genome is not sequenced, is cloned and the properties of recombinant protein expressed in *E. coli* are investigated. The target CE-like gene is actually CE and the protein is desirable for industrial use from the point of its thermotolerance and stability in high temperature and broad range of pH.

7.2. Materials and methods

7.2.1. Bacterial strain and plasmid

R. marinus JCM9785 was provided by Japan Collection of Microorganisms, RIKEN BRC (Wako, Japan). *E. coli* DH5α and *E. coli* BL21 (DE3)-Codonplus^{TM} RIL were used in the propagation of plasmid DNA and the production of a recombinant protein respectively. A plasmid vector of pET-22b was used in the expression of the *R. marinus* JCM9785 (RmCE) gene in *E. coli*.

7.2.2. Detection of CE activity in the cell free extract of *R. marinus* JCM9785

R. marinus JCM9785 was aerobically cultivated in 3 L of Marine Broth 2216, supplemented with 2 g/L konjak glucomannan (Rheolex; Shimizu Chemical; Hiroshima, Japan) and 0.2 g/L antifoamer (KM72; Shin-Etsu Chemical; Tokyo) for 24 h at 70°C. The cells were harvested by centrifugation and resuspended in about 200 mL of 10 mM K-phosphate buffer (pH 7.0, buffer A). The suspended cells were disrupted by sonication, and then the cell debris was removed by centrifugation. The resulting extract was used in the assay of CE activity, as follows: Cell-free extract (0.5 mL) was mixed with an equal volume of 200 mM lactose in 50 mM Na-phosphate buffer (pH 7.0), and incubated at 40°C for 48 h. Then the reaction mixture was analyzed by HPLC as described in previous chapter. The reaction product was purified by HPLC and the components of monosaccharide were analyzed as well

7.2.3. Purification of cellobiose 2-epimerase from the cell-free extract of *R. marinus* JCM9785

R. marinus JCM9785 was aerobically cultivated in 15 L of culture medium. Bacterial cells harvested by centrifugation were resuspended in 1 L of buffer A and disrupted by sonication. The cell debris was removed by centrifugation. Then ammonium sulfate was added to the supernatant to 90% saturation, and the sample was stored at 4ºC overnight. Precipitated protein, recovered by centrifugation, was dissolved in 200 mL of buffer A and dialyzed against buffer A. The resulting sample was applied onto a Toyopearl DEAE-650M column (ϕ5 x 42 cm; Tosoh) equilibrated with buffer A. The non-adsorbed fraction was obtained by thorough washing with buffer A. This column chromatographic procedure was repeated 2 times, but enzyme

activity was detected only in the non-adsorbed fractions. Next, ammonium sulfate was added to the collected sample up to 0.5 M and the sample was subjected to Toyopearl Butyl-650M (Tosoh) column chromatography, where a column (ϕ2.6 x 35 cm) was equilibrated with buffer A containing 0.5 M ammonium sulfate. After the non-adsorbed protein was eluted completely, the adsorbed protein was eluted by a descending linear gradient of ammonium sulfate from 0.5 to 0 M (total elution volume, 1 L). The active fractions were pooled and concentrated up to 5 mL by ultrafiltration with Amicon Ultra-15 (Millipore)). Then the concentrated sample was applied to a Sephacryl S-200 column (GE Healthcare; ϕ2.6 x 87 cm) equilibrated with buffer A containing 0.1 M NaCl. Column chromatography was performed at flow rate of 0.3 mL/min. The pooled active fractions were dialyzed against buffer A, and were used as the final enzyme preparation. The purity of the protein was confirmed by SDS-PAGE. The protein concentration was determined by the Bradford method. BSA (Bio-Rad) was used as a standard protein.

7.2.4. N-Terminal sequence analysis

Purified RmCE of 11 μg was subjected to SDS-PAGE and the separated protein was transferred to a PVDF membrane (Immobilon-P^{SQ}; Millipore) by electroblotting using a semi-dry blotting apparatus. The band of RmCE, detected by staining with Coomassie Brilliant Blue R-250, was cut off from the membrane and applied to N-terminal sequence analysis using a protein sequencer, Procise 492cLC (Applied Biosystems).

7.2.5. Cloning of the gene

The sequence of CE-like genes of *R. marinus* JCM9785 was identified and cloned. Based on the expectation that the DNA sequences of CE-like gene and its surroundings are similar in both *R. marinus* JCM9785 and *R. marinus* DSM4252 of which the latter is genome sequenced, PCR was performed with the primers designed on the basis of the up- and downstream sequence of CE-like gene (Gene ID: ACY49317) of *R. marinus* DSM4252: 5'-TGCTGGATTACGTCATGCACACG-3' (antisense orientation) and 5'-CTGCAGCAGCAGGTGATCGGAC-3' (sense orientation). Dimethylsulfoxide at 2% v/v was added to the PCR mixture to facilitate amplification of the DNA fragment with a GC-rich template. The sequence of the amplified PCR product was analyzed. Then complete CE-like gene of *R. marinus* JCM9785 was cloned into *Nde*I – *Xho*I site in an expression vector, pET22b. The sequences of the primers used for PCR were as follows: 5'-AAACATATGGTGAGCACGGAGACCATC-3' (sense, *Nde*I site underlined) and 5'-AAACTCGAGCTACCGGGATCGAACGTG-3' (antisense, *Xho*I site underlined).

7.2.6. Production and purification of recombinant enzyme

To produce recombinant RmCE, a single colony of *E. coli* transformant harboring the expression plasmid was inoculated with 3 mL of LB medium containing 100 μg/mL of ampicillin, and cultured at 30°C overnight. Then 0.2 mL of the culture fluid was transferred to a fresh medium at 200 mL and this was cultured as well until A_{600} reached 0.5. Then 0.2 mL of 100 mM IPTG (final concentration, 0.1 mm) was added to induce the production of the recombinant protein, and the culture fluid was further incubated at 16°C for 24 h. The cells were collected by centrifugation and

resuspended in 20 mL of 20 mM sodium phosphate buffer (pH 7.0). They were disrupted by sonication as described above, and the cell debris was removed by centrifugation. The resulting supernatant was incubated at 70°C for 30 min and centrifuged to remove aggregated protein. Then supernatant obtained was dialyzed against buffer A and used for enzyme characterization.

7.2.7. Enzyme assay

Enzyme assay was performed as the same method as described in chapter 6 except the reaction temperature was set at 60ºC. One U of enzyme activity was defined as the amount of enzyme that forms 1 μmol of epilactose from lactose in 1 min at 60ºC and pH 7.0.

7.2.8. Effects of pH and temperature

The enzymatic characteristics of RmCE were investigated with an *E. coli* recombinant enzyme sample. Optimum pH and temperature were evaluated by measuring the initial reaction rates under the conditions of the enzyme assay modified in terms of reaction pH and temperature respectively. To identify the optimum pH, 20 mM Britton-Robinson buffer (pH 3-10) was used as the reaction buffer. In the analysis of the optimum temperature, the reaction rate at 50-100ºC was measured.

pH and temperature stabilities were assessed by measuring residual activity under standard conditions following the pH and temperature treatments. pH treatment was performed by incubating 150 μL of enzyme solution (2.2 mg/mL) in 20 mM Britton-Robinson buffer (pH 3.0-12.0), 50 mM KCl-HCl (pH 2.0), and 100 mM KCl-KOH (pH 13.0) for 24 h at 4°C. For temperature treatment, 0.5 mL of 0.2 mg/mL

of the enzyme in 20 mM Na-phosphate buffer (pH 7.0) was incubated at 50-100ºC for 30 min, and then immediately cooled on ice. The activity before the treatment was considered to be 100% of residual activity.

7.2.9. Kinetic analysis

The kinetic parameters of RmCE at 60ºC for cellobiose and lactose were determined from the initial reaction rates toward 10 to 100 mM of substrates by non-linear regression to the Michaelis-Menten equation. The reaction conditions, except for the substrate concentration, were the same as the standard conditions described above.

7.2.10. TLC analysis of the reaction products

The reaction mixtures of RmCE containing various sugars were analyzed by TLC as well. A reaction mixture consisting of 0.8 μg/mL of RmCE, 100 mm substrate described below, and 20 mM K-phosphate buffer (pH 6.5) was incubated at 60ºC for 24 h. Glucose, galactose, lactose, epilactose, cellobiose, cellotriose, mannobiose, gentiobiose (Wako Pure Chemical Industries), maltose, laminaribiose (Seikagaku), sophorose (Sigma-Aldrich), mannose, and GlcNAC were tested as substrates.

7.3. Results

7.3.1. Detection of cellobiose 2-epimerase activity in the cell-free extract of *R. marinus* JCM9785

The cell-free extract of *R. marinus* JCM9785 was incubated with lactose and the reaction mixture was analyzed by HPLC. A peak with the same retention time as authentic epilactose was detected (data not shown). The components of

monosaccharide of purified product showed two spots corresponding to mannose and galactose on TLC analysis (not shown), indicating that the glucose residue at the reducing end of lactose was enzymatically converted to mannose. Thus *R. marinus* JCM9785 produced a CE as predicted based on the high sequence similarity of ACY49317 protein from *R. marinus* DSM4252 to known CEs.

7.3.2. Production of recombinant enzyme

A gene homologous to the ACY49317 in *R. marinus* DSM4252 was obtained from the genome of *R. marinus* JCM9785 by PCR. The deduced amino acid sequence of the gene obtained was 94.2% identical to the ACY49317 protein (Fig. 7-1). In order to confirm that the cloned gene encoded RmCE, native RmCE was purified from the cell-free extract of *R. marinus* JCM9785 (Fig. 7-2a), and the N-terminal amino acid sequence and the masses of the tryptic peptides of the purified enzyme were analyzed. The N-terminal amino acid sequence of the purified native RmCE was ETIPDVRRL. This was included in the deduced amino acid sequence of the cloned gene (Fig. 7-1). Additionally, the peptide masses of the tryptic peptides of the native RmCE, analyzed by MALDI-TOF-MS, matched the theoretical values with 27.2% coverage of the entire amino acid sequence (Fig. 7-1, Table 7-1). These results unambiguously indicated that the cloned gene encoded RmCE in *R. marinus* JCM9785.

Next, the cloned gene was expressed in *E. coli*. RmCE was successfully produced in the soluble fraction of the *E. coli* cell (Fig. 7-2b). The total enzymatic activity produced in 200 mL of culture medium was 1,050 U, estimating that 12 mg of recombinant enzyme was produced based on the specific activity of the purified

recombinant enzyme. Heat treatment of the cell-free extract at 70ºC for 30 min was effective in the purification of recombinant RmCE. The resulting enzyme sample showed a single band on SDS-PAGE (Fig. 7-2b), and its specific activity was 87.5 U/mg.

7.3.3. Effects of temperature and pH on the activity and stability of *R. marinus* cellobiose 2-epimerase

The effects of temperature and pH on the activity and stability of recombinant RmCE was investigated. The activity of RmCEs significantly elevated with increasing temperature up to 80°C (Fig. 7-3a). At 80°C, 2.5-fold higher activity was shown than at 50°C. Similar activity was observed at 90°C, but decreased at 100°C. The thermal stability of RmCE was assessed by measuring residual activity after heat treatment for 30 min. Residual activity over 90% of the original activity was shown below 80°C, whereas very low and no residual activity was observed at 90°C and 100°C respectively (Fig. 7-3a).

The pH profile of the RmCE reaction was elucidated. The highest activity of RmCE was observed at pH 6.3 (Fig. 7-3b). Enzyme activity gradually decreased with increasing pH values over pH 6.3. Ninety percent of activity relative to the maximum activity (pH 6.3) was shown at pH 9.6, where no non-enzymatic epimerization occurred (data not shown). The reaction rate of epimerization at pH values higher than 9.6 could not be measured because significant non-enzymatic epimerization was observed. Enzymatic activity dropped at acidic pH, although the enzyme was fully stable even at pH 3.2. RmCE demonstrated the widest stable range of pH values among CEs known to date, retaining the original activity of RmCE in a range

of 3.2 to 10.8 after 24 h of incubation at 4ºC (Fig. 7-3b).

7.3.4. Substrate specificity

The reaction products of various carbohydrates were analyzed by TLC (Fig. 7-4). The reaction products of lactose, epilactose, cellobiose, mannnobiose, and cellotriose were detected though the amount of reaction product from cellotirose was small, whereas glucose, galactose, mannose, sophorose, laminaribiose, gentiobiose, and maltose did not serve as substrates for RmCE. In addition, RmCE was inactive toward ManNAC, a substrate of AGE. Similarly to all known CEs, RmCE is highly specific to oligosaccharides linked by the β-1,4-glycosidic linkage, and not active towards monosaccharides.

7.3.5. Kinetic analysis

The kinetic parameters of RmCE for cellobiose and lactose were determined (Table 7-2). RmCE showed similar K_m values for the two substrates, while the k_{cat} value for lactose (111 s^{-1}) was 1.4-fold higher than that of cellobiose (80.8 s^{-1}), which led to a higher preference for lactose over cellobiose, unlike known CEs (Chapter 6, Ito 2008, Senoura 2009, Taguchi 2008).

The conversion ratios of lactose and cellobiose for epilactose and Glc-Man respectively after the reactions reached full equilibrium were essentially equal, around 30%, at all the substrate concentrations tested (Fig. 7-5). In the reaction to 100 mM mannobiose and epilactose, the conversion ratios for the epimerized products were 69.5% and 67.9% respectively.

7.4. Discussion

In this study, a thermophilic and stable cellobiose 2-epimerase from *R. marinus* JCM9785 (Rmce) was characterized. Multiplealignment of the amino acid sequence of RmCE with those of known CEs from *R. albus*, *B. fragilis*, and *E. cellulosolvens*, *Anabaena* AGE, and porcine AGE suggested that RmCE has a similar structure to them. RmCE was predicted to consist of 12 α-helices to establish an $(\alpha/\alpha)_6$ barrel structure, like comparable enzymes (Fig. 7-1). All the amino acid residues important for catalysis, which have been confirmed by site-directed mutagenesis studies (Lee 2007, Itoh 2000), were completely conserved in RmCE. It is assumed that His259 and His390 of RmCE, corresponding to the putative catalytic His residues of RaCE, porcine AGE, and *Anabaena* AGE, may work as catalytic amino acid residues. Consistently with this assumption, the pK_a value of side chain of His is about 6.3, and RmCE is active in a range of pH 6-9 but not on the acidic side, although it was fully stable at such pH values (Fig. 7-3).

RmCE acted only on β-1,4-linked oligosaccharide, cellobiose, lactose, epilactose, mannobiose, and cellotriose like other CEs (Fig. 7-4). Although the structures of the epimerized products were not confirmed, the reaction products of the cellooligosaccharides, mannobiose, and epilactose were assumed to be epimerized cellooligosaccarides with a mannose residue at the reducing end, Man-Glc, and lactose respectively, based on the reaction pattern of RmCE toward lactose and those of known CEs. Kinetic analysis of RmCE revealed that it prefers for lactose over cellobiose in terms of k_{cat} and K_m values (Table 7-2). At present, the relationship of structure and function of CE is not fully understood.

It is not easy to compare the kinetic parameters of RmCE with those of the

other CEs, because the reaction temperature of RmCE was different, but RmCE showed much higher k_{cat} for lactose than the known CEs (Table 6-4, Table 7-2). This result would be caused by the high thermal stability of RmCE, and the enzyme reaction was performed at 60ºC where the other known enzymes cannot be examined due to their thermal lability. The high k_{cat} for lactose of RmCE is very attractive for industrial use to synthesis epilactose, since the enzyme reaction in the practical process is thought to be performed at much higher concentrations than the K_m value of lactose, and the k_{cat} value is the sole determinant of the reaction rate per mg of enzyme.

RmCE showed maximum activity at 80 to 90ºC and was stable up to 80ºC. This is the first report of the thermo-tolerance CE. The amino acid component ratios of RmCE and RaCE, the latter is most active at around 30ºC, were compared (Table 7-3). In RmCE, the contents of basic amino acids, Arg and His, are considerably higher than RaCE, whereas the content of Lys of RmCE is lower (Table 7-3). On the other hand, the contents of the acidic amino acids, Glu and Asp, of RmCE are close to and lower than RaCE respectively. It is known that basic amino acids play an important role in thermostability in thermophilic enzymes, because they coordinate the salt-bridge at the surface of the protein and toughen protein structure against high temperature (Perutz 1975, Tomazic 1988). Especially, the guanidinium group of Arg is able to form more than one electrostatic bond (Mrabet 1992), and increased Arg content has been correlated with heat stability in thermophilic enzymes (Merkler 1981). Indeed, the Arg content of RmCE was remarkably higher (2.7-fold) than that of RaCE (Table 7-3). Arg residues on the surface of RmCE might form salt-bridge interactions with acidic amino acid residues to make the protein structure

significantly rigid. Comparing the amino acid sequences, more Pro residues were situated in the putative loop connecting α-helix 1 and α-helix 2 of RmCE than the other CEs and AGEs (Fig. 7-1). Especially, three Pro residues are positioned near the N-terminal of putative α-helix 2, including a crucial Arg66. These Pro residues might stabilize this loop structure to maintain the structure of the active site at high temperatures as seen for thermostable oligo-1,6-glucosidase (Watanabe 1991).

With high thermal stability and high activity at weakly acidic pH, RmCE is the most useful for the production of epilactose among known CEs. Enzyme reaction at high temperature makes it possible to carry out the CE reaction at high substrate concentration, simplifying the purification of epilactose from the reaction mixture because the tedious concentration procedure to remove unreacted lactose by crystallization is made easy (Saburi 2010). In addition, non-enzymatic epimerization, which occurs at alkaline pH and high temperature, can be avoided because RmCE is most active at weakly acidic pH.

Figures and Tables

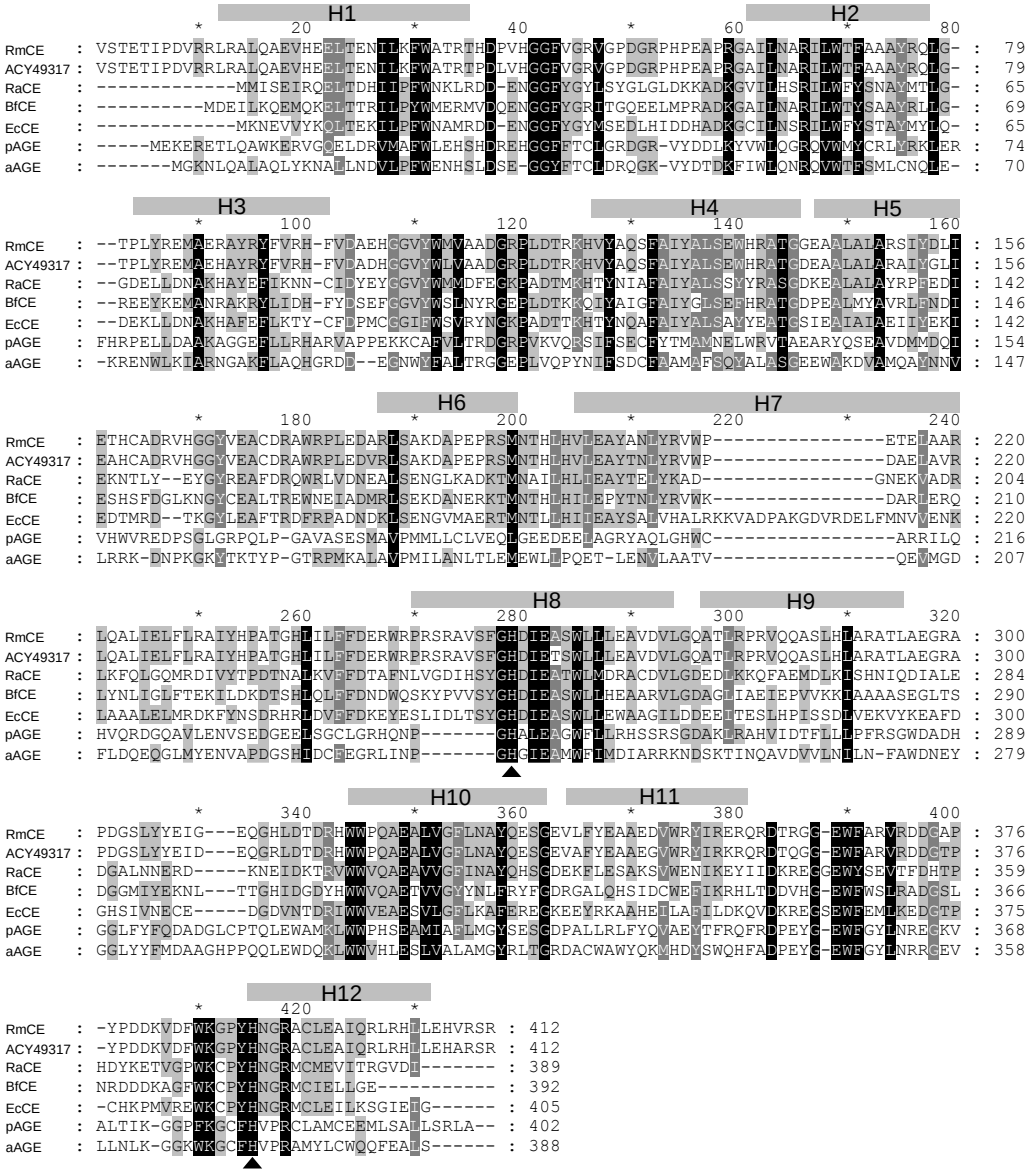

Fig. 7-1. Multiple alignment of amino acid sequences of CEs and AGEs.

The amino acid sequences of CEs and AGEs were aligned using the Clustal W program.[27] Black, dark gray, and light gray indicate complete, 80%, and 60% conservation respectively. Gray bars above a sequence represent predicted α-helices forming the catalytic $(\alpha/\alpha)_6$ barrel. Black triangles and circles show the putative catalytic His residues and the amino acid residues important for catalysis respectively. RmCE, *R. marinus* JCM9785 CE; ACY49317, ACY49317 protein from *R. marinus* DSM4252; RaCE, *R. albus* NE1 CE (Genbank ID: BAF81109); BfCE, *B. fragillis* NCTC9343 CE (Genbank ID: BAH23773.1); EcCE, *E. cellulosolvens* NE13 CE (Genbank ID: BAG68451.1); pAGE, pig AGE (Swiss-Prot ID: P17560.2); aAGE, *Anabaena* sp. CH1 AGE (Genbank ID: ABG57043.1). The N-terminal amino acid sequence of native RmCE and the sequences of tryptic peptides whose masses matched the theoretical values are underlined and boxed respectively.

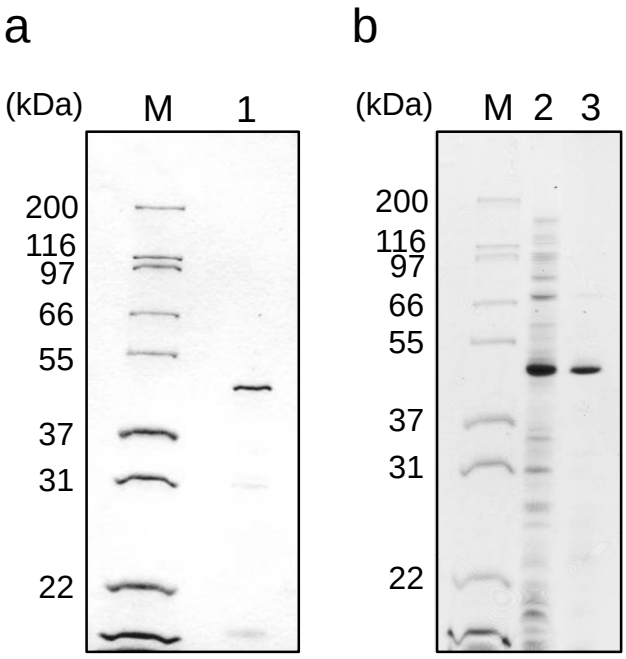

Fig. 7-2. SDS-PAGE analysis of native and recombinant RmCE.

SDS-PAGE was performed on a 15% polyacrylamide gel, and protein was detected by Coomasie Brilliant Blue staining. a, SDS-PAGE of the native RmCE purified from the cell-free extract from *R. marinus* JCM9785. One μg of protein was loaded on the gel. The molecular masses of the size markers are shown on the left. M, size marker; 1, purified native RmCE. b, SDS-PAGE of the recombinant RmCE produced in *E. coli*. 2, Cell-free extract of *E. coli* transformant producing recombinant RmCE (5 μg of protein was analyzed). 3, Purified recombinant RmCE (1 μg).

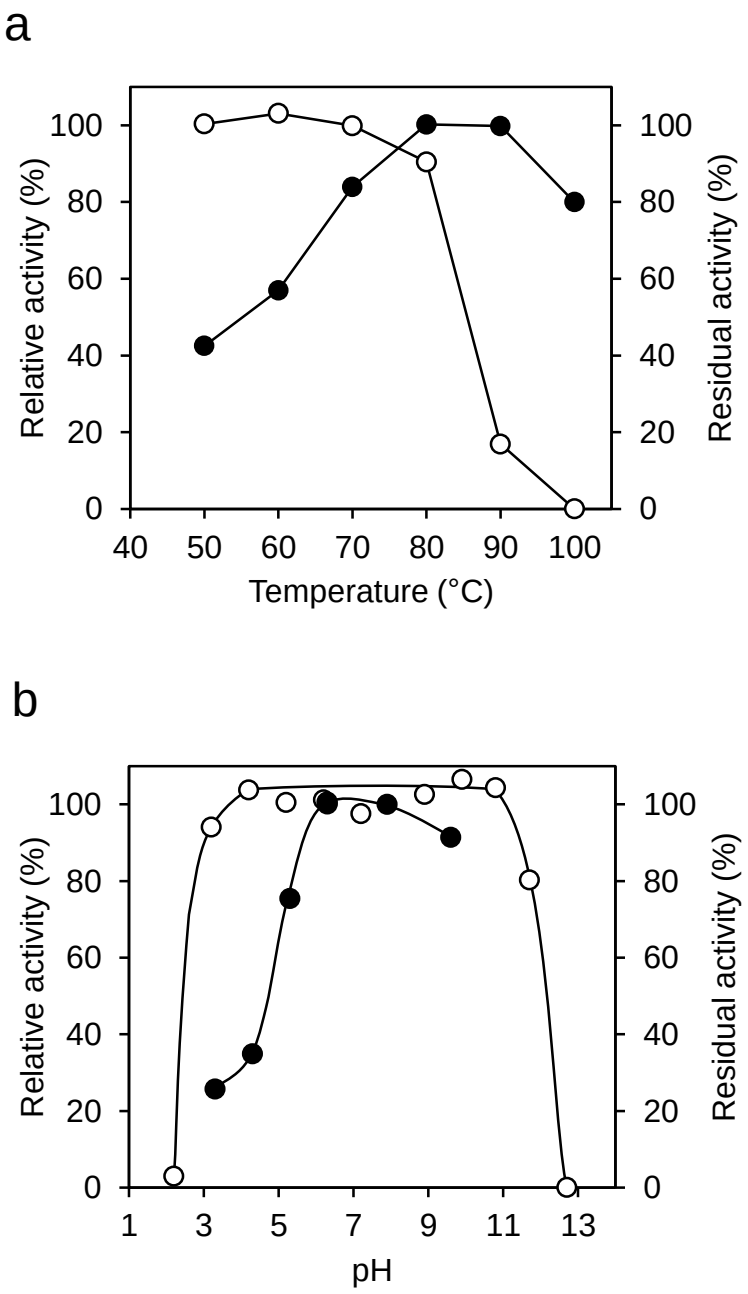

Fig. 7-3. Effects of temperature and pH on RmCE activity and stability.

a, Effect of temperature. Solid and hollow circles indicate relative activity at the indicated temperature and the residual activity after heat treatment for 30 min, respectively. b, Effect of pH. Solid and hollow circles indicate relative activity at the indicated pH and the residual activity after pH treatment for 24 h at 4ºC respectively.

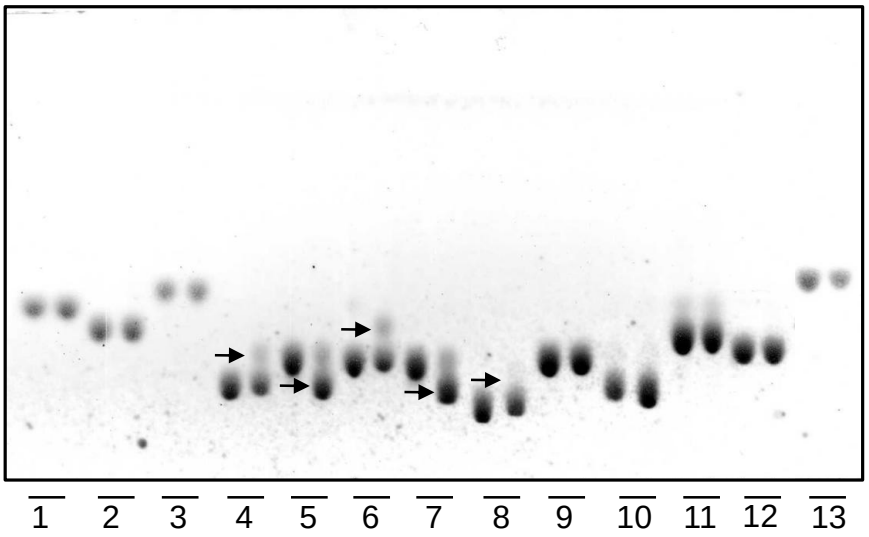

Fig. 7-4. TLC analysis of the reaction product of RmCE for various sugars.
The reaction of RmCE to various sugars was analysed by TLC to elucidate the substrate specificity of RmCE. The left and right lanes for each number indicate the samples before and after the reaction respectively. The reaction products are indicated by arrows. 1, glucose; 2, galactose; 3, mannose; 4, lactose; 5, epilactose; 6, cellobiose; 7, mannobiose; 8, cellotriose; 9, maltose; 10, gentiobiose; 11, laminaribiose; 12, sophorose; 13, ManNAC.

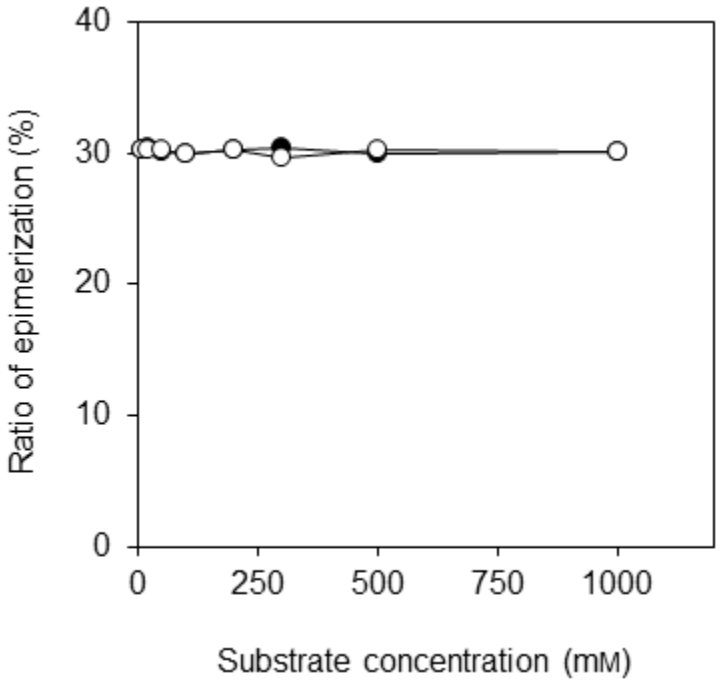

Fig. 7-5. Conversion ratios of RmCE reaction at various substrate concentrations.

The epimerization ratios at equilibrium in the reactions to varying concentrations of substrate were assessed. The reaction mixtures consisting of 10-1000 mM lactose or cellobiose, 5 mM K-phosphate buffer (pH 6.5), and RmCE (30 U/g-substrate solid) were incubated at 60°C for 24 h. The amount of products was measured by HPLC after the reactions had fully reached equilibrium. Close and open circles indicate lactose and cellobiose, respectively.

Table 7-1. MALDI-TOFMS of tryptic peptide mixture of RmCE.

Mass measured	Mass calculated	Start residue	End residue	Sequence
0584.34	0584.32	093	096	YFVR
0614.36	0614.35	248	251	WRPR
0680.36	0680.35	030	034	FWATR
0714.43	0714.43	060	066	GAILNAR
0822.40	0822.39	363	369	GGEWFAR
0903.51	0903.52	404	410	HLLEHVR
0947.53	0947.53	077	084	QLGTPLYR
1113.56	1113.58	175	183	AWRPLEDAR
1171.64	1171.61	211	220	VWPETELAAR
1215.75	1215.75	221	230	LQALIELFLR
1384.67	1384.71	047	059	VGPDGRPHPEAPR
1475.74	1475.72	382	393	VDFWKGPYHNGR
1836.94	1836.97	014	029	ALQAEVHEELTENILK

Measured and calculated molecular masses are given as protonated mono-isotopic masses.

Table 7-2. . Kinetic aarameters of RmCE for cellobiose and lactose.

Origin	Cellobiose			Lactose		
	k_{cat} (s^{-1})	K_m (mM)	k_{cat}/K_m ($s^{-1} \cdot mM^{-1}$)	k_{cat} (s^{-1})	K_m (mM)	k_{cat}/K_m ($s^{-1} \cdot mM^{-1}$)
R. marinus JCM9785	80.8	27.2	2.97	111	28.8	3.85

The reaction was carried out at 60ºC.

Table 7-3. Numbers of acidic and basic amino acids in RmCE and RaCE.

Amino acid	RmCE	RaCE
Asp	24 (5.8)	36 (9.3)
Glu	32 (8.3)	33 (8.5)
Lys	5 (1.2)	27 (6.9)
Arg	46 (11.2)	16 (4.1)
His	21 (5.1)	12 (3.1)
Total	412	389

Amino acid content (%) is provided in parentheses.

Chapter 8. General discussion and concluding remarks

8.1. General discussion

8.1.1. α-Glucosidase from *Halomonas* sp. H11 (HaG)

α-Glucosidase is an industrially important enzyme because it is capable of synthesizing oligosaccharides and glucosides. When the author started the studies on glucoside synthesis by α-glucosidase, the industrially available α-glucosidases were limited to a few. To develop value added and new glucosides, enzymes with innovative type of reaction such as specific glucosylation and high yield or rate of production of glucoside can be attractive biocatalysts especially in food, cosmetic and pharmaceutical industry.

In Capter 2, 3 and 4, the author found a novel and unique α-glucosidase (HaG) from moderate halophilic bacterium *Halomonas* sp. H11 that has potential for efficient synthesis of various glucosides. Its narrow substrate specificity for hydrolysis for almost only maltose, *p*NPG and sucrose is one of the novel features of HaG that might cause not to accumulate byproducts such as oligosaccharides and higher glucosylated compounds in the glucosides synthesis by HaG. As described in Chapter 3, HaG can use low molecular weight alcohols as acceptor molecules in transglucosylation to produce alkyl glucosides. Furthermore the synthesis efficiency of α-glucosylglycerol (αGG) using HaG was superior to that of *A. niger* α-glucosidase which was reported as the industrial biocatalyst for producing αGG. In the glucoside synthesis, a high yield and rate of production, and a few amount/kind of byproducts are industrially principal matters to save cost. To purify the synthesized product,

fewer varieties of byproducts also help to simplify the purification procedure. From these points of view, HaG is a promising candidate tor the efficient production of glucosides. A key region contributing narrow substrate specificity and high transglucosylation ability of HaG will be proved by molecular engineering methods.

Addition to the high transglucosylation activity toward alcohols and strictry narrow substrate specificity, HaG has some interesting properties to be further investigated. For example, HaG is significantly stimulated by monovalent cations such as K^+, Rb^+, NH_4^+, and Cs^+. Surprisingly the k_{catapp}/K_{mapp} value for maltose hydrolysis of HaG was increaced to 969-fold with 10 mM K^+ from that of the absence of cations. Furthermore, the optimum reaction temperature of HaG was raised to 40°C from 30°C in the presence of 10 mM NH_4^+. To my knowledge, there is no precedence of such extreme effects on enzyme activity and reaction temperature by monovalent cations, therefore HaG must be a very attractive enzyme for the basic biochemical researches. The author expects that a study of the interactions of monovalent cations and HaG will provide some insights to aid understanding of the environmental adaptation of the enzyme.

To utilize HaG for glucoside synthesis, glucosylation of 6-gingerol was investigated in Chapter 5. The transglucosylation ability of another eight known enzymes, namely α-glucosidases from *Aspergillus niger*, *Aspergillus nidulans* ABPU1, *Acremonium strictum* and *Saccharomyces cerevisiae,* and CGTases from *Geobacillus stearothermophilus, Bacillus coagulans*, *Bacillus* sp. No. 38-2, and *Bacillus clarkii* 7364 were also evaluated. Notably only HaG could transfer glucose residue to 6-gingerol to synthesize 5-α-Glc-gingerol while no transglucosylation occurred when any other seven enzymes were tested (Fig. 5-2). HaG

regioselectively and dominantly synthesizes 5-α-Glc-gingerol which is a novel chemical compound first reported in this work. The stability and water solubility of 5-α-Glc-gingerol are much superior to those of 6-gingerol. It is a typical example to show how glucosylation is powerful technique to improve physical properties of the chemicals.

It is well known that α-glucosidases are ubiquitous enzymes present in a wide variety of bacteria, fungi, yeast, plants, and animals. However, as HaG demonstrated more efficient synthesis of αGG than the previous system using α-glucosidase from *A*. *niger*, and prominence synthesis of novel glucoside, 5-α-Glc-gingerol, it would be possible to find the enzymes of desired catalytic property if the screening systems are appropreate. The author believes that this work on HaG and glucoside synthesis stimulates not only food industry but also chemical and pharmaceutical related industries, and will contribute for the development of functional materials. On the other hand, some questions arisen in this study such as why HaG is activated by monovalent cations, why HaG has strictly narrow substrate specificity, and why only HaG can synthesize 5-α-Glc-gingerol, should be precisely investigated at a molecular level.

8.1.2. Cellobiose 2-epimerases (CEs) from aerobic bacteria

With an increasing demand for functional sugars, epilactose is one of the promising oligosaccharide for healthcare. Cellobiose 2-epimerase (CE) is the most desirable biocatalyst for the production of epilactose because it can convert low priced lactose to epilactose without any dangerous chemicals. However CEs reported so far were all from anaerobic bacteria and the most of them was heat labile,

preventing the industrial utilization of CE for epilactose production. To obtain more feasible CE, the author focused on nine genes with unknown function but relatively similar to the known CE form *R. albus*.

In Chapter 6, the author selected totaly eight CE-like genes of most of which have been annotated as AGEs (*N*-acylglucosamine 2-epimerases) and the other were ‘hypothetical protein’, from various aerobic bacteria, namely *Chitinophaga pinensis* NBRC 15968, *Flavobacterium johnsoniae* NBRC 14942, *Pedobacter heparinus* NBRC 12017, *Dyadobacter fermentans* ATCC700827, *Herpetosiphon aurantiacus* ATCC23779, *Saccharophagus degradans* ATCC43961, *Spirosoma linguale* ATCC33905 and *Teredinibacter turnerae* ATCC39867, and revealed that they are all CEs but not AGEs. Each CE has unique properties on effects of pH and temperatures, and kinetic parameters (Table 6-3, Table 6-4, Fig. 7-3, Table 7-2). Interestingly bacteria possessing CE also have mannosyl glucose phosphorylase (MGP)-like genes in their genome, impying mannann degradation pathway might be in common with them. For more secure insights, a research on metabolic engineering will be required.

Continuously in Chapter 7, the author discribed the screening and identification of CE from *R. marinus* JCM9785 (RmCE) showing high thermotolerance and stablity at a wide range of pH. These properties of RmCE are ideal for the industrial use for the production of epilactose. The reaction preferency of RmCE at morderate acidic pH (pH 6.3) is also suitable for the production of epilactise because non-enzymatic reaction to generate lactulose by non-enzymatic epimerization of lactose occurs at alkarine pH and high temperature conditions. Arg contents in RmCE was significantly higher than the former reported

non-thermotorelant CE from *R. albus* (RaCE), suggesting that Arg residues in RmCE are making salt-bridge interactions with acidic amino acid residues to make the protein structure significantly rigid. Comparing analysis of thermoterelant RmCE and the other CEs obtained in Chapter 6, will give some insights for designing thermotorelant enzymes. Moreover the author expects that epilactose produced by RmCE will be avairable in industrial scale in the near future.

8.2. Concluding remarks

(1) The author screened α-glucosidase that can efficiently transfer glycosyl residue to glycerol, and the enzyme with high transglucosylation activity was found from a moderate halophilic marine bacterium, *Halomonas* sp. H11 strain, isolated from a surface of coral.

(2) α-Glucosidase from *Halomonas* sp. H11 (HaG) was purified and the enzymatic characteristics were determined. HaG was active at 30°C and neutral pH. HaG had unique properties as follows; i) significant stimulation by monovalent cations such as NH_4^+, K^+, Rb^+, and Cs^+, ii) very narrow hydrolytic specificity for substrate chain-length and glucosidic bonds, and iii) strong transglucosylation activity toward glycerol. An unique phenomenon that optimum reaction temperature of HaG was risen to 40°C in the presence of 10 mM NH_4^+ was observed.

(3) The kinetic parameters of hydrolysis of HaG for *p*NPG and maltose in a non-essential activator model and Michaelis-Menten model were determined. It was revealed that both K_m and k_{cat} for both substrates were improved by the presence of monovalent cations such as NH_4^+, K^+, Rb^+, and Cs^+. It was noteworthy that k_{cat}/K_m value for *p*NPG was increased to 969-fold by K^+.

(4) The transglucosylation ability of HaG was evaluated. HaG transfered one glucose residue to short cahin length alcohols such as glycerol, ethanol, plopylene glycol, 1-propanol and 2-propanol to produce alkyl glucoside without an accumulation of byproducts such as di- or more glucosylated compounds and maltotriose.

(5) The synthesis reaction of α-glucosylglycerol (αGG) using HaG and α-glucosidase from *A. niger* was compared. HaG showed more efficient production rate and yield of αGG than those of *A. niger* α-glucosidase. Monovalent cation contributed to accelerate the transglucosylation reaction rate of HaG.

(6) A gene encoding HaG were cloned and sequenced. It was revealed that HaG was a novel α-glucosidase classified into GH family 13. Its homologues were distributed in bacteria adapted saline environment.

(7) Transglucosylation ability of HaG and another eight enzymes, namely α-glucosidases from *Aspergillus niger*, *Aspergillus nidulans* ABPU1, *Acremonium strictum* and *Saccharomyces cerevisiae,* and cyclodextrin glucanotransferase (CGTases) from *Geobacillus stearothermophilus, Bacillus coagulans*, *Bacillus* sp. No. 38-2, and *Bacillus clarkii* 7364 were evaluated using 6-gingerol as a glycosyl acceptor. Interestingly only HaG could synthesize α-glucosylated 6-gingerol.

(8) The author determined the structure of α-glucosylated 6-gingerol as (*S*)-5-(*O*-α-d-glucopyranosyl)-1-(4-hydroxy-3-methoxyphenyl)decan-3-one (5-α-Glc-gingerol) by MS and NMR analyses. This glucoside was a novel compound first synthesized in this work. Since HaG site-specifically and regioselectively transfered glycosyl residue to 6-gingerol, 5-α-Glc-gingerol could

be synthesized by HaG with high yield (molecular yield was about 60% based on 6-gingerol).

(9) The physiological propertied of 5-α-Glc-gingerol was investigated. It was water-soluble and more stable than naked 6-gingerol against acid and heat. 5-α-Glc-gingerol was resistant to rat intestinal enzyme meant glucosidic bond of 5-α-Glc-gingerol was not digested by α-glucosidase containing in rat intestin.

(10) The author screened cellobiose 2-epimerase (CE) that can be utilized in industrial process. First, the author cloned and determined enzymatic characteristics of CE-like genes which had been annotated as *N*-acylglucosamine 2-epimerases (AGEs) from nine aerobic bacteria, *Chitinophaga pinensis* NBRC 15968, *Flavobacterium johnsoniae* NBRC 14942, *Pedobacter heparinus* NBRC 12017, *Dyadobacter fermentans* ATCC700827, *Herpetosiphon aurantiacus* ATCC23779, *Saccharophagus degradans* ATCC43961, *Spirosoma linguale* ATCC33905 and *Teredinibacter turnerae* ATCC39867, and revealed that they are all CEs but not AGEs by substrate specificity analyses.

(11) The effects of temperature and pH, and kinetic parameters for cellobiose and lactose of eight CEs from aerobic bacteria were determined. The optimum temperature of each CE was as follows; 50°C (DfCE), 45°C (HaCE and SlCE), and 35°C (the others). DfCE, HaCE and SlCE were stable up to 50°C, and the optimum pH and pH stability were different each other.

(12) Phylogenetic analysis of revealed CEs and genetically related enzymes, AGEs, aldose-ketose isomerases (AKIs) and mannose 6-phosphate isomerases (PMI) were performed. Bacteria possessing genes belonging to the CE cluster tended

to have mannosyl glucose phosphorylase (MGP)-like genes together.

(13) CE from a thermophilic marine bacterium, *R. marinus* JCM9785 (RmCE) was purified and identified. The enzymatic characteristics of RmCE expressed by recombinant *E. coli* was determined. RmCE showed highest activity at 80°C to 90°C at pH 6.3. It was also stable at a wide range of pHs. Arg contents in RmCE was significantly higher than the former reported non-thermotorelant CE from *R. albus* (RaCE), suggesting that Arg residues in RmCE are making salt-bridge interactions with acidic amino acid residues to make the protein structure significantly rigid.

(14) RmCE was the most suitable for the industrial use among nine CEs identified in this work and known CEs previously reported. The author expects that RmCE will contribute for the epilactose production in industrial process.

References

Amein, M.; Leatherwood, J. M. Mechanism of cellobiose epimerase. *Biochem. Biophys. Res. Commun.*, 1969, 36, 223–227.

Aerts, D.; Verhaeghe, T. F.; Roman, B. I.; Stevens, C. V.; Desmet, T.; Soetaert, W. Transglucosylation potential of six sucrose phosphorylases toward different classes of acceptors. *Carbhydr. Res.*, 2011, 346, 1860–1867.

Aga, H.; Yoneyama, M.; Sakai, S.; Yamamoto, I. Synthesis of 2-*O*-α-D-glucopyranosyl L-ascorbic acid by cyclomaltodextrin glucanotransferase from *Bacillus stearothermophilus*. *Agric. Biol. Chem*., 1991, 55, 1751–1756.

Aghajari, N.; Feller, G.; Gerday, C.; Haser, R. Crystal structures of the psychrophilic alpha-amylase from *Alteromonas haloplanctis* in its native form and complexed with an inhibitor. *Protein Sci*., 1998, 7, 564–572.

Aghajari, N.; Feller, G.; Gerday, C.; Haser, R. Structural basis of alpha-amylase activation by chloride. *Protein Sci*., 2002, 11, 1435–1441.

Aghajari, N.; Feller, G.; Gerday, C.; Haser, R. Structures of the psychrophilic *Alteromonas haloplanctis* alpha-amylase give insights into cold adaptation at a molecular level. *Structure*, 1998, 6, 1503–1516.

Altschul, S. F.; Gish, W.; Miller, W.; Myers, E. W.; Lipman, D. J. Basic local alignment search tool. *J*. *Mol*. *Biol*., 1990, 215, 403–410.

Baranowski, J. D. Storage stability of a processed ginger paste. *J. Food. Sci*., 1985, 50, 932–933.

Barrow, G. I.; Feltham, R. K. A. Cowan and Steel's manual for the identification of medical bacteria, 3rd ed., Cambridge University Press, 1993.

Berthelot, K.; Delmotte, F. M. Purification and characterization of an alpha-glucosidase from *Rhizobium* sp. (*Robinia pseudoacacia* L.) strain USDA 4280. *Appl*. *Environ*. *Microbiol*., 1999, 65, 2907–2911.

Bertrand, A.; Morel, S.; Lefoulon, F.; Rolland, Y.; Monsan, P.; Remaud-Simeon, M. Leuconostoc mesenteroides glucansucrase synthesis of flavonoid glucosides by acceptor reactions in aqueous-organic solvents. *Carbohydr. Res*. 2006, 341, 855–863.

Bhattarai, S.; Tran, V. H.; Duke, C. C. The stability of gingerol and shogaol in aqueous solutions. *J. Pharm. Sci.*, 2001, 90, 1658–1664.

Bock, K.; Pedersen, C.; Pedersen, H. Carbon-13 nuclear magnetic resonance data for oligosaccharides. *Adv. Carbohydr. Chem. Biochem.*, 1984, 42, 193–225.

Bradford, M. M. A rapid and sensitive method for the quantitation of microgram quantities of protein utilizing the principle of protein-dye binding. *Anal. Biochem.*, 1976, 72, 248–254.

Brayer, G. D.; Luo, Y.; Withers, S. G. The structure of human pancreatic alpha-amylase at 1.8 Å resolution and comparisons with related enzymes. *Protein Sci*., 1995, 4, 1730–1742.

Cantarel, B. L.; Coutinho, P. M.; Rancurel, C.; Bernard, T.; Lombard, V.; Henrissat, B. The Carbohydrate-Active EnZymes database (CAZy): an expert resource for Glycogenomics. *Nucleic Acids Res.*, 2009, 37, 233–238.

Centeno, M. S.; Guerreiro, C. I.; Dias, F. M.; Morland, C.; Tailford, L. E.; Goyal, A.; Prates, J. A.; Ferreira, L. M.; Caldeira, R. M.; Mongodin, E. F.; Nelson, K. E.; Gilbert, H. J.; Fontes, C. M. Galactomannan hydrolysis and mannose metabolism in *Cellvibrio mixtus*. *FEMS Microbiol Lett.*, 2006, 261, 123–132.

Chiba, S. Molecular mechanism in alpha-glucosidase and glucoamylase. *Biosci. Biotech. Biochem*., 1997, 61, 1233–1239.

Chiba, S. α-Glucosidases, In *Handbook of amylases and related enzymes*, 1st ed.; Amylase Research Society of Japan, Ed.; Pergamon Press: Oxford, 1988, pp 104–116.

D'Amico, S.; Gerbay, C.; Feller, G. Structural similarities and evolutionary relationships in chloride-dependent alpha-amylases. *Gene*, 2000, 253, 95–105.

Dixon, M.; Webb, E. C. Enzyme inhibition and activation. *In* Enzymes, 3rd ed.; M. Dixon, and E. C. Webb. Ed.; Academic Press, New York, NY., 1979, pp 389–391.

Feller, G.; Bussy, O.; Houssier, C.; Gerday, C. Structural and functional aspects of chloride binding to *Alteromonas haloplanctis* alpha-amylase. *J*. *Biol*. *Chem*., 1996, 271, 23836–23841.

Feller, G.; Payan, F.; Theys, F.; Qian, M.; Haser, R.; Gerday, C. Stability and structural analysis of alpha-amylase from the antarctic psychrophile *Alteromonas haloplanctis* A23. *Eur*. *J*. *Biochem*., 1994, 222, 441–447.

Goedl, C.; Sawangwan, T.; Mueller, M.; Schwarz, A.; Nidetzky, B. A high-yielding biocatalytic process for the production of 2-*O*-(alpha-D-glucopyranosyl)-*sn*-glycerol, a natural osmolyte and useful moisturizing ingredient. *Angew*. *Chem*. *Int*. *Ed*. *Engl*., 2008, 47, 10086–10089.

Goujon, M.; McWilliam, H.; Li, W.; Valentin, F.; Squizzato, S.; Paern, J.; Lopez, R. A new bioinformatics analysis tools framework at EMBL-EBI. *Nucleic Acids Res*., 2010, 38, W695–699.

Govindarajan, V. S. Ginger--chemistry, technology, and quality evaluation: part 1.

Crit. Rev. Food. Sci. Nutr., 1982, 17, 1–96.

Hanahan, D. Studies on transformation of *Escherichia coli* with plasmids. *J. Mol. Biol.*, 1983, 166, 557–580.

Harada, N.; Zhao, J.; Kurihara, H.; Nakagata, N.; Okajima, K. Effects of topical application of alpha-D-glucosylglycerol on dermal levels of insulin-like growth factor-i in mice and on facial skin elasticity in humans. *Biosci*. *Biotechnol*. *Biochem*., 2010, 74, 759–765.

Hincha, D. K.; Hagemann, M. Stabilization of model membranes during drying by compatible solutes involved in the stress tolerance of plants and microorganisms. *Biochem*. *J*., 2004, 383, 277–283.

Ho, S. N.; Hunt, H. D.; Horton, R.M.; Pullen, J. K.; Pease, L. R. Site-directed mutagenesis by overlap extension using the polymerase chain reaction. *Gene*, 1989, 77, 51–59.

Hoelzle, I.; Streeter, J. G. Stimulation of α-glucosidases from fast-growing rhizobia and *Agrobacterium tumefaciens* by K^+, NH^+_4, and Rb^+. *Can*. *J*. *Microbiol*., 1989, 36, 223–227.

Hondoh, H.; Saburi, W.; Mori, H.; Okuyama, M.; Nakada, T.; Matsuura, Y.; Kimura, A. Substrate recognition of α-1,6-glucosidic linkage hydrolyzing enzyme, dextran glucosidase from *Streptococcus mutans*. *J*. *Mol*. *Biol*., 2008, 378, 911–920.

Hung, V. S.; Hatada, Y.; Goda, S.; Lu, J.; Hidaka, Y.; Li, Z.; Akita, M.; Ohta, Y.; Watanabe, K.; Matsui, H.; Ito, S.; Horikoshi, K. alpha-Glucosidase from a strain of deep-sea *Geobacillus*: a potential enzyme for the biosynthesis of complex carbohydrates. *Appl*. *Microbiol*. *Biotechnol*., 2005, 68, 757–765.

Isa, Y.; Miyakawa, Y.; Yanagisawa, M.; Goto, T.; Kang, M. S.; Kawada, T.; Morimitsu, Y.; Kumota, K.; Tsuda, T. 6-Shogaol and 6-gingerol, the pungent of ginger, inhibit TNF-alpha mediated downregulation of adiponectin expression via different mechanisms in 3T3-L1 adipocytes. *Biochem*. *Biophys*. *Res*. *Commun*., 2008, 373, 429–434.

Isegawa, Y.; Sheng, J.; Sokawa, Y.; Yamanishi, K.; Nakagomi, O.; Ueda, S. Selective amplification of cDNA sequence from total RNA by cassette-ligation mediated polymerase chain reaction (PCR): application to sequencing 6.5 kb genome segment of hantavirus strain B-1. *Mol*. *Cell*. *Probes*, 1992, 6, 467-475.

Ito, S.; Hamada, S.; Ito, H.; Matsui, H.; Ozawa, T.; Taguchi, H.; Ito, S. Site-directed mutagenesis of possible catalytic residues of cellobiose 2-epimerase from *Ruminococcus albus*. *Biotechnol. Lett*., 2009, 31, 1065–1071.

Ito, S.; Hamada, S.; Yamaguchi, K.; Umene, S.; Ito, H.; Matsui, H.; Ozawa, T.; Taguchi, H.; Watanabe, J.; Wasaki, J.; Ito, S. Cloning and sequencing of the cellobiose 2-epimerase gene from an obligatory anaerobe, *Ruminococcus albus*. *Biochem. Biophys. Res. Commun.*, 2007, 360, 640–645.

Ito, S.; Taguchi, H.; Hamada, S.; Kawauchi, S.; Ito, H.; Senoura, T.; Watanabe, J.; Nishimukai, M.; Ito, S.; Matsui, H. Enzymatic properties of cellobiose 2-epimerase from *Ruminococcus albus* and the synthesis of rare oligosaccharides by the enzyme. *Appl. Microbiol. Biotechnol.*, 2008, 79, 433–441.

Ito, T.; Mikami, B.; Hashimoto, W.; Murata, K. Crystal structure of YihS in complex with D-mannose: structural annotation of Escherichia coli and Salmonella enterica yihS-encoded proteins to an aldose-ketose isomerase. *J. Mol. Biol.*, 2008, 377, 1443–1459.

Itoh, T.; Mikami, B.; Maru, I.; Ohta, Y.; Hashimoto, W.; Murata, K. Crystal

structure of N-acyl-D-glucosamine 2-epimerase from porcine kidney at 2.0 Å resolution. *J. Mol. Biol.*, 2000, 303, 733–744.

Ju, S. A.; Park, S. M.; Lee, Y. S.; Bae, J. H.; Yu, R.; An, W. G.; Suh, J. H.; Kim, B. S. Administration of 6-gingerol greatly enhances the number of tumor-infiltrating lymphocytes in murine tumors. *Int. J. Cancer.* 2011, 130, 2618–2628.

Kato, N.; Suyama, S.; Shirokane, M.; Kato, M.; Kobayashi, T.; Tsukagoshi, N. Novel alpha-glucosidase from Aspergillus nidulans with strong transglycosylation activity. *Appl. Environ. Microbiol*., 2002, 68, 1250–1256.

Kaye, J. Z.; Márquez, M. C.; Ventosa, A.; Baross, J. A. *Halomonas neptunia* sp. nov., *Halomonas sulfidaeris* sp. nov., *Halomonas axialensis* sp. nov. and *Halomonas hydrothermalis* sp. nov.: halophilic bacteria isolated from deep-sea hydrothermal-vent environments. *Int*. *J*. *Syst*. *Evol*. *Microbiol*., 2004, 54, 499–511.

Kelly, C.T.; Fogarty, W. Microbial alpha–glucosidases. *Process Biochem*., 1983, 18, 6–12.

Klähn, S.; Hagemann, M. Compatible solute biosynthesis in cyanobacteria. *Environ*. *Microbiol*. 2011, 13, 551–562.

Kometani, T.; Nishimura, T.; Nakae, T.; Takii, H.; Okada, S. Synthesis of neohesperidin glycosides and naringin glycosides by cyclodextrin glucanotransferase from an alkalophilic *Bacillus species*. *Biosci. Biotechnol. Biochem.*, 1996, 60, 645–649.

Kurosu, J.; Sato, T.; Yoshida, K.; Tsugane, T.; Shimura, S.; Kirimura, K.; Kino, K.; Usami, S. Enzymatic synthesis of alpha-arbutin by alpha-anomer-selective glucosylation of hydroquinone using lyophilized cells of *Xanthomonas campestris* WU-9701. *J*. *Biosci*. *Bioeng*. 2002, 93, 328–330.

Laemmli, U. K. Cleavage of structural proteins during the assembly of the head of bacteriophage T4. *Nature*, 1970, 227, 680–685.

Larson, S.B.; Greenwood, A.; Cascio, D.; Day, J.; McPherson, A. Refined molecular structure of pig pancreatic alpha-amylase at 2.1 Å resolution. *J*. *Mol*. *Biol*. 1994, 235, 1560–1584.

Lee, Y.; Wu, H.; Chang, Y.; Wang, W.; Hsu, W. The central cavity from the (alpha/alpha)$_6$ barrel structure of *Anabaena* sp. CH1 N-acetyl-D-glucosamine 2-epimerase contains two key histidine residues for reversible conversion. *J. Mol. Biol.*, 2007, 367, 895–908.

Leemhuis, H.; Kelly, R. M.; Dijkhuizen, L. Engineering of cyclodextrin glucanotransferases and the impact for biotechnological applications. *Appl. Microbiol. Biotechnol*., 2010, 85, 823–835.

Luley-Goedl, C.; Nidetzky, B. Carbohydrate synthesis by disaccharide phosphorylases: reactions, catalytic mechanisms and application in the glycosciences. *Biotechnol. J.*, 2010, 5, 1324–1338.

Maurus, R.; Begum, A.; Kuo, H. H.; Racaza, A.; Numao, S.; Andersen, C.; Tams, J. W.; Vind, J.; Overall, C. M.; Withers, S. G.; Brayer, G. D. Structural and mechanistic studies of chloride induced activation of human pancreatic alpha-amylase. *Protein Sci*., 2005, 14, 743–755.

McCarter, J. D.; Withers, S. G. Mechanisms of enzymatic glycoside hydrolysis. *Curr. Opin. Struct. Biol*., 1994, 4, 885–892.

McCarter, J. D.; Withers, S. G. Unequivocal identification of Asp-214 as the catalytic nucleophile of *Saccharomyces cerevisiae* alpha-glucosidase using 5-fluoro glycosyl fluorides. *J*. *Biol*. *Chem*. 1996, 271, 6889–6894.

Merkler, D. J.; Farrington, G. K.; Wedler, F. C. Protein thermostability. Correlations between calculated macroscopic parameters and growth temperature for closely related thermophilic and mesophilic bacilli. *Int. J. Pept. Protein Res.*, 1981, 18, 430–442.

Miwa, I.; Okuda, J.; Maeda, K.; Okuda, G. Mutarotase effect on colorimetric determination of blood glucose with beta-D-glucose oxidase. *Clin*. *Chim*. *Acta*. 1972, 37, 538–540.

Mrabet, N. T.; van den Broeck, A.; van den Brande, I.; Stanssens, P.; Laroche, Y.; Lambeir, A.; Matthijssens, G.; Jenkins, J.; Chiadmi, M.; van Tilbeurgh. H.; Rey, F.; Janin, J.; Quax, W. J.; Lasters, I,; De Maeyer, M.; Wodak, S. J. Arginine residues as stabilizing elements in proteins. *Biochemistry*, 1992, 31, 2239-2253.

Murase, H.; Yamauchi, R.; Kato, K.; Kunieda, T.; Terao, J. Synthesis of a novel vitamin E derivative, 2-(alpha-D-glucopyranosyl) methyl-2,5,7,8-tetramethylchroman-6-ol, by alpha-glucosidase-catalyzed transglycosylation. *Lipids*, 1997, 32, 73–78.

Nakagawa, H.; Dobashi, Y.; Sato, T.; Yoshida, K.; Tsugane, T.; Shimura, S.; Kirimura, K.; Kino, K.; Usami, S. Alpha-anomer-selective glucosylation of menthol with high yield through a crystal accumulation reaction using lyophilized cells of *Xanthomonas campestris* WU-9701. *J. Biosci. Bioeng*., 2000, 89, 138–144.

Nakagawa, K.; Kawasaki, H. DNA sequence analysis, *In* Identification manual of Actinomycetes, the society for actinomycetes Japan Ed., Business Center for Academic societies Japan, Tokyo. 2001, pp 83–117.

Nakano, H.; Kiso, T.; Okamoto, K.; Tomita, T.; Manan, M. B.; Kitahata, S. Synthesis of glycosyl glycerol by cyclodextrin glucanotransferases. *J*. *Biosci*. *Bioeng.,* 2003*,* 95, 583-588.

Nakao, M.; Nakayama, T.; Kakudo, A.; Inohara, M.; Harada, M.; Omura, F.; Shibano, Y. Structure and expression of a gene coding for thermostable alpha-glucosidase with a broad substrate specificity from Bacillus sp. SAM1606. *Eur*. *J*. *Biochem*., 1994, 220, 293–300.

Nielsen, M.; Lundegaard, C.; Lund, O.; Petersen, T. N. CPHmodels-3.0--remote homology modeling using structure-guided sequence profiles. *Nucleic Acids Res.*, 2010, 38, W576–581.

Nishimukai, M.; Watanabe, J.; Taguchi, H.; Senoura, T.; Hamada, S.; Matsui, H.; Yamamoto, T.; Wasaki, J.; Hara, H.; Ito, S. Effects of epilactose on calcium absorption and serum lipid metabolism in rats. *Agric. Food Chem.*, 2008, 56, 10340–10345.

Nitta, A.; Takenaka, F.; Iki, M.; Matsumura, E.; Sakaguchi, M. Antitumor agents containing alpha-D-glucosylglycerols and food and cosmetics containing them 2007, JP patent 2007-262023.

Nolan, M. et al. Complete genome sequence of *Rhodothermus marinus* type strain (R-10). *Stand. Genomic Sci.*, 2009, 1, 283–290.

Park, C. S.; Kim, J. E.; Choi, J. G.; Oh, D. K. Characterization of a recombinant cellobiose 2-epimerase from *Caldicellulosiruptor saccharolyticus* and its application in the production of mannose from glucose. *Appl. Microbiol. Biotechnol.*, 2011, 92, 1187–1196.

Perutz, M. F.; Raidt, H. Stereochemical basis of heat stability in bacterial ferredoxins and in haemoglobin A2. *Nature*, 1975, 255, 256–259.

Pluskal, M. G.; Przekop, M. B.; Kavonian, M. R.; Vecoli, C.; Hicks, D. A. Immobilon PVDF transfer membrane. a new membrane substrate for western blotting of proteins. *Bio Techniques*, 1986, 4, 272–283.

Qian, M.; Haser, R.; Payan, F. Structure and molecular model refinement of pig pancreatic alpha-amylase at 2.1 Å resolution. *J*. *Mol*. *Biol*., 1993, 231, 785-799.

Ramasubbu, N.; Paloth, V.; Luo, Y.; Brayer, G. D.; Levine, M. J. Structure of human salivary alpha-amylase at 1.6 Å resolution: implications for its role in the oral cavity. *Acta Crystallogr*. *D*. *Biol*. *Crystallogr*. 1996, 52, 435–446.

Saburi, W.; Mori, H.; Saito, S.; Okuyama, M.; Kimura, A. Structural elements in dextran glucosidase responsible for high specificity to long chain substrate. *Biochim*. *Biophys*. *Acta,* 2006, 1764, 688–698.

Saburi, W.; Yamamoto, T.; Taguchi, H.; Hamada, S.; Matsui, H. Practical preparation of epilactose produced with cellobiose 2-epimerase from *Ruminococcus albus* NE1. *Biosci. Biotechnol. Biochem.*, 2010, 74, 1736–1737.

Saitou, N.; Nei, M. The neighbor-joining method: a new method for reconstructing phylogenetic trees. *Mol. Biol. Evol.*, 1987, 4, 406–425.

Sambrook, J.; Russell, D. W. “Molecular Cloning: a Laboratory Manual” 3rd ed., Cold Spring Harbor Laboratory Press, Cold Spring Harbor, New York, NY., 2001.

Sánchez-Porro, C.; Kaur, B.; Mann, H.; Ventosa, A. *Halomonas titanicae* sp. nov., a halophilic bacterium isolated from the RMS Titanic. *Int*. *J*. *Syst*. *Evol*. *Microbiol*. 2010, 60, 2768–2774.

Sato, T.; Nakagawa, H.; Kurosu, J.; Yoshida, K.; Tsugane, T.; Shimura, S.; Kirimura, K.; Kino, K.; Usami, S. Alpha-anomer-selective glucosylation of (+)-catechin by the crude enzyme, showing glucosyl transfer activity, of *Xanthomonas campestris* WU-9701. *J. Biosci. Bioeng*., 2000, 90, 625–630.

Senoura, T.; Ito, S.; Taguchi, H.; Higa, M.; Hamada, S.; Matsui, H.; Ozawa, T,; Jin, S.; Watanabe, J.; Wasaki, J.; Ito, S. *Biochem. Biophys. Res. Commun.*,

2011, 408, 701–706.

Senoura, T.; Taguchi, H.; Ito, S.; Hamada, S.; Matsui, H.; Fukiya, S.; Yokota, A.; Watanabe, J.; Wasaki, J.; Ito, S. Identification of the cellobiose 2-epimerase gene in the genome of *Bacteroides fragilis* NCTC 9343. *Biosci. Biotechnol. Biochem.*, 2009, 73, 400–406.

Shaikh, F. A.; Withers, S. G. Teaching old enzymes new tricks: engineering and evolution of glycosidases and glycosyl transferases for improved glycoside synthesis. *Biochem. Cell. Biol.*, 2008, 86, 169–177.

Shirai, T.; Hung, V. S.; Morinaka, K.; Kobayashi, T.; Ito, S. Crystal structure of GH13 alpha-glucosidase GSJ from one of the deepest sea bacteria. *Proteins*, 2008, 73, 126–133.

Shulter, C. H. Enzymes activated by monovalent cations. *Science*, 1970, 168, 789–795.

Sievers, F.; Wilm, A.; Dineen, D.; Gibson, T. J.; Karplus, K.; Li, W.; Lopez, R.; McWilliam, H.; Remmert, M.; Söding, J.; Thompson, J. D.; Higgins, D. G. Fast, scalable generation of high-quality protein multiple sequence alignments using Clustal Omega. *Mol*. *Syst*. *Biol*., 2011, 7:539. doi:10.1038/msb.2011.75.

Strobl, S.; Maskos, K.; Betz, M.; Wiegand, G.; Huber, R.; Gomis-Rüth, F. X.; Glockshuber, R. Crystal structure of yellow meal worm alpha-amylase at 1.64 Å resolution. *J. Mol*. *Biol*., 1998, 278, 617–628.

Suzuki, T.; Nishimukai, M.; Shinoki, A.; Taguchi, H.; Fukiya, S.; Yokota, A.; Saburi, W.; Yamamoto, T.; Hara, H.; Matsui, H. Ingestion of epilactose, a non-digestible disaccharide, improves postgastrectomy osteopenia and anemia in rats through the promotion of intestinal calcium and iron absorption. *J. Agric. Food Chem.*, 2010, 58, 10787–10792.

Suzuki, T.; Nishimukai, M.; Takechi, M.; Taguchi, H.; Hamada, S.; Yokota, A.; Ito, S.; Hara, H,; Matsui, H. The nondigestible disaccharide epilactose increases paracellular Ca absorption via rho-associated kinase- and myosin light chain kinase-dependent mechanisms in rat small intestines. *J. Agric. Food Chem.*, 2010, 58, 1927–1932.

Suzuki, Y.; Suzuki, K. Enzymatic formation of 4^{G}-alpha-D-Glucopyranosyl-rutint. *Agric. Biol. Chem.*, 1991, 5, 181–187.

Taguchi, H.; Senoura, T.; Hamada, S.; Matsui, H.; Kobayashi, Y.; Watanabe, J.; Wasaki, J.; Ito, S. Cloning and sequencing of the gene for cellobiose 2-epimerase from a ruminal strain of *Eubacterium cellulosolvens*. *FEMS Microbiol. Lett.*, 2008, 287, 34–40.

Takaku, H.; Manufacture of oligosaccharides. In *Handbook of amylases and related enzymes*, 1st ed.; Amylase Research Society of Japan, Ed.; Pergamon Press: Oxford, 1988, pp.212–222.

Takenaka, F.; Uchiyama, H. Synthesis of alpha-D-glucosylglycerol by alpha-glucosidase and some of its characteristics. *Biosci. Biotechnol. Biochem*., 2000, 64, 1821–1826.

Takenaka, F.; Uchiyama, H.; Imamura, T. Identification of alpha-D-glucosylglycerol in sake. *Biosci*. *Biotechnol*. *Biochem*., 2000, 64, 378–385.

Tamegai, H.; Furukawa, T.; Nitta, J.; Chikuma, S.; Miyazaki, M.; Nogi, Y.; Arakawa, S.; Kato, C.; Horikoshi, K. *Halomonas* sp. strain DT-W, a halophile from the 11,000 m-depth of the Mariana Trench. *Extremophiles*, 2006, 5, 27–33.

Tamura, K.; Peterson, D.; Peterson, N.; Stecher, G.; Nei, M.; Kumar, S. MEGA5: molecular evolutionary genetics analysis using maximum likelihood, evolutionary

distance, and maximum parsimony methods. *Mol. Biol. Evol.*, 2011, 28, 2731–2739.

Thompson, J. D.; Higgins, D. G.; Gibson, T. J. CLUSTAL W: improving the sensitivity of progressive multiple sequence alignment through sequence weighting, position-specific gap penalties and weight matrix choice. *Nucleic Acids Res.*, 1994, 22, 4673–4680.

Tomazic, S. J.; Klibanov, A. M. Why is one *Bacillus* alpha-amylase more resistant against irreversible thermoinactivation than another? *J. Biol. Chem.*, 1988, 263, 3092–3096.

Tyler, T.; Leatherwood, J. M. Epimerization of disaccharides by enzyme preparations from *Ruminococcus albus*. *Arch. Biochem. Biophys.*, 1967, 119, 363–367.

Usami, S., et al. 2001, Production of glycoside with α-glucosidase and new alpha-glucosidase and its production. JP patent 2001-46096.

Vreeland, R. H. 2005. Genus I. *Halomonas*. , *In* Bergey's manual of systematic bacteriology.2 nd ed., Vol. 2. (The proteobacteria), part B, The gammaproteobacteria, D. J.Brenner, N. R. Kreig, J. T. Staley, and G. M. Garrity Ed., Springer, New York, NY., 2005, pp 300–313.

Watanabe, K.; Chishiro, K.; Kitamura, K.; Suzuki, Y. Proline residues responsible for thermostability occur with high frequency in the loop regions of an extremely thermostable oligo-1,6-glucosidase from *Bacillus thermoglucosidasius* KP1006. *J. Biol. Chem.*, 1991, 266, 24287–24294.

Watanabe, K.; Hata, Y.; Kizaki, H.; Katsube, Y.; Suzuki, Y. The refined crystal structure of *Bacillus cereus* oligo-1,6-glucosidase at 2.0 Å resolution: structural characterization of proline-substitution sites for protein thermostabilization. *J.*

Mol. *Biol*., 1997, 269, 142–153.

Wohlfarth, A.; Severin, J.; Galinski, E. A. The spectrum of compatible solutes in heterotrophic halophilic eubacteria of the family *Halomonadaceae*. *J*. *Gen*. *Microbiol*. 1990, 136, 705–712.

Yamamoto, I.; Muto, N.; *J*. *Nutr*. *Sci*. *Vitaminol*., 1992, Spec-No: 161–164.

Yamamoto, T.; Unno, T.; Sugawara, M.; Goda, T. Properties of a nigeose and nigerosylmaltooligosaccharides-suppplemented syrup. *J. Appl. Glycosci*., 1999, 46, 475–482.

Yoshida, K.; Takenaka, F.; Nitta, A.; Iki, M. 2007, α-D-Glucopyranosyl glycerol derivatives as antiallergic agents, health foods, and cosmetics. JP patent 2007-137862.

Acknowledgements

To complete this work, I have been helped by many people for 4 years (2008-2012). First of all, I am grateful to Professor Dr. Hideo Nakano (Nagoya University) for kind constructive comments and warm encouragement to construct this degree thesis. I am deeply thankful to Mr. Atsushi Tona, Dr. Mikio Yamamoto, Dr. Atsushi Totsuka, Dr. Masayasu Takada, and Dr. Takeshi Yamamoto at Nihon Shokuhin Kako Co., Ltd. for giving me an opportunity to perform this work. At the same time, I also thank Professor Dr. Toshiaki Kudo (Nagasaki University) for offering a unique microorganism collection of the ocean. It was critical matter to get started this work. I also thank Professor Dr. Hirokazu Matsui, Associate Proffessor Dr. Haruhide Mori at Hokkaido University, who are concerning to the work for CE screening.

To achieve whole this work, I particularly thank Assistant Professor Dr. Wataru Saburi (Hokkaido University) for teaching me a throughout of the experiments and kind support for writing papers. I thank Professor Dr. Shigenori Kumazawa and Associate Professor Dr. Yasuaki Kawarasaki for measuring the NMR and mass spectra (University of Shizuoka). I also thank Professor Dr. Tetsuo Kobayashi (Nagoya University) for kindly supplying a fungal strain.

All of this work was performed at research institute of Nihon Shokuhin Kako Co., Ltd. (Fuji, Shizuoka). I thank co-workers at Nihon Shokuhin Kako. Especially I thank Dr. Koki Wada, Mr. Yoshinori Nakagawa and Mr. Yutaka Kimoto for insightful discussion. I also thank Mr. Kenta Aizawa and Mr. Hideaki Ishida for supporting NMR and MS analyses.

Finally I appreciate the generous support and encouragement by my family.

The author, Teruyo Ojima

List of publications

Ojima, T.; Saburi, W.; Yamamoto, T.; Kudo, T., Characterization of *Halomonas* sp. strain H11 α-glucosidase activated by monovalent cations and its application for efficient synthesis of α-D-glucosylglycerol. *Appl. Environ. Microbiol*., 2012, 78, 1836-1845

Ojima, T.; Aizawa, K.; Saburi, W.; Yamamoto, T., α-Glucosylated 6-gingerol: chemoenzymatic synthesis using α-glucosidase from *Halomonas* sp. H11, and its physical properties. *Carbohydr*. *Res*., 2012, 354, 59-64

Ojima, T,; Saburi, W,; Sato, H,; Yamamoto, T,; Mori, H,; Matsui H., Biochemical characterization of a thermophilic cellobiose 2-epimerase from a thermohalophilic bacterium, *Rhodothermus marinus* JCM9785. *Biosci*. *Biotechnol*. *Biochem*., 2011, 75, 2162-2168.

Ojima, T.; Saburi, W.; Yamamoto, T.; Mori, H.; Matsui, H., Identification of cellobiose 2-epimerases from various aerobes. *Biosci*. *Biotechnol*. *Biochem., In press.*

List of related publications

Kamiya, T.; Ojima, T.; Sugimoto, K.; Nakano, H.; Kawarasaki, Y., Quantitative Y2H screening: cloning and signal peptide engineering of a fungal secretory LacA gene and its application to yeast two-hybrid system as a quantitative reporter. *J. Biotechnol*., 2010, 146, 151-159.

Kojima, T.; Nagao, N.; Ando, D.; Ojima, T.; Kawarasaki, Y.; Kobayashi, I.; Nakajima, M.; Nakano, H., Emulsion culture: a miniaturized library screening system based on micro-droplets in an emulsified medium. *J. Biosci. Bioeng*., 2011, 112, 299-303.

Sato, H.; Saburi, W.; Ojima, T.; Taguchi, H.; Mori, H.; Matsui, H., Immobilization of thermostable cellobiose 2-epimerase from *Rhodothermus marinus* JCM9785 and continuous production of epilactose. *Biosci. Biotechnol. Biochem*. 2012, 76, 1584-1587.

Supplemental Figure

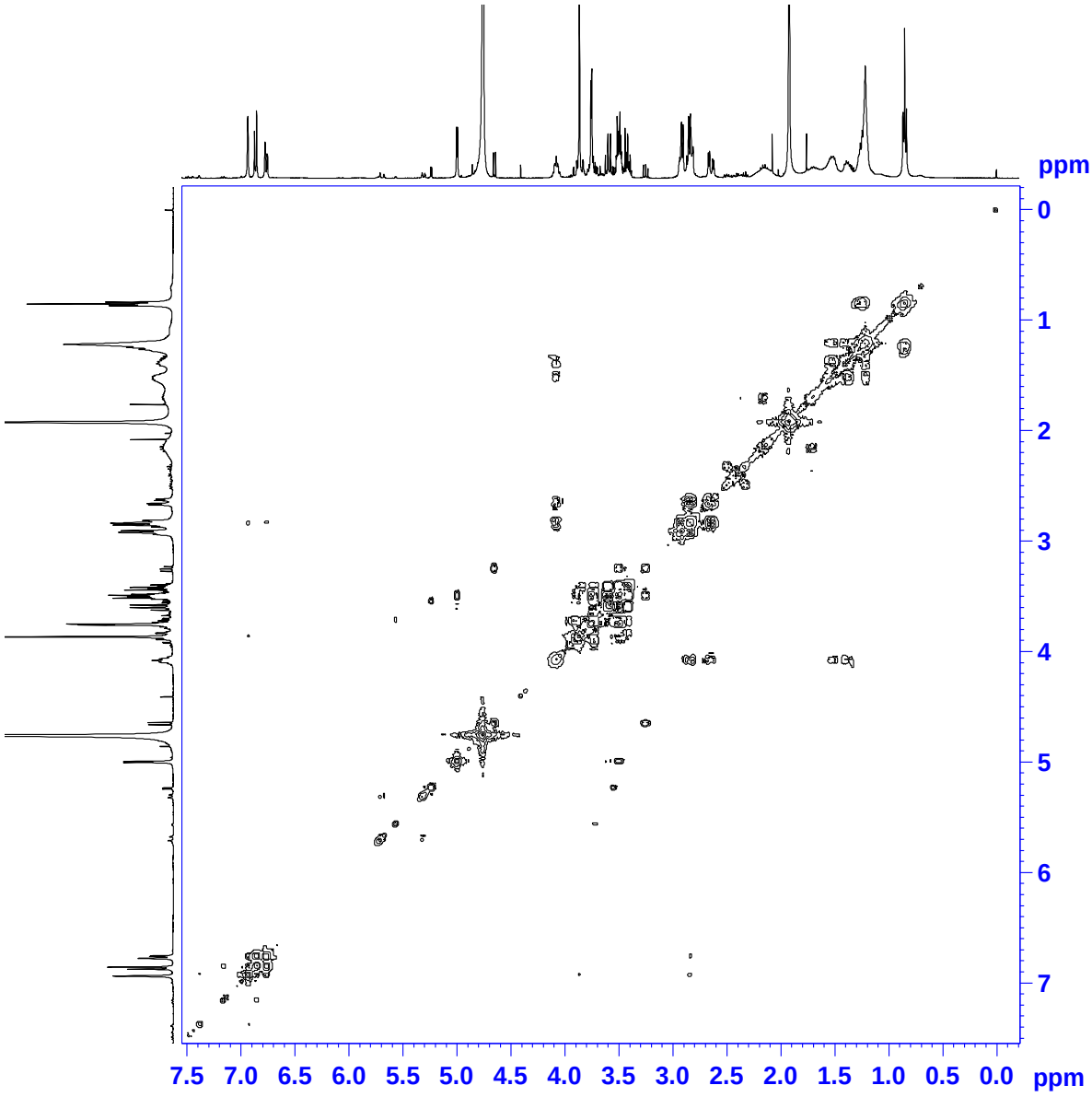

Supplemental Fig. 1. NMR spectra.

HH-COSY (whole view)

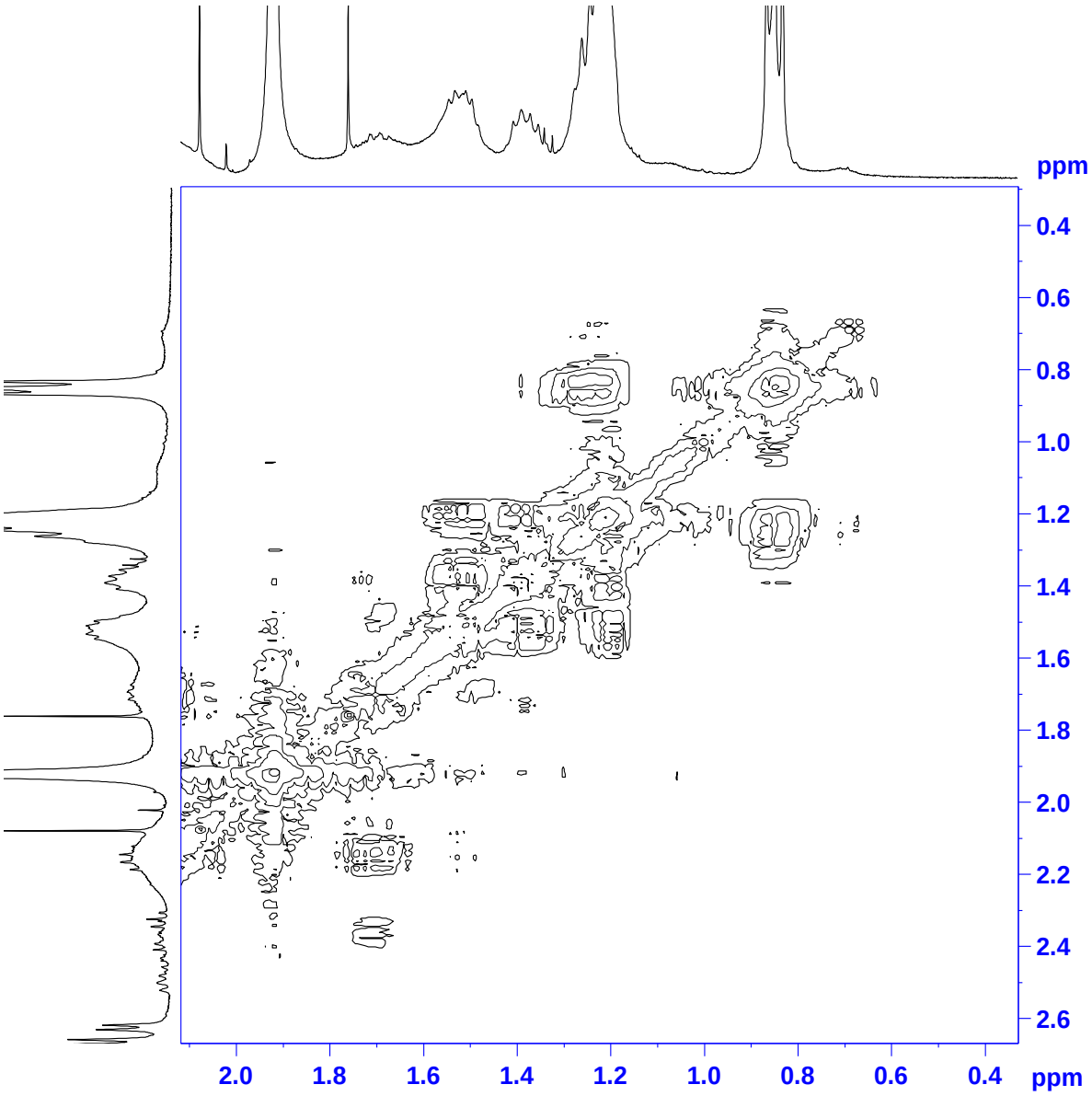

Supplemental Fig. 1. NMR spectra (continued).

HH-COSY (enlarged view 1)

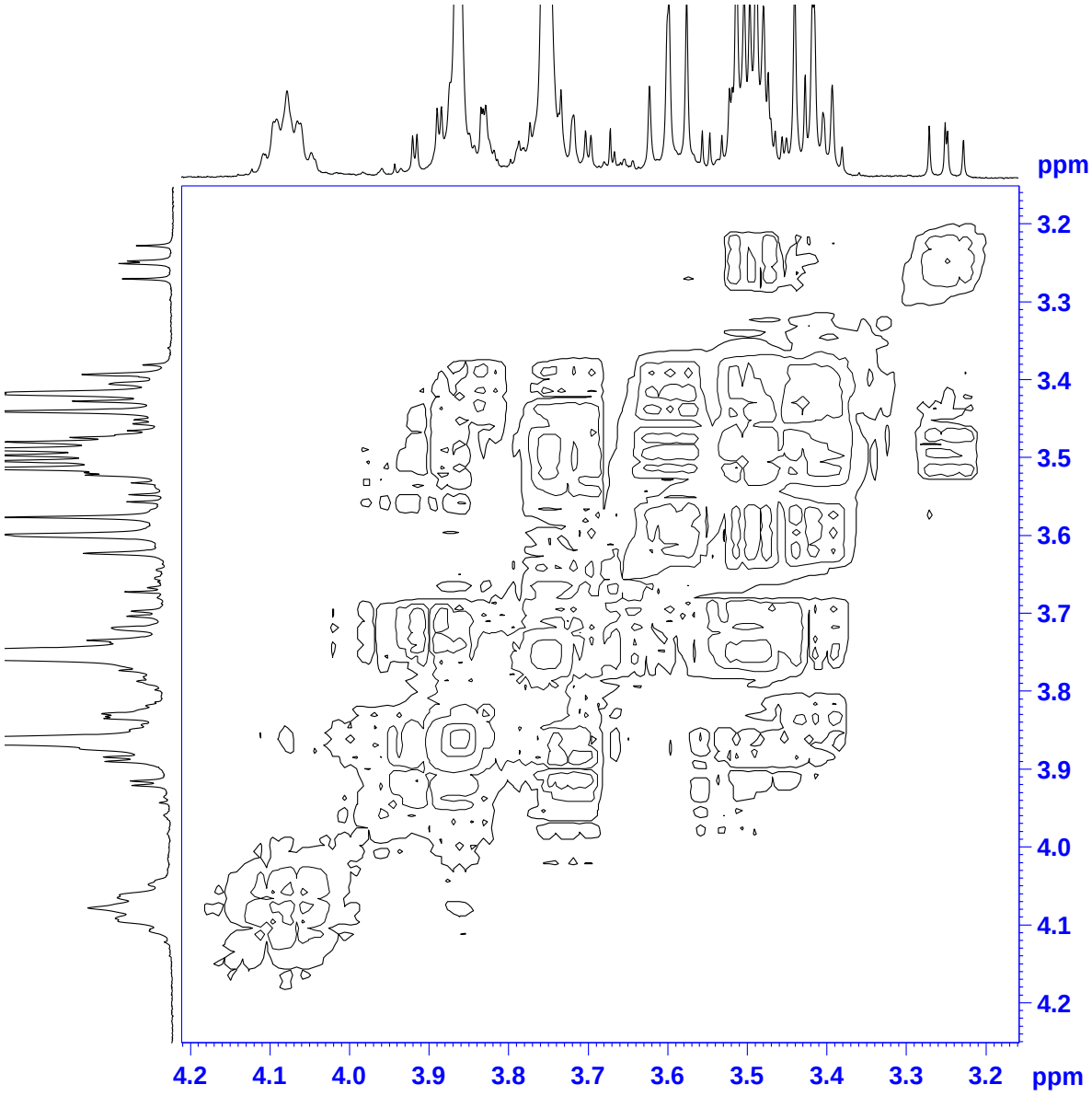

Supplemental Fig. 1. NMR spectra (continued).

HH-COSY (enlarged view 2)

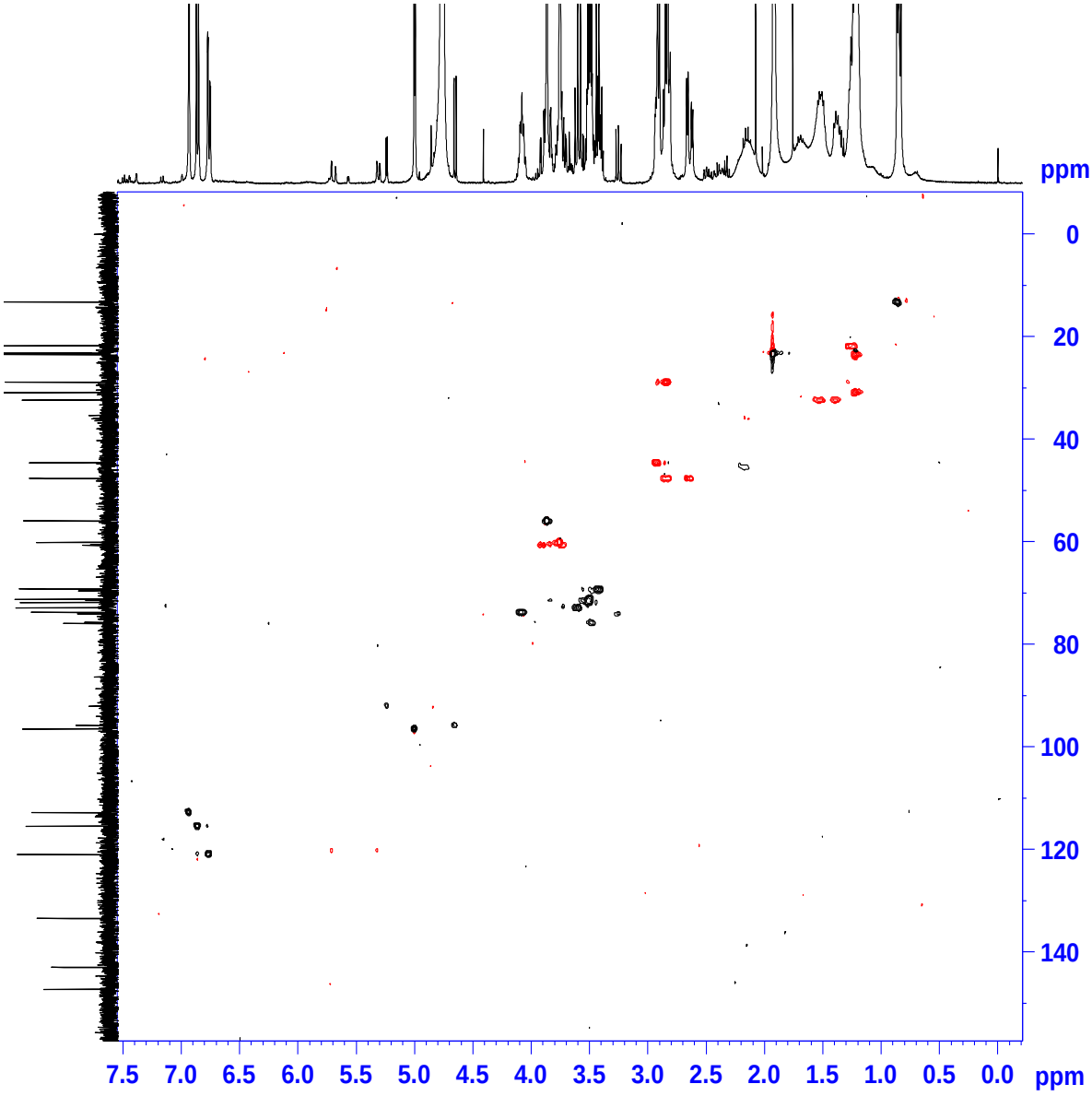

Supplemental Fig. 1. NMR spectra (continued).

HSQC (whole view)

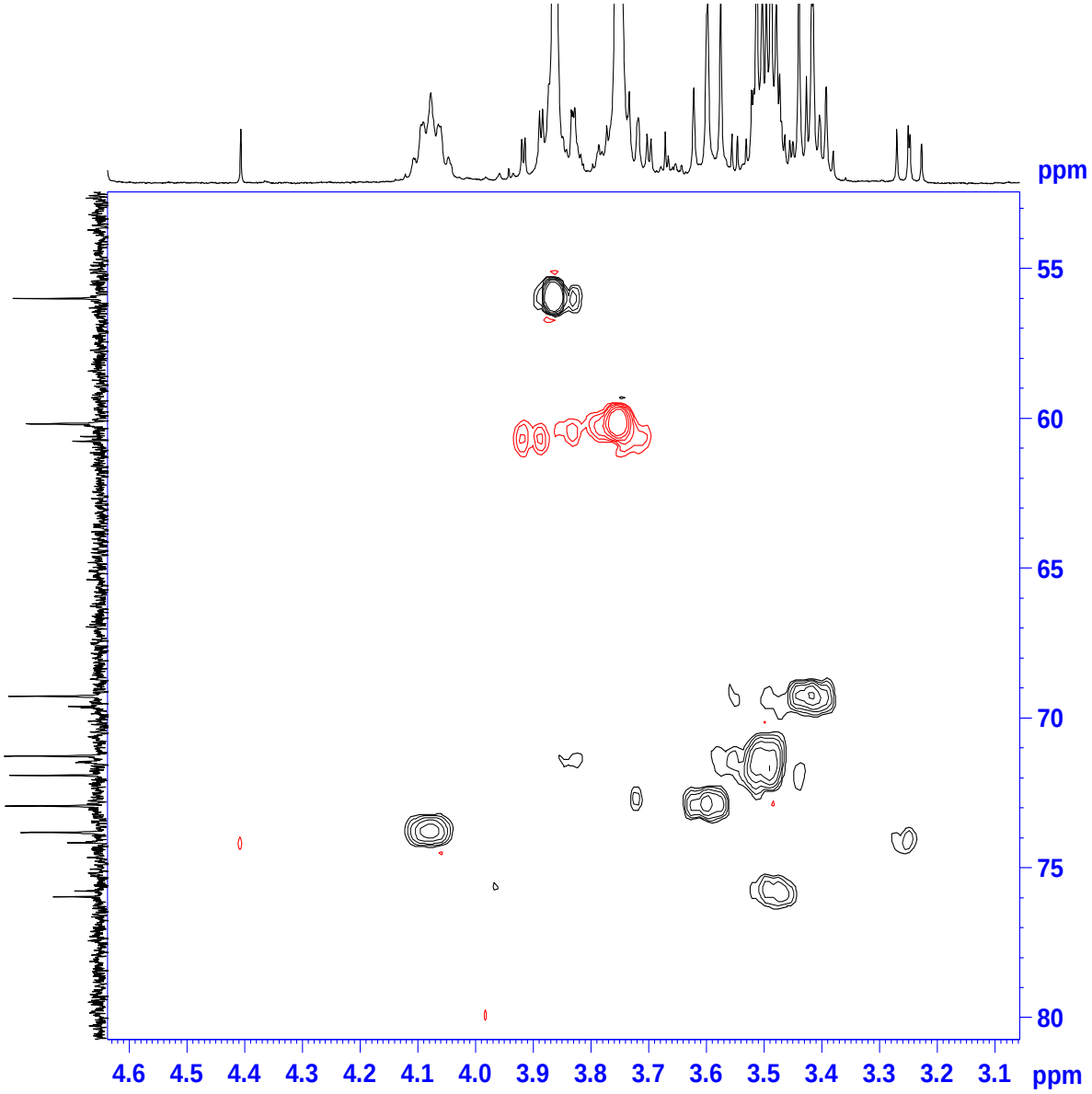

Supplemental Fig. 1. NMR spectra (continued).

HSQC (enlarged view 1)

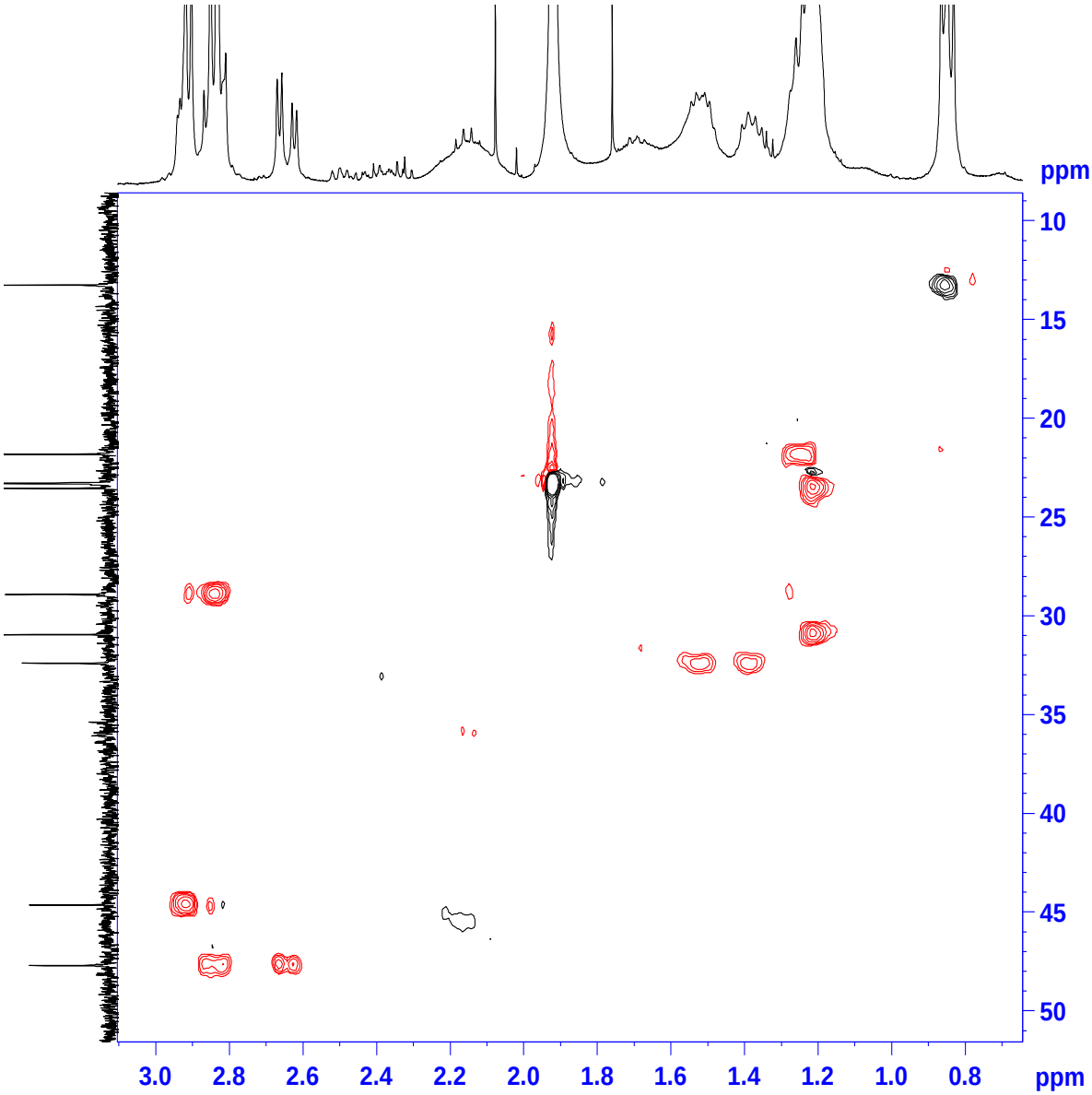

Supplemental Fig. 1. NMR spectra (continued).

HSQC (enlarged view 2)

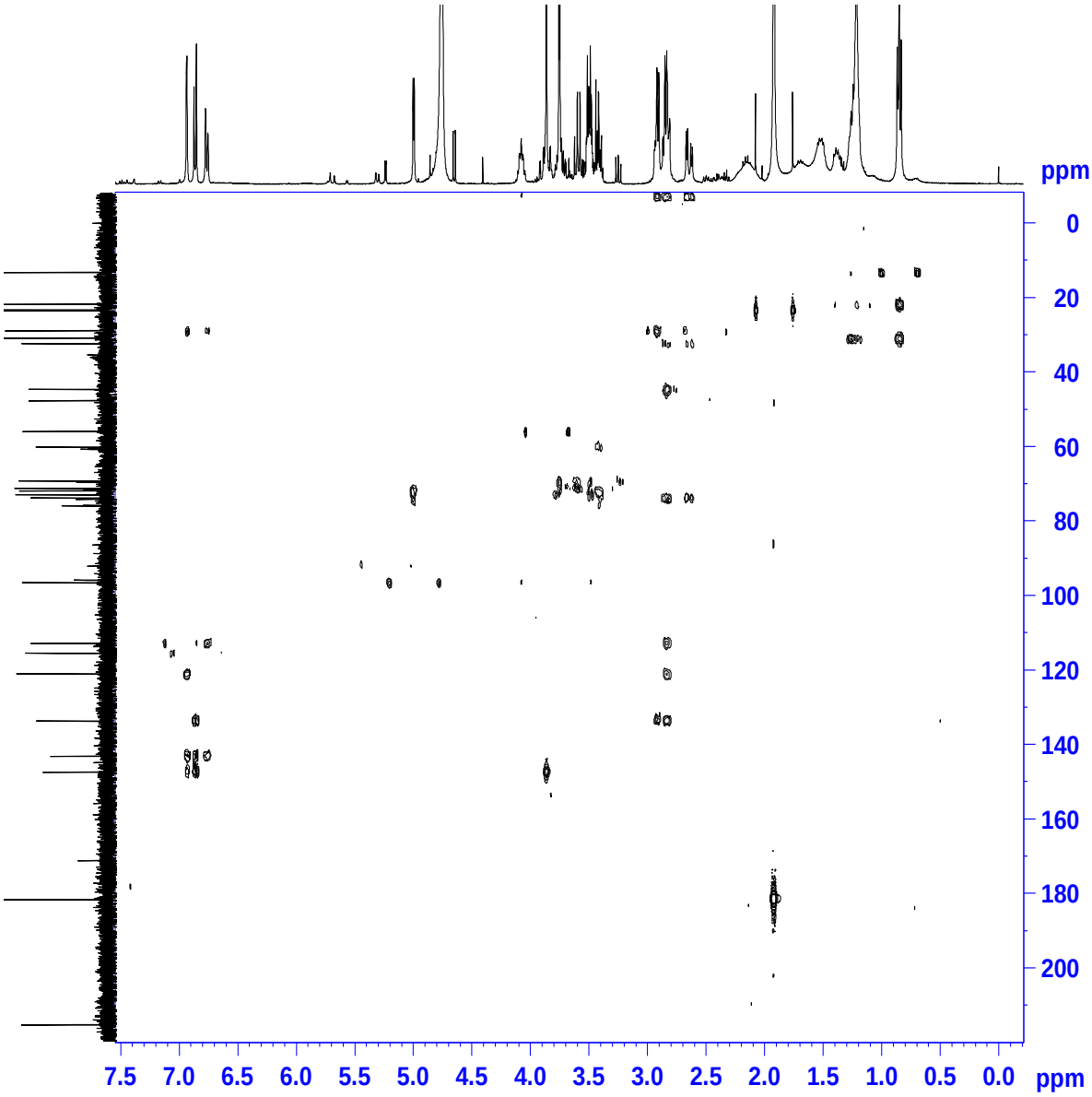

Supplemental Fig. 1. NMR spectra (continued).

HMBC (whole view)

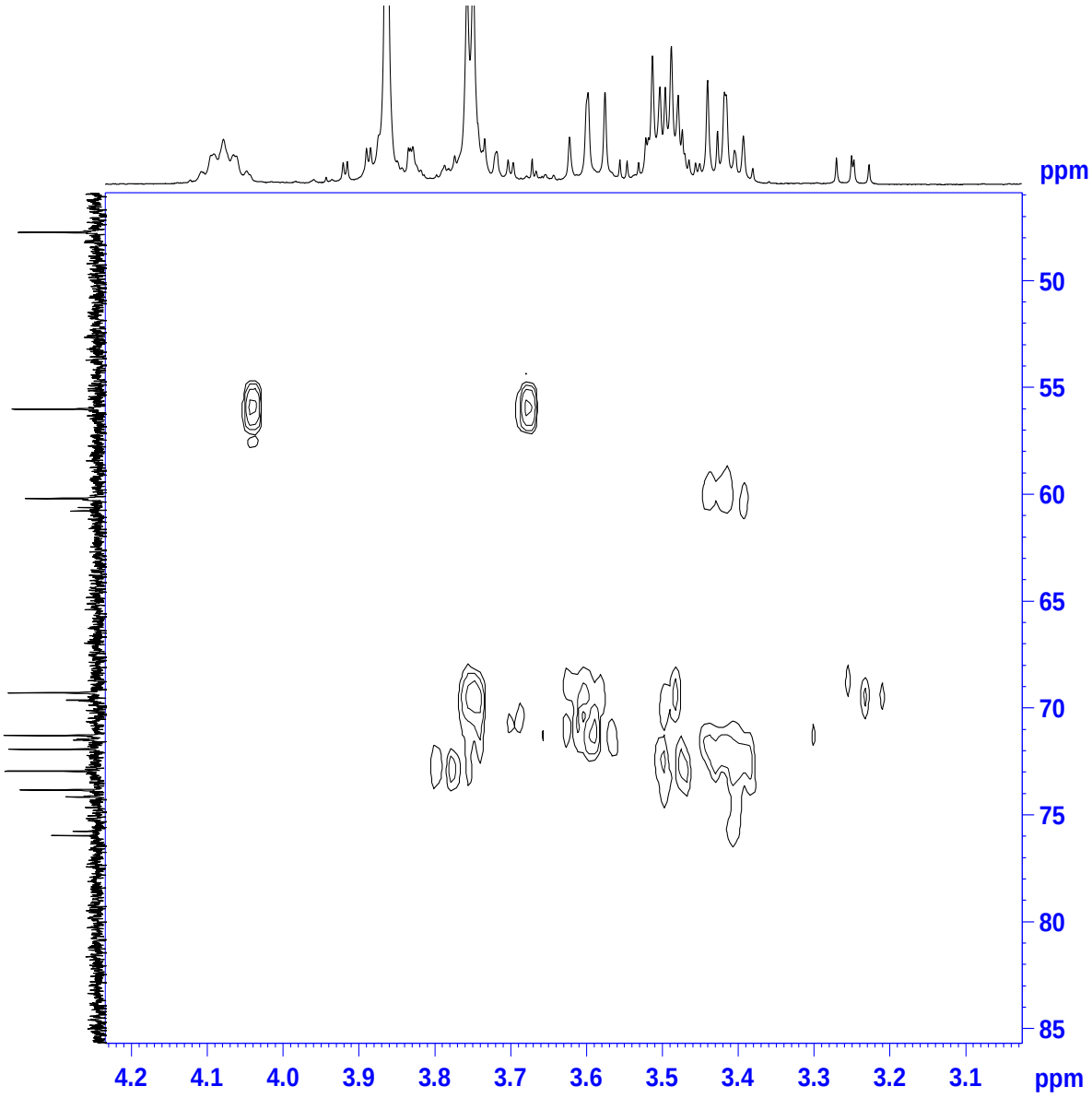

Supplemental Fig. 1. NMR spectra (continued).
HMBC (enlarged view 1)

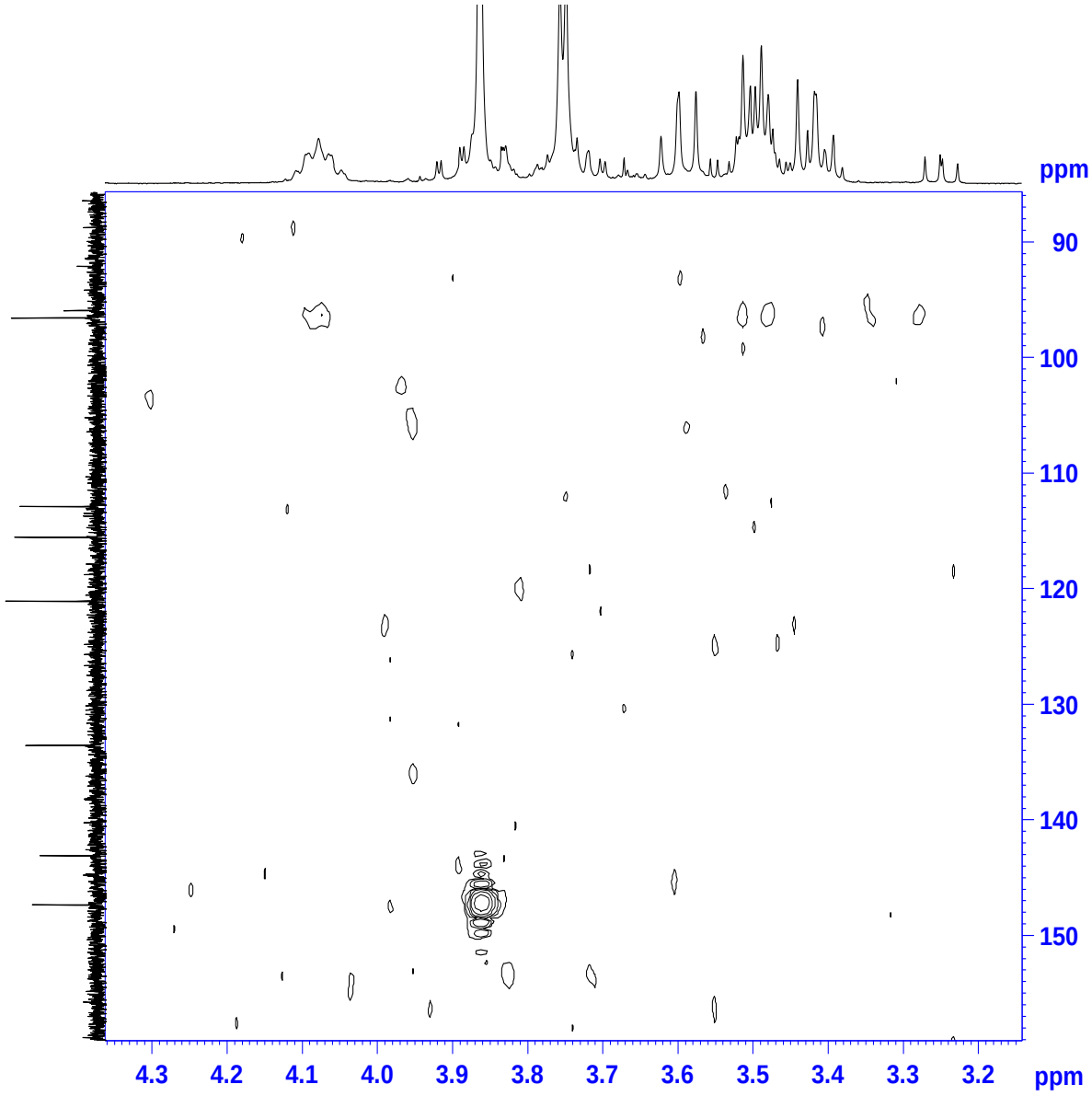

Supplemental Fig. 1. NMR spectra (continued).

HMBC (enlarged view 2)

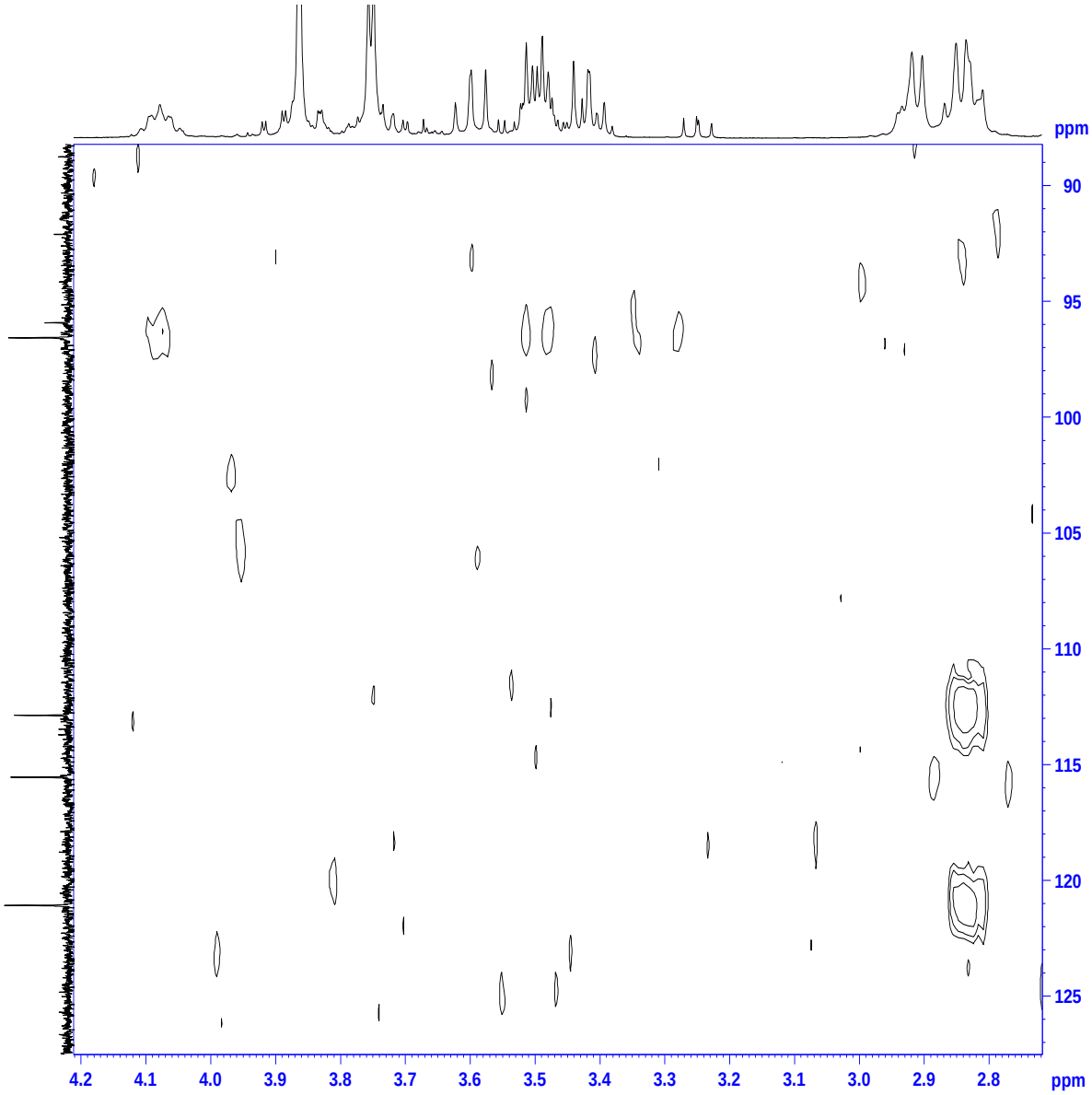

Supplemental Fig. 1. NMR spectra (continued).

HMBC (enlarged view 3)

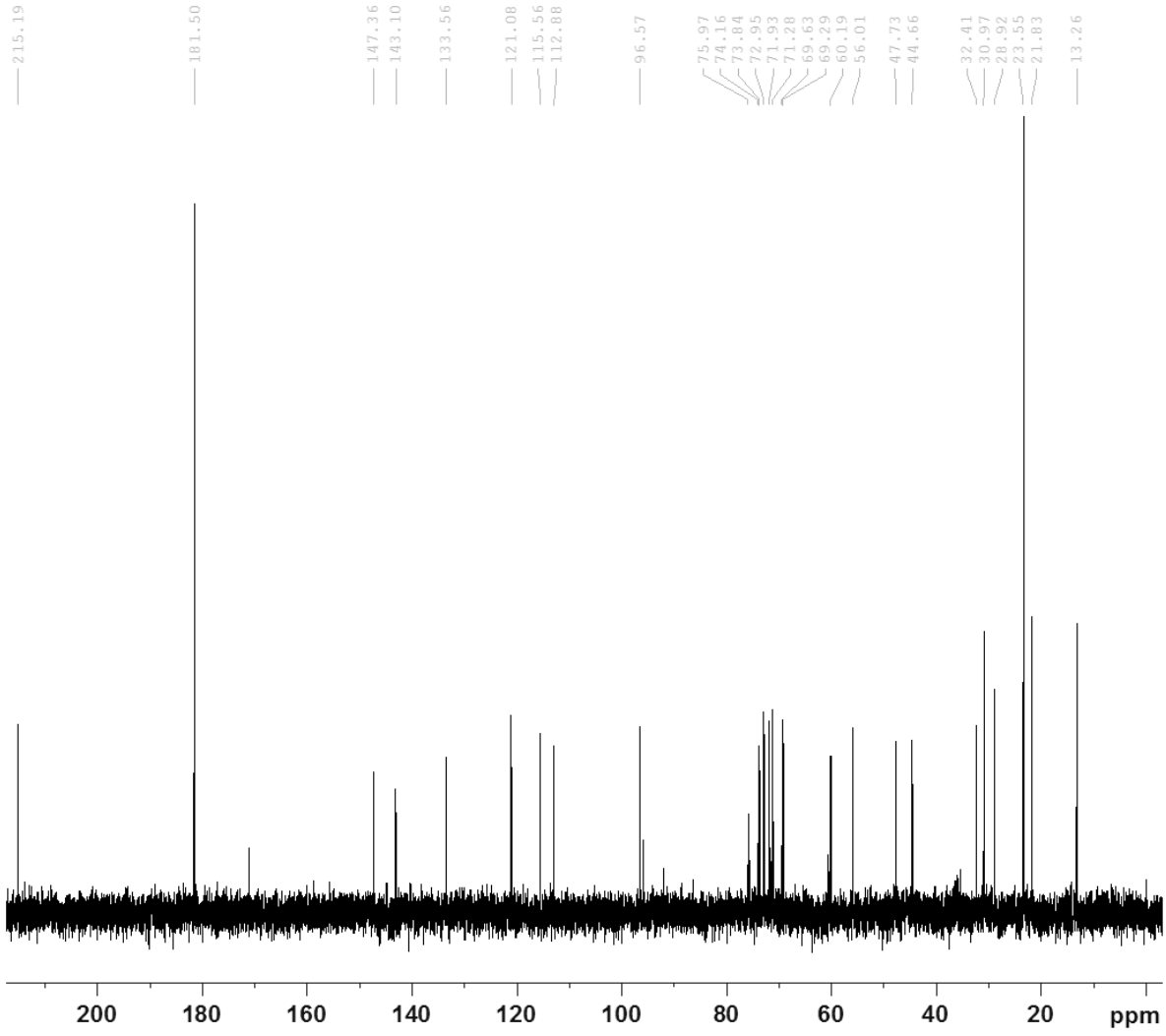

Supplemental Fig. 1. NMR spectra (continued).

^{13}C-NMR spectrum (whole view)

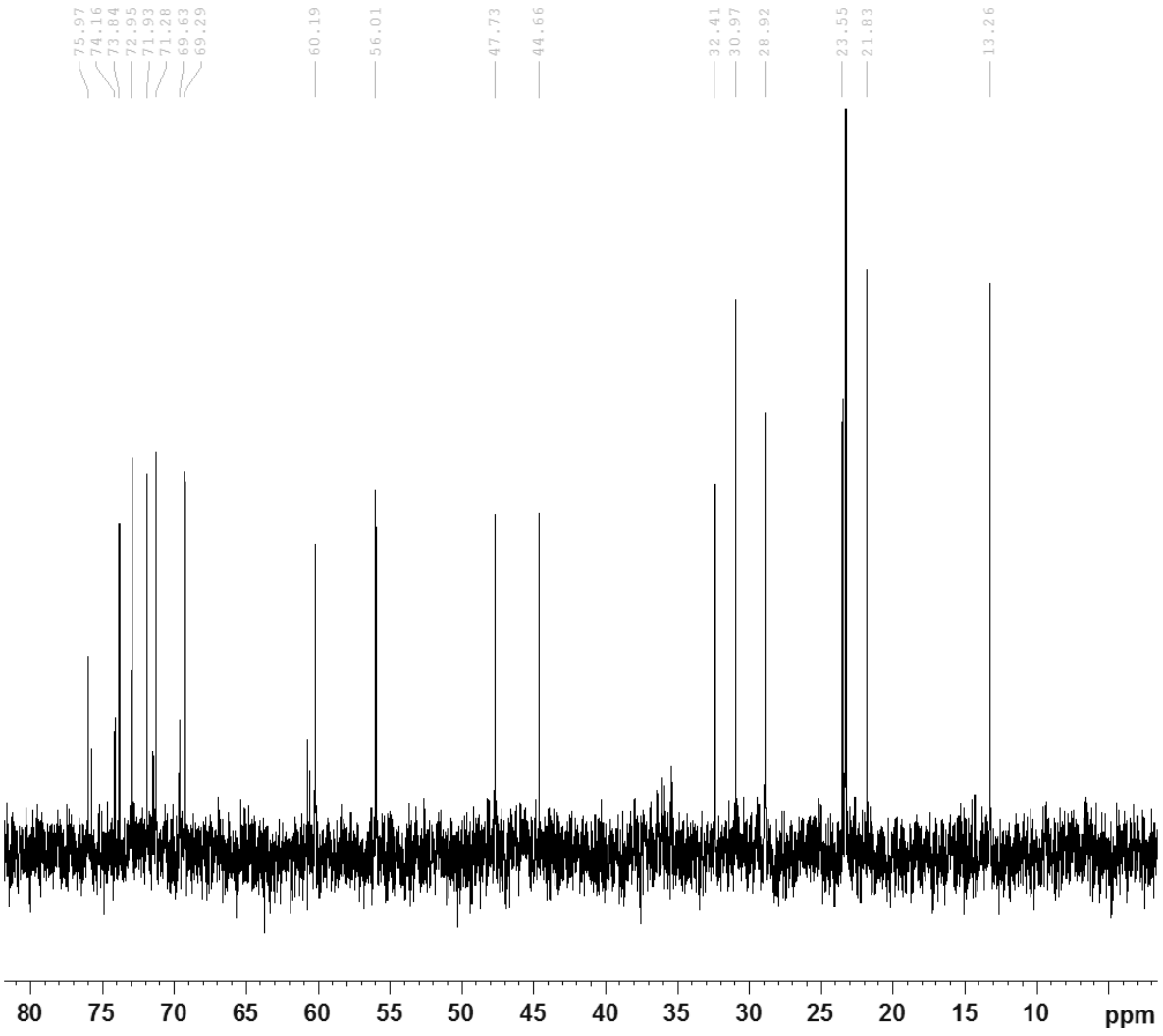

Supplemental Fig. 1. NMR spectra (continued).

^{13}C-NMR spectrum (enlarged view)

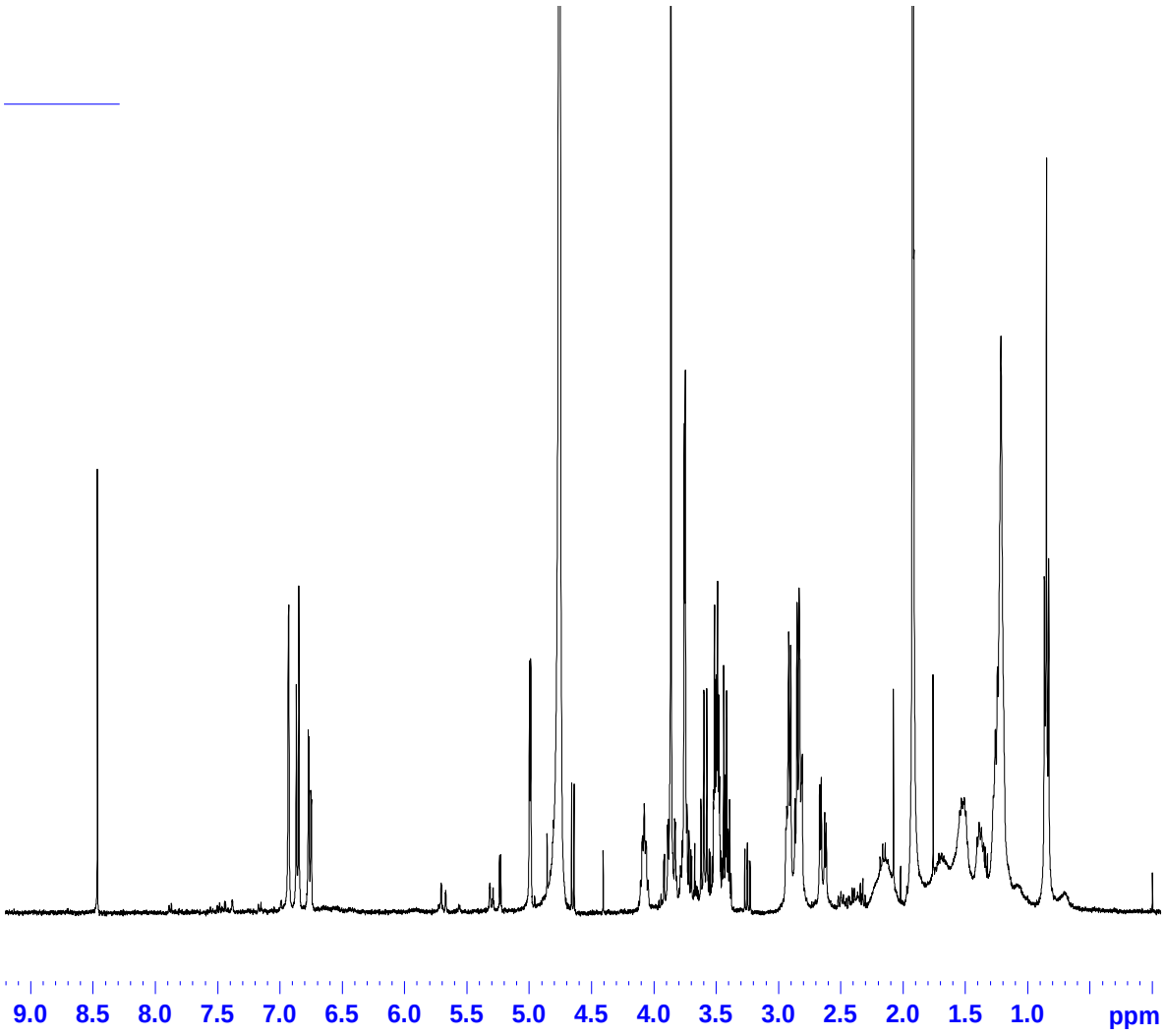

Supplemental Fig. 1. NMR spectra (continued).

^{1}H-NMR spectrum (whole view)

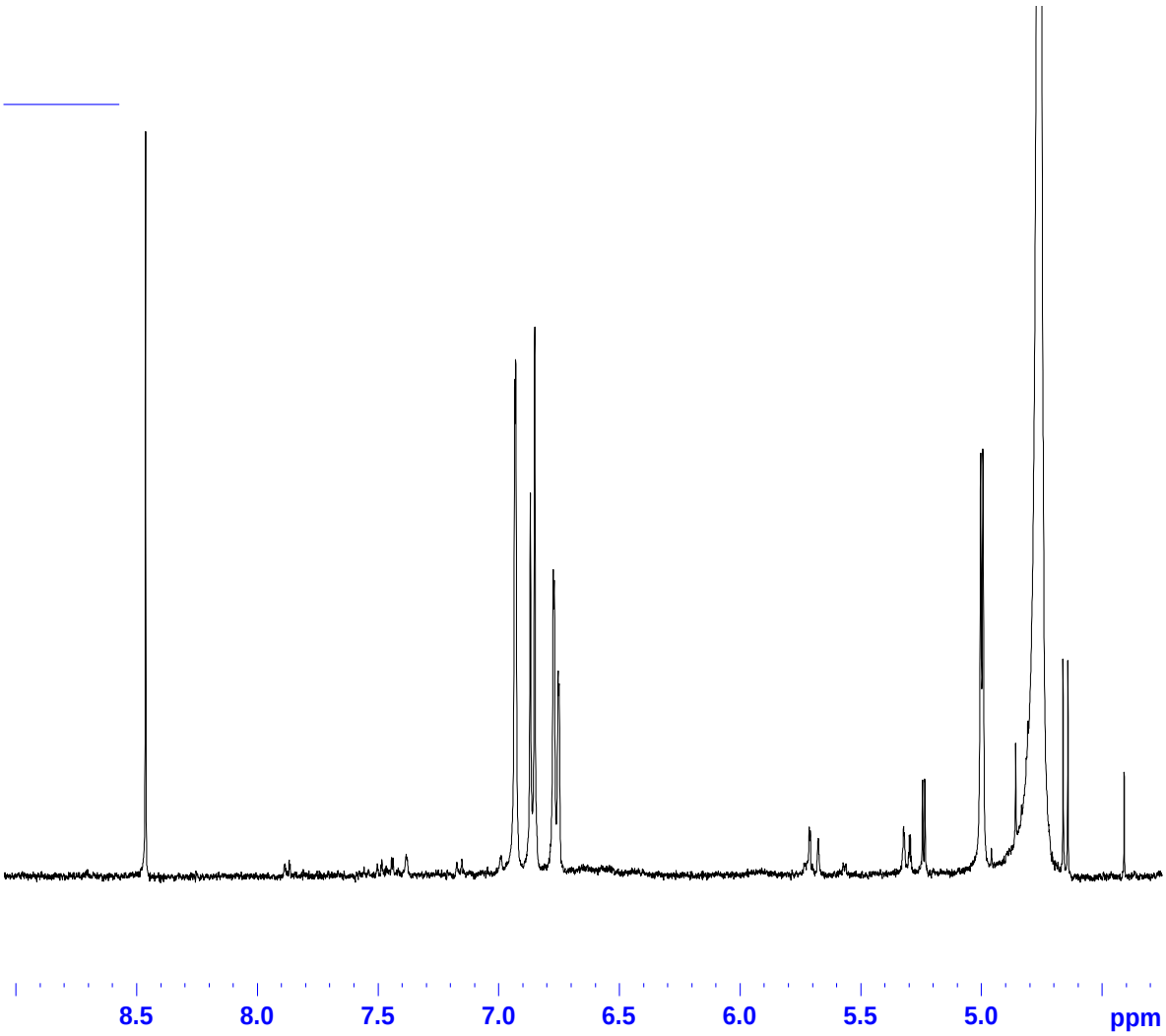

Supplemental Fig. 1. NMR spectra (continued).

^{1}H-NMR spectrum (enlarged view 1)

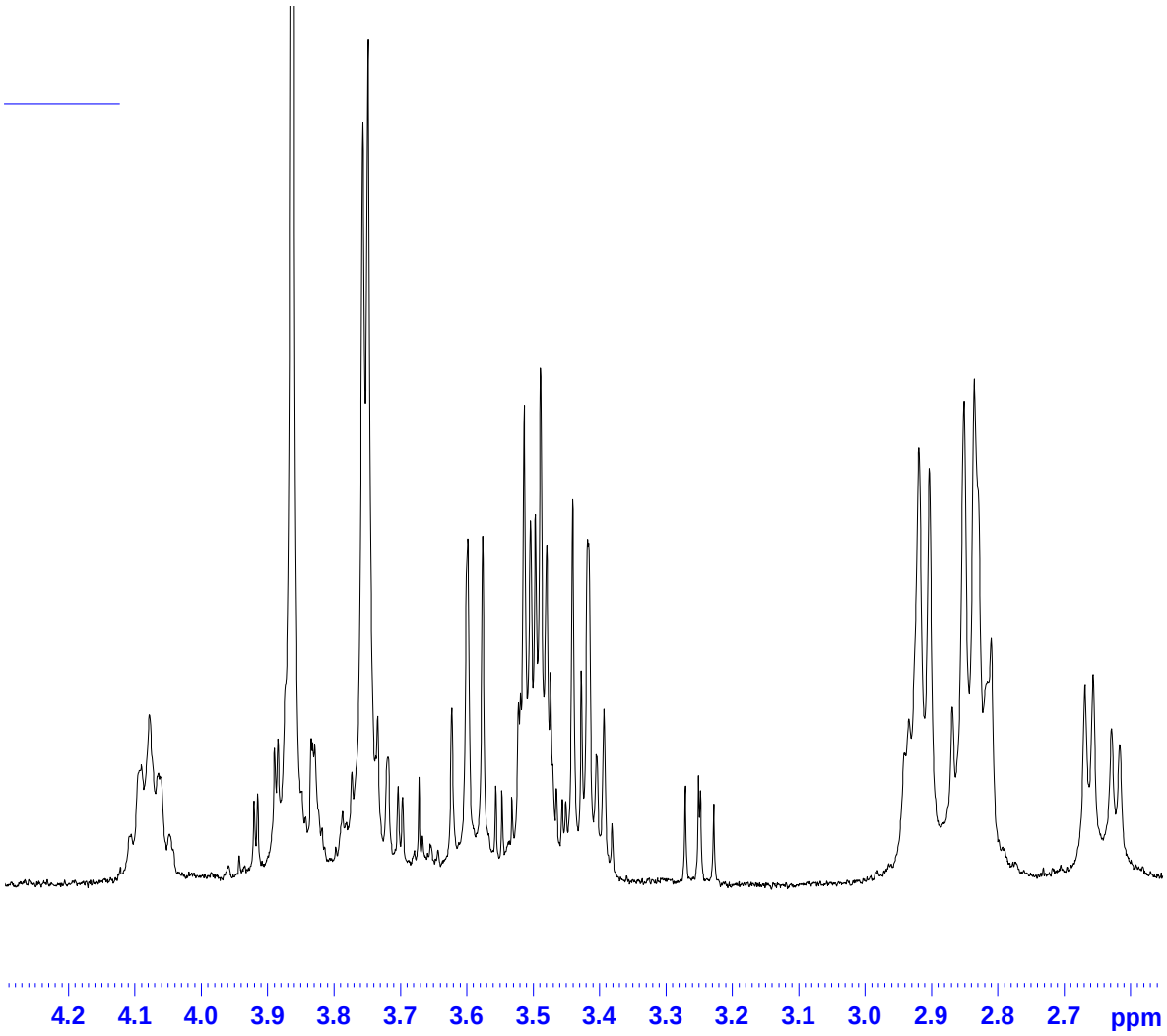

Supplemental Fig. 1. NMR spectra (continued).

^{1}H-NMR spectrum (enlarged view 2)

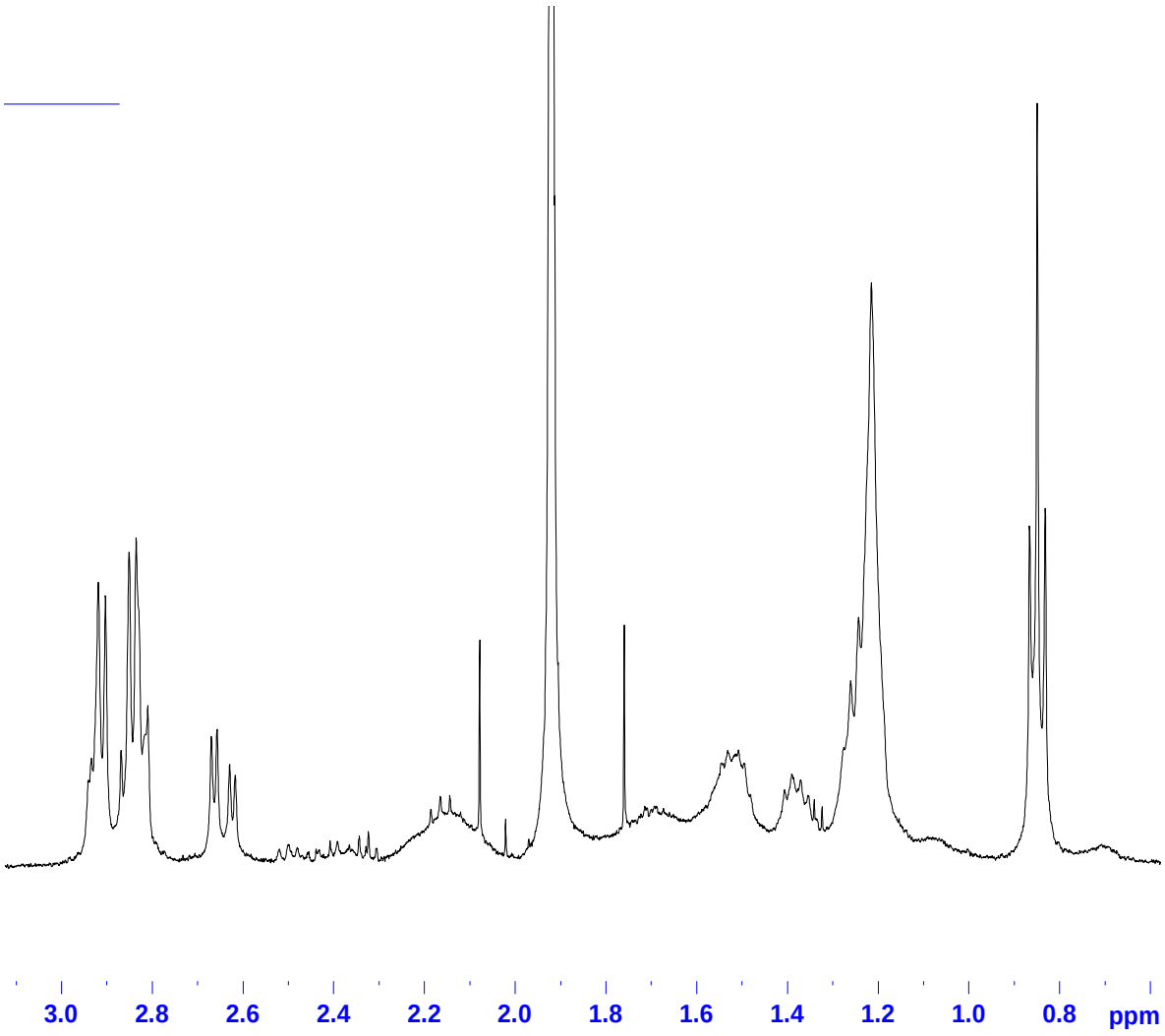

Supplemental Fig. 1. NMR spectra (continued).

^{1}H-NMR spectrum (enlarged view 3)